

EFFECTS OF SUBSTRATE ON DENDROCHRONOLOGIC STREAMFLOW
RECONSTRUCTION: PARIA RIVER, UTAH; WITH FRACTAL
APPLICATION TO DENDROCHRONOLOGY.

by

David Earl Grow

Copyright © David Earl Grow 2002

A Dissertation Submitted to the Faculty of the
SCHOOL OF RENEWABLE NATURAL RESOURCES

In Partial Fulfillment of the Requirements
For the Degree of

DOCTOR OF PHILOSOPHY
WITH A MAJOR IN WATERSHED MANAGEMENT

In the Graduate College

THE UNIVERSITY OF ARIZONA

THE UNIVERSITY OF ARIZONA ®
GRADUATE COLLEGE

As members of the Final Examination Committee, we certify that we have
read the dissertation prepared by David Earl Grow

entitled Effects of Substrate on Dendrochronologic

Streamflow Reconstructions: Paria River, Utah;

With Fractal Application to Dendrochronology.

and recommend that it be accepted as fulfilling the dissertation
requirement for the Degree of Doctor of Philosophy

Jeffrey S. Dean
Jeffrey S. Dean

12/11/02

Date 11/27/02

Date

Peter F. Ffolliott

12/12/02

Date 11/27/02

Date

Katherine K. Hirschboeck

12/12/02

Date 12/12/02

Date

David M. Meko

12/09/02

Date 12/09/02

Date

Thomas W. Swetnam

Final approval and acceptance of this dissertation is contingent upon
the candidate's submission of the final copy of the dissertation to the
Graduate College.

I hereby certify that I have read this dissertation prepared under my
direction and recommend that it be accepted as fulfilling the dissertation
requirement.

Thomas W. Swetnam

Dissertation Director

Thomas W. Swetnam

12/09/02

Date

STATEMENT BY AUTHOR

This dissertation has been submitted in partial fulfillment of requirements for an advanced degree at The University of Arizona and is deposited in the University Library to be made available to borrowers under rules of the Library.

Brief quotations from this dissertation are allowable without special permission, provided that accurate acknowledgment of source is made. Requests for permission for extended quotation from or reproduction of this manuscript in whole or in part may be granted by the copyright holder.

SIGNED: David Earl Graw

ACKNOWLEDGMENTS

I would like to thank my wife, Beth, for her continuing support and encouragement; Dr. Robert D. Hall, whose encouragement and occasional, gentle kick in the butt provided the original impetus for this degree; Dr. Jerry R. Miller and Sue Miller for my initial exposure to dendrochronology; Dr. Charles W. Stockton for providing practical statistical enlightenment; Dr. Richard Hereford of the U.S.G.S. for providing the opportunity to work with dendrochronology and streamflow reconstructions in southern Utah; Dr. P.K. Kulatilake for opening the door to fractals; Christine Hallman for validating tree-ring measurements; Dennie Bowden and Dick Warren for crossdating assistance; Rex Adams for all around laboratory guidance; the entire Laboratory of Tree Ring Research staff and faculty; and Thomas Harlan, whose experience, commentary, and insights proved invaluable during our field excursions. Naturally, many thanks go to my committee: Jeffrey S. Dean, Peter F. Ffolliott, Katherine K. Hirschboeck, David M. Meko, and Thomas W. Swetnam. The U.S. Forest Service, National Park Service, Bureau of Land Management, and the Grand Staircase - Escalante National Monument personnel were instrumental in obtaining sampling permits in southern Utah and northern Arizona.

TABLE OF CONTENTS

	Page
LIST OF ILLUSTRATIONS.....	8
LIST OF TABLES.....	10
ABSTRACT.....	11
CHAPTER 1. INTRODUCTION.....	13
Statement of the Problem.....	15
Substrate, Discharge Reconstructions, and Fractals... <td style="text-align: right;">18</td>	18
Hypotheses To Be Tested.....	20
Primary Hypothesis.....	20
Secondary Hypothesis.....	21
Previous Work.....	21
Dendrochronology in the Paria River Basin.....	21
Streamflow Reconstructions of Some Selected Rivers.....	23
Background.....	24
Geology, Soils, and Topography.....	24
Geology of the Basin.....	25
Substrate Characteristics.....	25
Paria River Basin Meteorology.....	27
Historical Background.....	30
Land-Use Changes.....	30
Water Use and Diversions.....	31

TABLE OF CONTENTS - *Continued*

Fractal Geometry.....	32
General Background.....	32
Fractals and River Basins.....	35
Hurst's Exponent and the Fractal Dimension ..	36
Self-Similar Versus Self-Affine Fractals.....	38
Roughness-Length Method Used in This Study...	43
Autocorrelation and Self-Affine Fractals.....	44
CHAPTER 2. METHODS.....	46
Field.....	46
Species Selection.....	46
Sampling Site Criteria.....	46
Laboratory.....	47
Sample Preparation and Chronology Development....	47
Data Analysis.....	48
Chronology Assessment.....	48
Fractal Analysis: Roughness-Length Method.....	51
Water Year Partitions.....	59
Streamflow Reconstructions.....	65
CHAPTER 3. RESULTS.....	69
Chronology Assessment.....	69
Cross-Correlation.....	71
Autocorrelation Assessment.....	72
Streamflow Reconstructions.....	74

TABLE OF CONTENTS - *Continued*

Reconstruction Validation.....	78
Substrate Analysis.....	80
Statistical Significance of Reconstructions.....	82
Fractal Analysis.....	84
Fractal Transformations.....	87
Fractal Transform Reconstructions.....	91
CHAPTER 4. DISCUSSION.....	95
Chronology Confidence.....	95
Streamflow Reconstructions and Meteorology.....	95
Substrate Analysis.....	99
Fractal Analysis.....	101
Fractal Transformations.....	105
Fractal Transform Reconstructions.....	107
Spatial Variability of Sites.....	108
CHAPTER 5. CONCLUSIONS.....	110
APPENDIX A. TREE-RING CHRONOLOGIES.....	113
APPENDIX B. STREAMFLOW RECONSTRUCTIONS.....	120
APPENDIX C. FRACTAL TRANSFORM RECONSTRUCTIONS.....	184
REFERENCES.....	203

LIST OF ILLUSTRATIONS

Figure 1, Gauged discharge and mean annual reconstructed discharge for the Paria River.....	16
Figure 2, Map of the Paria River Basin in southern Utah.....	22
Figure 3, Mean monthly precipitation and discharge distribution in the Paria River Basin.....	29
Figure 4, Fractal self-similarity.....	40
Figure 5, Example of fractal self-affinity.....	41
Figure 6, Time series example of fractal self-affinity..	41
Figure 7, Removal of growth trend.....	49
Figure 8, Log (ω) vs. log σ (ω) to determine fractal parameters.....	54
Figure 9, Log (ω) vs. log σ (ω) of annual discharge and site DSM indices.....	56
Figure 10, Annual discharge and precipitation for two sites in the Paria River Basin.....	61
Figure 11, Winter 2 discharge and precipitation for two sites in the Paria River Basin.....	63
Figure 12, Annual discharge, standard, and residual tree-ring indices.....	64
Figure 13, Scatter plots and histogram of residuals.....	67
Figure 14, Time series plot, lagged scatter plot, and ACF of residuals.....	68

LIST OF ILLUSTRATIONS - *Continued*

Figure 15, Winter 2 discharge reconstruction using sites CB and HCL.....	76
Figure 16, Substrate and adjusted coefficient of determination for Winter 2 discharge reconstruction.....	81
Figure 17, Results of fractal smoothing for site CB standard chronology.....	89

LIST OF TABLES

Table 1, Sampling site soil summary.....	26
Table 2, Paria River water budget.....	31
Table 3, Fractal parameters for site DSM.....	54
Table 4, Summary of chronology statistics.....	69
Table 5, Between-site chronology correlation matrix.....	72
Table 6, Summary of autocorrelation coefficients.....	73
Table 7, Adjusted coefficients of determination of discharge reconstructions.....	75
Table 8, Reconstruction validation summary.....	79
Table 9, Substrate correlation coefficient summary.....	84
Table 10, Fractal dimensions and Hurst exponents of tree-ring and hydrologic series.....	86
Table 11, Fractal parameters used to smooth tree-ring series.....	88
Table 12, Fractal parameters of modified tree-ring series.....	90
Table 13, Annual fractally modified streamflow reconstruction statistics.....	92
Table 14, Winter 2 fractally modified streamflow reconstruction statistics.....	93
Table 15, Discharge reconstruction summary.....	94

ABSTRACT

Two piñon (*Pinus edulis*) tree-ring chronologies developed on each of three substrates (sandstone, shale, and alluvial fan deposits) in southern Utah for the period 1702 to 1997 demonstrate that geologic substrate affects dendrochronologic streamflow reconstructions. Chronologies from alluvial fan deposits explain the most variance of cool-season (October 1 to May 31) flow with an adjusted coefficient of determination (R_a^2) equal to 0.59. Chronologies from sandstone deposits account for 52 percent of the variance, while those on shale deposits account for 45 percent. Correlation coefficients among the three substrates are significantly different at the 95% confidence level.

The highest single-site annual discharge reconstruction (October 1 to September 30), $R_a^2 = 0.25$, is provided by chronologies from shale deposits. The highest substrate-pair annual discharge reconstruction, $R_a^2 = 0.27$, is provided by chronologies from alluvial fan deposits. The highest summer discharge reconstruction (July 4 to September 3), $R_a^2 = 0.14$, is provided by chronologies from sandstone. Over 90 percent of the summer reconstructions are below $R_a^2 = 0.10$.

The different substrate response is attributed to varying amounts of clay in each substrate affecting infiltration and available water for tree growth. Low summer reconstruction values are attributed to spatially and temporally variable thunderstorms.

The fractal parameters (fractal dimension and Hurst exponent), calculated using the roughness-length method, describe the long-term persistence of each tree-ring series and of the hydrologic record. The fractal dimensions range from 1.739 to 1.939 for the tree-ring series for the calibration period, and from 1.884 to 1.946 for the entire chronology periods. The fractal dimension for the annual hydrologic record is 1.802, and 1.819 from October 1 through May 31. Modification of each tree-ring series based on the ratios of the Hurst exponent of each series forced the fractal dimensions of the tree-ring series to be closer to that of the hydrologic series. Fractal modification of the tree-ring series failed to improve streamflow reconstructions, but the modification of the tree-ring and hydrologic series suggests a more realistic reconstruction. Fractal analysis is useful to examine the stationarity of tree-ring series.

CHAPTER 1. INTRODUCTION

Dendrochronological streamflow reconstructions have been performed since the mid 1930s. Early 1900s streamflow studies (Hardman and Reil, 1936; Hawley, 1937; Schulman, 1945; 1951) were not strict reconstructions as the term is used today. These early studies generally compared tree-ring records with streamflow, and made estimates for wet and dry periods for pre-gauged streamflow. To facilitate comparison between precipitation and streamflow, the series were commonly smoothed using a 'Hahn' filter, a three year moving average with double weight given to the central value.

Tree-ring growth is directly related to precipitation (Fritts, 1976; Loaiciga et al., 1993). Streamflow reconstructions represent precipitation less water lost to evapotranspiration (Jones et al., 1984; Meko and Stockton, 1984). Therefore, the climate and vegetation peculiar to a specific basin will directly influence the dendrochronologic streamflow reconstructions for that basin. Fritts (1976) reports that substrate and soil differences affect tree-ring width. The substrate controls infiltration, local drainage, and nutrient supply to the tree. A tree is therefore an integrator of the local environment, and the tree-ring

record reflects not only precipitation but also the substrate on which the trees are growing.

In discussing runoff histories, Schulman (1945) mentions that criteria necessary for an effective dendrochronologic index are site selection, crossdating, and sensitivity; selection of the appropriate species, proper crossdating of the samples, and sensitivity of the sample to the environmental variable in question. While Schulman (1945) did not provide a detailed description of the geologic substrate, he did mention that some samples in the Pacific Northwest were collected mostly on granitic type rocks. Wright and Mooney (1965) and Fritts (1969) discussed the distribution of bristlecone pines (*Pinus longaeva*) in the White Mountains of California. These studies concluded that growth patterns of bristlecone pines were controlled by the dolomitic substrate on which the bulk of the trees and the oldest trees occurred. Fritts (1969) also mentioned that tree rings were generally wider on sandstone than on the dolomite. Cleaveland and Stahle (1989) reconstructed streamflow of the White River in Arkansas, and mentioned that the samples were taken on well drained upland and poorly drained wetland habitats. Numerous other investigators (Stockton, 1976; Smith and Stockton, 1981; Cook and Jacoby, 1983; Phipps, 1972, 1983; Jones et al.,

1984; Meko and Graybill, 1995; Meko et al., 2001) performed streamflow reconstructions, and contributed a plethora of statistical techniques and approaches to the reconstruction process. None of these studies directly addressed the role of substrate on the tree-ring record.

Statement of the Problem

Tree-ring sample selection has emphasized the sensitivity of the species to the environmental variable being investigated (e.g., temperature or precipitation) (Fritts, 1976). The selection process has focused on species, elevation, and aspect as criteria for selecting the proper specimens. Little attention has been paid to the effects of soil type and substrate on tree-ring width. Soil texture affects infiltration of water, evaporation of water from the soil, translocation of clays and minerals, and distribution of roots (Jenny, 1941; Fritts and Holowaychuck, 1959; Birkeland, 1984). Therefore, the type of soil and substrate will determine the water content of the soil available for tree growth, rooting depth, and nutrient supply. Consequently, soils will affect tree-ring width.

Tree-ring widths commonly underestimate high and low extremes of streamflow by tree rings during the calibration period, and this is probably an artifact of regression and

the biological characteristics of trees (Fig. 1). Regression necessarily compresses reconstructions towards the mean of the calibration data, resulting in underestimation of high, and overestimation of low flows.

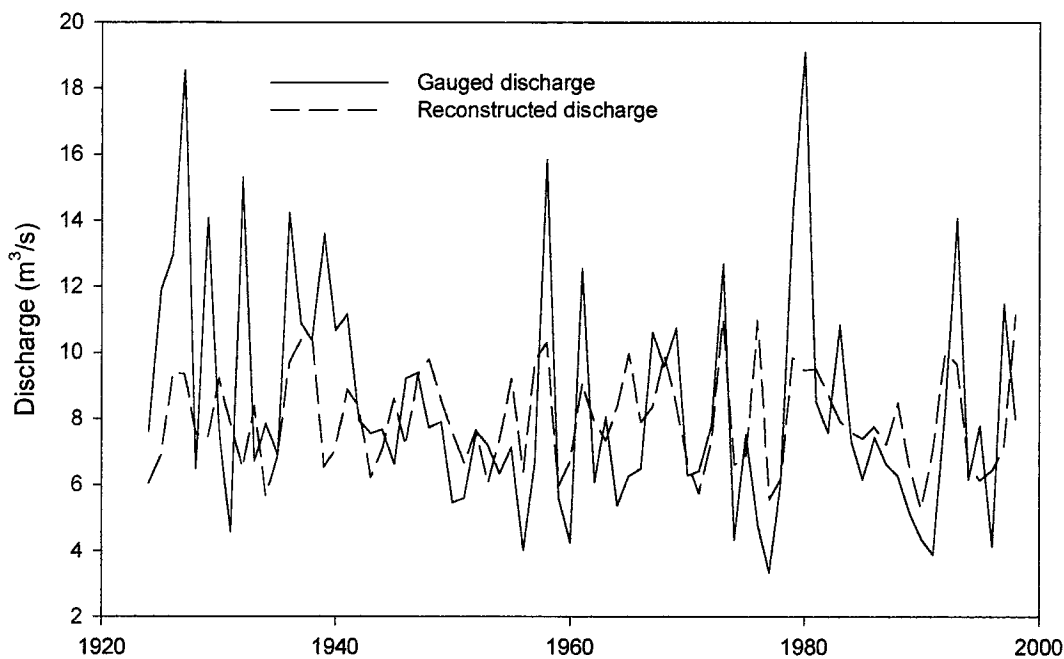


Figure 1. Gauged discharge and reconstructed mean annual discharge for the Paria River using Douglas-fir (*Pseudotsuga menziesii*). Note that there is a compression of the variance of the reconstructed values relative to the observed values, as well as a slight shift in the alignment of some of the peaks (Unpublished data from D. Grow, 2000).

The biological processes of tree-ring growth require only a particular amount of water. Therefore, excess water above what is required might not be reflected in the tree-ring record, but can be recorded in the hydrological gauge records. Additionally, the tree-ring record is a composite of the environmental conditions of tree growth. For example, the tree-ring record reflects a combination of precipitation, temperature, evapotranspiration, nutrient supply, disease, insect infestations, and physical damage caused by such factors as lightning strikes, tree-fall breaking branches, or mammals eating or clawing the bark. Isolating a single environmental variable becomes problematic. However, separation of these different signals can be largely accomplished by site and tree selection.

Transformations of raw data (for example, logarithmic or quadratic) can be performed on hydrological or tree-ring data to force a more normal distribution of the data to improve statistical inference (Loaiciga et al., 1993; Cleaveland, 2000). Recently, Meko (2001) adjusted the first-order autocorrelation of tree-ring indices to be closer to that of a hydrologic series, in an effort to improve streamflow reconstructions. Cleaveland and Stahle (1989) examined inhomogeneities in the hydrologic record and found that inhomogeneities increase the error component in

streamflow reconstructions. One method to overcome the inhomogeneities uses the ratio of the slopes of the discharge record lines to modify the hydrologic record to improve comparability of the inhomogeneous subsections of the record (Loaiciga et al., 1993). My study explores the use of the fractal dimensions of the tree-ring and hydrologic records to improve statistical inference by modifying the tree-ring series with the ratios of the slopes of the fractal parameters of the tree-ring and hydrologic series. By forcing the fractal parameters of each series to be closer, improved discharge reconstructions is a reasonable assumption.

Substrate, Discharge Reconstructions, and Fractals

Different time scales need to be considered when examining soils and substrates, tree growth, and the hydrologic record. Soils can take hundreds or thousands of years to develop (Jenny, 1941; Birkeland, 1984). The longevity of soil development dictates that soils are integrators of long-term climatic, biological, topographical, and geologic dynamics. Trees are integrators of their environment as well, and record climatic and environmental fluctuations, although not on the same time span as soils. Over the life of a tree, soils do not change

appreciably, and are not considered a factor affecting yearly ring-width variability (Fritts, 1976), but the type of soil and substrate at a site controls the available water for vegetative growth, and the soil type will affect tree-ring width.

The discharge record is an integrator of the geology, vegetation, and climate of a basin upstream of the gauging station. The discharge recorded at a gauging station is the residual remaining after evaporation, vegetation use, infiltration to groundwater, and storage of water within the basin. Because soil texture controls infiltration and regulates the amount of water evaporated from the soil, the type of substrate controls the rate at which water enters and exits a system. For example, coarse grained sands will percolate water much faster than shale or clay (Fetter, 1980). Therefore, depending on the frequency, intensity, and spatial distribution of precipitation events, substrate affects how soon or if discharge is recorded at a gauging station. There can be a lag of several days to years when water enters and exits a system.

The time-scale differences of the integrators (soils, trees, and discharge) present difficulties when performing streamflow reconstructions. The time-scale differences among the integrators introduce error because of the lag in

response of one variable to another. What is needed is a mechanism to assess the long-term behavior of each of the integrators to determine characteristics peculiar to each one. Fractals can provide such a mechanism by producing a scaling factor between the tree-ring record and the hydrologic record based on properties inherent within each series.

The objectives of my study are twofold: 1) to directly address the effects of substrate on dendrochronological streamflow reconstructions, and 2) to determine the facility of using the fractal dimensions of tree-ring chronologies and the hydrologic record as scaling factors in dendrochronological applications.

Hypotheses To Be Tested

Primary Hypothesis

Geological substrate controls local hydrological systems. Drainage characteristics peculiar to different substrates are reflected in the tree-ring record, and trees on a particular substrate produce a chronology that provides improved streamflow reconstructions over trees on other substrates.

Secondary Hypothesis

The fractal parameters describe the long-term persistence of the profiles of tree-ring series and discharge records. The ratios between the variables are scaling factors that can be used to equalize the persistence and synchronize the peaks and troughs in tree-ring indices and the normalized gauged streamflow. These adjustments will improve streamflow reconstructions.

Previous Work

Dendrochronology in the Paria River Basin

A few dendrochronological investigations have been conducted in the Paria River basin, the site of this study (Fig 2). Schulman (1950; 1956) developed chronologies using bristlecone pine (*Pinus longaeva*), Douglas-fir (*Pseudotsuga menziesii*), juniper (*Juniperus sp.*), and piñon (*Pinus edulis*) trees from Bryce Canyon National Park, Tropic Canyon, and Red Canyon. The oldest chronology developed at that time dated to A.D. 1095. Shroder (1978) conducted a dendrogeomorphic study of rock glaciers on Table Cliffs Plateau (on the northeast corner of the Paria River basin). The chronologies developed using Englemann spruce (*Picea engelmannii*), limber pine (*Pinus flexilis*), and Douglas-fir date to A.D. 1750.

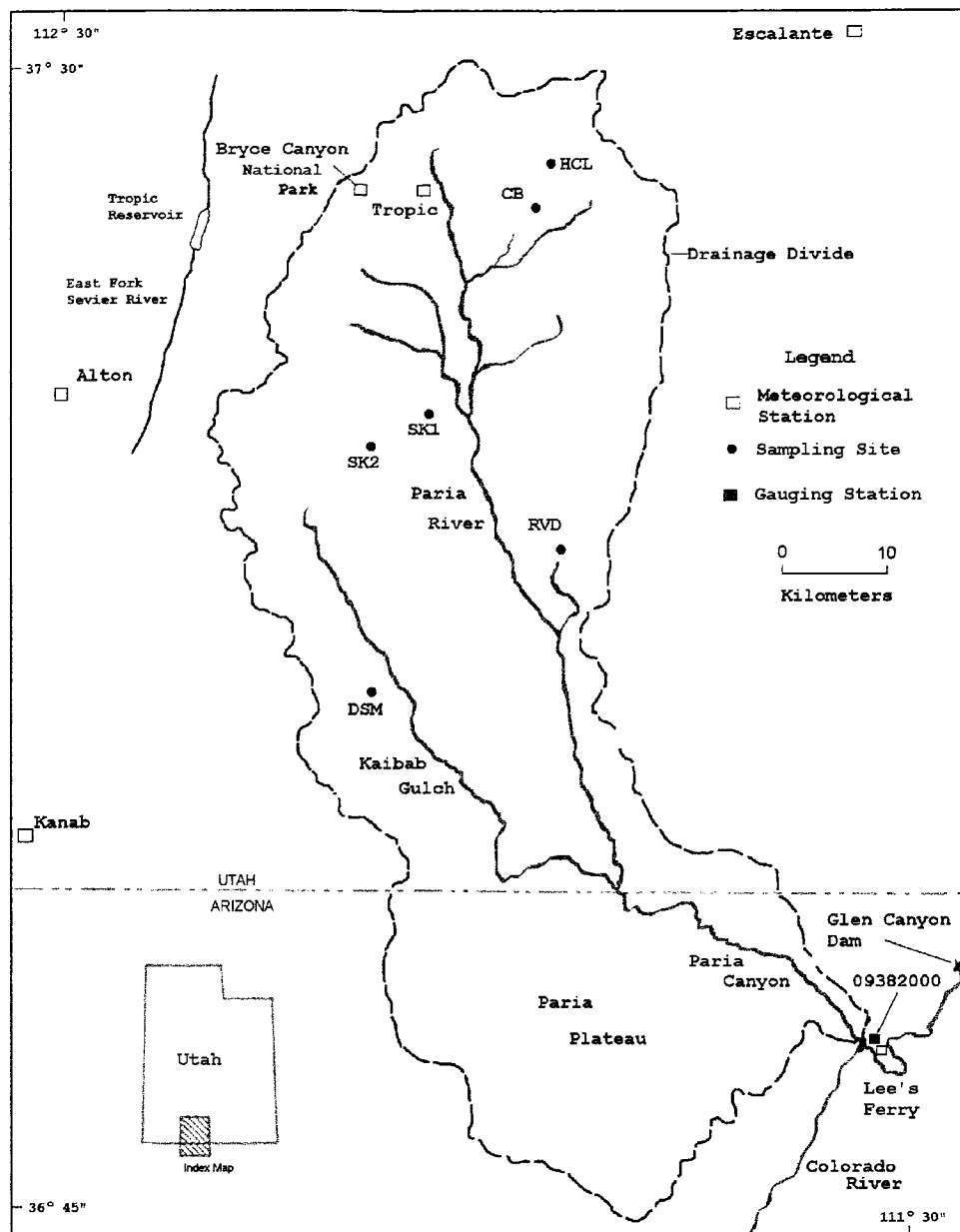


Figure 2. Map of the Paria River basin in southern Utah showing locations of sampling sites, U.S.G.S. gauging stations, and meteorological stations (Modified from Graf et al., 1991). Key to sites:
CB = Coal Bench, HCL = Lower Henderson Canyon,
DSM = Deer Springs Mesa, RVD = Round Valley Draw,
SK1 = Skutumpah Road site number 1, and
SK2 = Skutumpah Road site number 2.

In the early 1980s, Graybill and LaMarche investigated bristlecone pine on Table Cliffs Plateau, and developed a chronology from A.D. 804 to 1983 (Laboratory of Tree-Ring Research, unpublished data). More recently, cottonwoods (*Populus fremontii*) were examined to estimate the minimum ages of flood deposits and terraces along the Paria River (R. Hereford, 2000, U.S.G.S., pers. comm.). The oldest tree dates to the 1820s.

Streamflow Reconstructions of Some Selected Rivers

Hereford et al. (1996) reconstructed streamflow of the Virgin River from 1690 to 1992. In this study, ring width accounted for 59% of the variability in gauged water year streamflow from 1910 to 1992.

Stockton (1976) performed a 450 year streamflow reconstruction of the Colorado River based on streamflow data from Lee's Ferry. His tree-ring width reconstruction accounted for 82% of the variance in streamflow during the calibration period.

Graybill (1989) reconstructed discharge for the Salt and Verde Rivers in Arizona. Reconstructions accounted for between 52% and 67% of the variance in the calibration period. This reconstruction used both living trees and archaeological samples.

Background

Geology, Soils, and Topography

The area chosen for this study is the Paria River basin in southern Utah and northern Arizona (Fig. 1). During previous dendrochronological research in this basin, I observed that piñon trees were widely scattered on different substrates within the basin. The widespread presence of piñon and exposure of geologic strata provide an opportunity to address the effects of substrate on tree-ring chronologies and streamflow reconstructions.

The drainage area is 365,188 hectares and the topography is mesa and scarp, with elevations ranging from 952 meters at the gauge at Lee's Ferry to 3,140 meters in the upper basin on Aquarius Plateau. The Paria River joins the Colorado River at the head of Marble Canyon near the North Rim of the Grand Canyon. The vegetation of the area consists of juniper-piñon in the lowlands, and mixed conifer on the plateaus: Douglas-fir, limber pine, Engelmann spruce, and bristlecone pine. Ponderosa pine frequents the mid elevations, and is also found in isolated patches on north-facing hillslopes at lower elevations.

Geology of the Basin

The basin consists of three distinct geological zones: 1) the upper basin is composed of the carbonate Wasatch Formation of Tertiary age, 2) the central basin amphitheater is composed primarily of Tropic shale of Cretaceous age, and 3) the lower basin plateaus are composed of Jurassic age Navajo sandstone. Late Holocene alluvium covers most valley floors, and forms a terrace one to five meters above stream channels. The bulk of bedrock is loosely cemented, and is a readily available source of sediment (Hereford, 1986; Kelsey, 1998; Fillmore, 2000). Bare rock exposures are abundant throughout the basin.

Substrate Characteristics

Soils throughout the basin are predominantly fine, sandy loams, very deep, and well drained (Swensen and Bayer, 1990). The tree-ring sample sites are located on three different soil series (Tab. 1). Sites HCL and CB are located on the Hernandez-Clapper Series; DSM and RVD on the Podo Series; and SK1 and SK2 on the Cannonville Series. The Hernandez-Clapper series is formed in alluvium from sandstone and limestone. The Podo series is formed from sandstone residuum and alluvium. The Cannonville series is formed from shale residuum. The clay content of the soil

series ranges from 5 to 50%, and permeability ranges from 0.15 to 15.24 centimeters per hour (Tab. 1). These features affect the infiltration capacity, hydraulic conductivity, transmissivity, and available water capacity of the different substrates (Birkeland, 1984; Brooks et al., 1997; Ritter et al., 2002).

Table 1. Sampling site soil summary (From Swenson and Bayer, 1990)

Site	Soil series	Clay content (%)	Permeability (cm/hour)
CB	Hernandez-Clapper	18 - 27	1.52 - 5.08
HCL	Hernandez-Clapper	18 - 27	1.52 - 5.08
DSM	Podo	5-25	5.08 - 15.24
RVD	Podo	5-25	5.08 - 15.24
SK1	Cannonville	40 - 50	0.15 - 0.51
SK2	Cannonville	40 - 50	0.15 - 0.51

Key to site codes:

CB = Coal Bench, HCL = Lower Henderson Canyon, DSM = Deer Springs Mesa, RVD = Round Valley Draw, SK1 = Skutumpah Road site number 1, SK2 = Skutumpah Road site number 2.

Paria River Basin Meteorology

The precipitation in the basin is delivered by two types of storm systems and is influenced by topography (Hereford, 1986; Graf et al., 1991; Bradford et al., 2000). Winter and spring precipitation originates primarily from synoptic-scale storm systems, generally as frontal systems. Summer and fall precipitation originates primarily from convective thunderstorms, some of which can be enhanced by moisture from dissipating eastern Pacific Ocean tropical storms. Summer thunderstorms are spatially and temporally variable. Surface water supply in the basin primarily originates from snow melt during April, May, and June (Bradford et al., 2000).

Precipitation as rain in and around the basin ranges from 20 to 76 centimeters per year; snowfall depth ranges from 63 to 280 centimeters, with the higher amounts falling on the upper plateaus. Mean annual temperature ranges from 3.3 to 9.4 degrees Celsius (Swensen and Bayer, 1990).

Precipitation distribution is biseasonal with rain falling from July to October, and snowfall/rain falling from November to June (Hereford, 1986). Mean annual precipitation at Bryce Canyon National Park (~2,438 meter elevation) averages 41 centimeters of rain and 240 centimeters of snow fall. Mean annual precipitation at Tropic (~1920 meter

elevation) averages 31 centimeters of rain and 99 centimeters of snowfall (Fig. 3) (Swensen and Bayer, 1990).

Estimated pan evaporation for Bryce Canyon National Park is 78 centimeters, and 93 centimeters at Tropic from May through October (Swensen and Bayer, 1990). Estimated pan evaporation exceeds recorded rainfall for each station. Although the estimated evaporation is not the actual evaporation, the potential for removing a large portion of water from the local system is present. Removing a large portion of water introduces a source of error between precipitation and discharge records.

Precipitation and discharge records provide some insight into possible error introduced into streamflow reconstructions (Fig. 3). Although discharge tracks precipitation fairly well, winter and spring (January-April) discharge records exceed precipitation records. Elevated late summer discharge records (July-October) also exceed precipitation records. The differences can result from the spatial variability of summer thunderstorms, and the paucity of meteorological stations in the lower basin. The differences reflect transmission losses due to evapotranspiration and water storage within the basin.

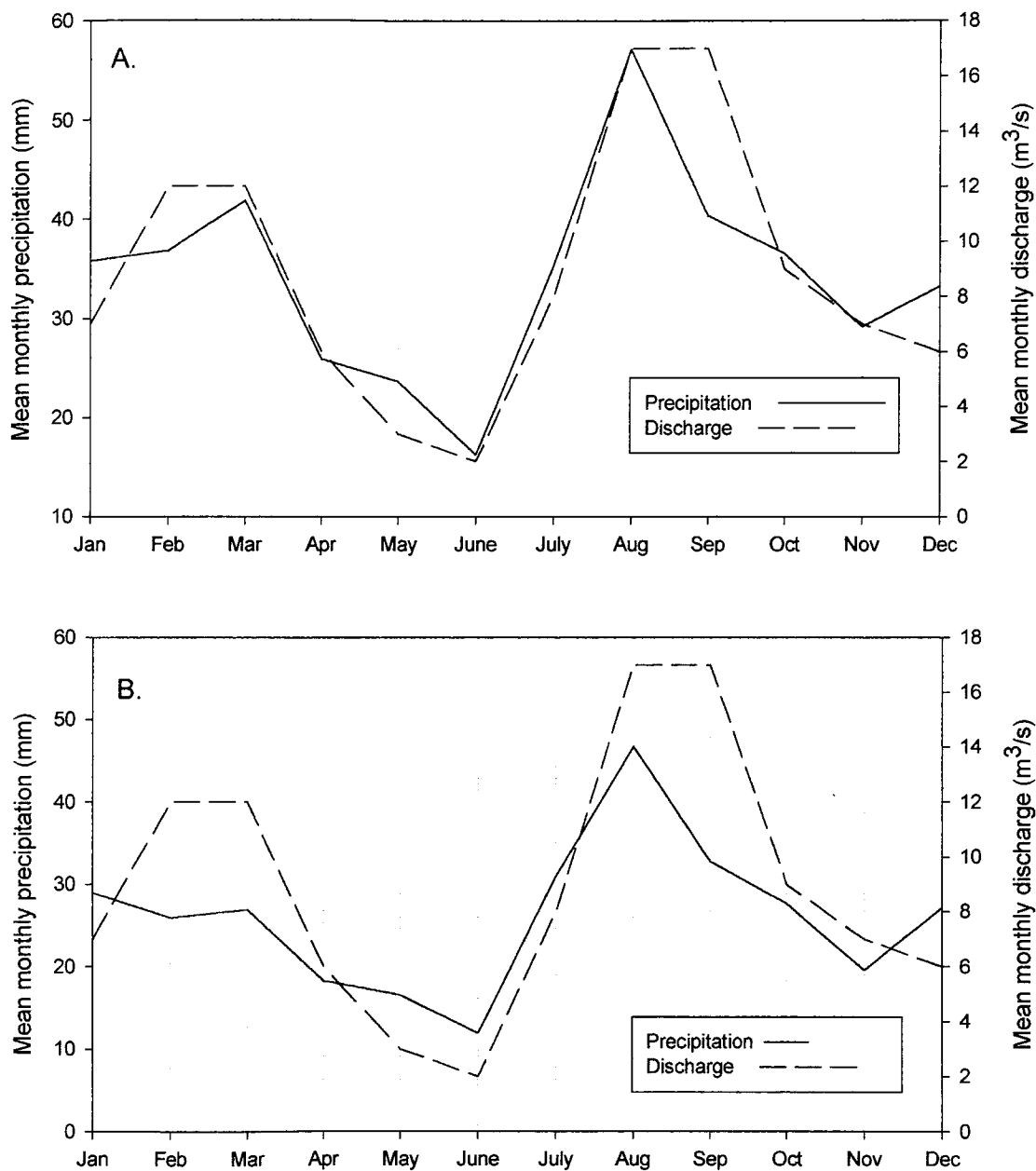


Figure 3. Mean monthly precipitation and Paria River discharge distribution at 2 sites in the Paria River basin: Bryce Canyon National Park (A), and Tropic (B). Discharge is mean monthly cubic meters per second for the period of record (1924– 1997) at the Lee's Ferry gauge.

Historical Background

Land-Use Changes

In the early 1900s, the U.S. Forest Service began incorporating a large portion of the plateau areas (Aquarius and Paunsaugunt Plateaus) surrounding the basin into the Dixie National Forest. By 1945, the present Dixie National Forest boundaries were established. Consequent to this procedure was the elimination of an appreciable amount of rangeland available for grazing, as well as the establishment of controls for forest management and timber harvesting. In 1924, the area settled by Ebenezer Bryce in 1875 was designated as the Utah National Park; in 1928, revisions and modifications included the renaming of the area to Bryce Canyon National Park (Bradford et al., 2000).

In 1996, the southern portion of the basin was encompassed by the newly designated Grand Staircase-Escalante National Monument, part of which has recently been reclassified as 'Wilderness' area, meaning that little if any anthropogenic modifications will be permitted. Apart from nominal private inholdings within these areas, the above actions have effectively protected the headwaters of the Paria River and its tributaries from anthropogenic degradation. The majority of current agricultural land use is in the greater Paria River

floodplain, and consists of cattle grazing and forage crop farming (Bradford et al., 2000).

Water Use and Diversions

In 1901, the Tropic Reservoir, with a capacity of 2,282,000 cubic meters was built on the East Fork of the Sevier River to divert water for irrigation to Bryce Valley (Bradford et al., 2000). This import is the only major diversion into the Colorado River via the Paria River, and amounts to about 6,000,000 cubic meters per year. The water budget summary from 1961 to 1990 shows that imports and returns less depletions decrease the total outflow to 1,234,000 cubic meters per year (Tab. 2).

Table 2. Summary of Paria River Water Budget ($m^3/year$), 1961-1990. (From Bradford et al., 2000)

Yield	25,000,000
Agricultural Depletion	4,317,000
Municipal and Industrial Depletion	370,000
Wet/Open Water Depletion	2,467,000
Imports	5,920,000
Outflow	24,670,000

Fractal Geometry

General Background

Attempts at streamflow reconstruction have utilized the tools and techniques available to the investigators during their respective times. As advances in technology improved the tools available for analyses, new techniques were developed that beforehand would have been impractical or impossible. For example, calculators and computers quickly replaced the slide rule for mathematical calculations while improving the speed, accuracy, and complexity of calculations. Subsequent to the emergence of personal computers was the relative ease of writing programs to perform more complex functions for data handling and analysis. This progression of thought and technology has led to some recent concepts of data modeling. One example is the use of fractals (Tarboton et al., 1988; Rosso et al., 1991; Garcia-Ruiz and Otálora, 1992). Fractals have been used extensively for describing natural phenomena (Mandelbrot, 1977; 1983), and rivers and river basins were one of the first natural phenomena to be examined using fractals (Takayasu, 1993).

'Fractal dimension' is not a new concept (Mandelbrot, 1977). For approximately 2300 years, mathematicians, scientists, and engineers have been indoctrinated in

Euclidean geometry. This standard geometry provides a way of looking at objects in space with a concept of dimensions: a point has no dimension, a line has one dimension, a plane has two dimensions, and a solid object has three dimensions. These integer dimensions ultimately lead to easily handled equations to solve engineering and technological problems. Problems arose when scientists began to realize that nature did not generally fit into nice lines, planes, and solids of Euclidean geometry. For example, clouds are not perfect spheres, mountains are not cones, and rivers are not straight lines.

During the late 1800s, mathematicians became embroiled over the concept of a non-differentiable curve as a direct result of not being able to fit some of their observations into Euclidean space. In 1918, Hausdorff first postulated the concept of a new 'dimension'. The Hausdorff 'dimension' is really a topological space in which a feature can be described with dimensions that are not integers. This concept was relatively dormant (really confined to a few forward thinking mathematicians) until Benoit Mandelbrot coined the term 'fractal' (Mandelbrot, 1977) and put the concept into common usage. In his early work, Mandelbrot worked on the time series of fluctuating cotton prices over time in developing his concept of fractals (Mandelbrot,

1977). A fractal can be defined as 'a set for which the Hausdorff dimension strictly exceeds the topological dimension' (Mandelbrot, 1967; 1977; 1983). Simply put, a line has a Euclidean (topological) dimension of 1, and a plane has a Euclidean dimension of 2. The fractal concept allows a feature to partially fill the space of a plane, more than just a line, with a resulting dimension between 1 and 2. This is now commonly called a fractal dimension. For example, a fractal dimension might have the value of 1.26, or 1.78 depending on the complexity of the feature. This approach provides a mechanism to describe irregular shapes and surfaces in nature (Gleick, 1987).

Since the mid 1970s, numerous investigators have applied the concepts of fractals to a number of disciplines. For example, Rodriguez-Iturbe and Rinaldo (1997) described rivers and river basins using fractals; Turcotte (1992; 1994) has used fractals in geological and fluvial applications. He found that fractals can improve the description of extreme flood events. Kulatilake et al. (1998) have applied fractals to geologic engineering in the assessment of fracture sets for mining purposes.

Fractals and River Basins

There has been a substantial amount of work done in the natural sciences within a fractal framework, but the investigators did not refer to their respective studies as fractal. These early works involved empirical investigations into many facets of fluvial hydrology and geomorphology. The concept of fractals is a power law relationship among variables (Turcotte, 1994).

An example of a scientific investigation that was not termed fractal at the time, but which actually defines a fractal relationship, is the work done by Hack (1957). Hack's Law describing the relationship between the area and length of drainage basins is:

$$L = 1.4 A^{0.6}$$

with L = length of the basin measured along the main channel to the divide, and A = area in square miles. The fractional exponent in Hack's Law is by definition a fractal dimension. The area / length relationship is a 2 dimensional representation of a 3 dimensional surface.

More recent investigations include work done by Pelletier and Turcotte (1999) and by Rodríguez-Iturbe and Rinaldo (1997). Pelletier and Turcotte (1999) demonstrate the fractal relationship of river discharge and tree-ring indices using the spectral analysis approach. While these

authors effectively describe the fractal relationships, the study is still one of descriptive analysis. Rodríguez-Iturbe and Rinaldo (1997) provide an in-depth discussion of the fractal analysis of river basins. Their discussion regarding irregular shapes is also one of description.

Kusumayudha et al. (2000) completed a study in Indonesia relating the fractal properties of the Oyo River, cave systems, and the topography of the area. This study did show the relationship among the variables being studied, but the research was still a basic fractal description of the features.

In summary, recent studies describe natural features using fractals. The next logical step is to apply fractals in a process based approach for predictive purposes.

Hurst's Exponent and the Fractal Dimension

In 1957, H.E. Hurst reported Nile River research results in an attempt to estimate the long-term storage capacity of Lake Nasser, the reservoir behind the Aswan Dam, for sustainable flow for irrigation and water supplies (Hurst et al., 1946; Hurst, 1957; Hurst et al., 1965). This work was facilitated by the long records of flow for the Nile River. Over several years, Hurst examined the discharge record, and

devised a relationship between the storage (R), which is the range of the maximum and minimum of the accumulated residuals from the mean flow, and the standard deviation (r) of the annual flow:

$$R/r = (N/2)^H$$

where N is the number of observations, and H is the measure of persistence over the entire span of record. Hurst referred to this relationship as the 'rescaled range' of the discharge record. Note that Hurst originally used 'K' to represent the storage exponent, but common practice has replaced the 'K' with 'H'. This work is one of the first long range and in-depth studies using time series to examine persistence in streamflow. Previous time series work concentrated on economics, for example, the fluctuation of cotton prices over time. In time series parlance, the long-term storage exponent (H) that Hurst defined for the Nile River is called persistence, that he referred to as 'deviation from randomness'.

During Hurst's endeavors with the Nile River, he also examined other long chronologies to compare the results of his technique to other arenas. Some of his early investigations included collaborations with A.E. Douglass to examine tree-ring indices and with Baron DeGeer to study varves (Hurst et al., 1965). For the time series that he

examined, the H values ranged from 0.52 to 0.94, with tree rings averaging 0.79. As the H value approaches 1.0, the persistence increases. An H value of 0.5 would represent no persistence. Hurst's H value is related to the fractal dimension (Df) by :

$$H = 2 - Df \quad (\text{Malinverno, 1990}),$$

$$\text{and } Df = 2 - H$$

for a two dimensional base, with Df = the fractal dimension, and H = the Hurst exponent, both describing the long-term persistence. The fractal dimension describes the strength of the persistence of the entire time series on a scale from 1 to 2, as opposed to relatively short-term persistence (first, second, or third order autocorrelation, for example) generally encountered in the analyses of tree rings (Malamud and Turcotte, 1999).

Self-Similar Versus Self-Affine Fractals

Fractals can be divided into two main groups: 1) self-similar and 2) self affine (Mandelbrot, 1977; Kulatilake et al., 1998). A self-similar fractal is a geometric feature that retains the same shape with isotropic magnification (Fig. 4). The self-similar fractals retain the same geometric ratios across different scales.

Self-similar fractals are the more familiar type, and have been published in various media. Koch curves, Peano curves, Cantor dusts, and Sierpinski figures are examples.

Self-affine fractals are scaled differently in different directions by anisotropic magnification. Consequently, as scale changes, the shapes appear to become distorted and irregular (Fig. 5). Self-affine fractals are generally encountered in nature. For example, the shapes of clouds, mountains, or the pattern of a river are self-affine fractals (Rodriguez-Iturbe and Rinaldo, 1997). Time series fall into the category of self-affinity (Fig. 6) (Malamud and Turcotte, 1999). For each increment in the horizontal direction (yearly increment), the increment in the vertical direction is multiplied by a scaling factor not equal to the yearly increment. For the length of the time series, the scaling factor is the fractal dimension of that series.

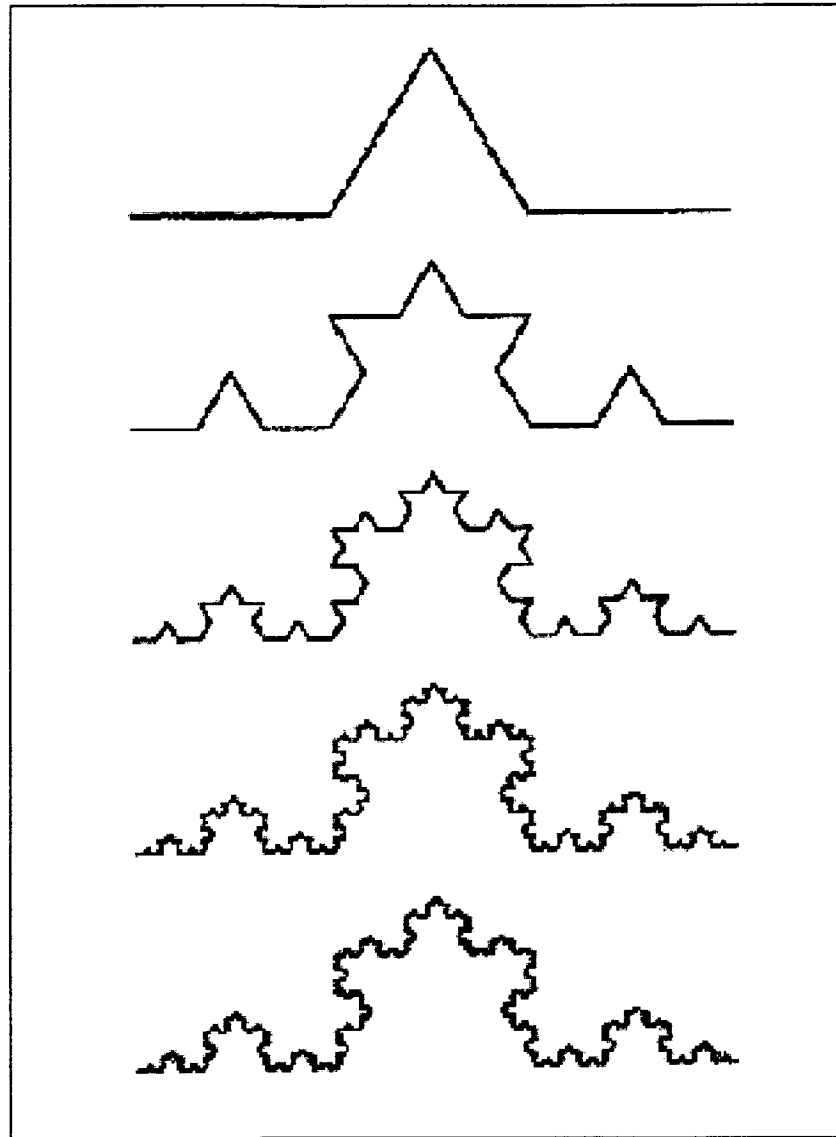


Figure 4. An example of fractal self-similarity. In the sequence of features, each subsequent feature is composed of a geometric shape with the same proportions as the topmost feature. This is referred to as isotropic magnification.

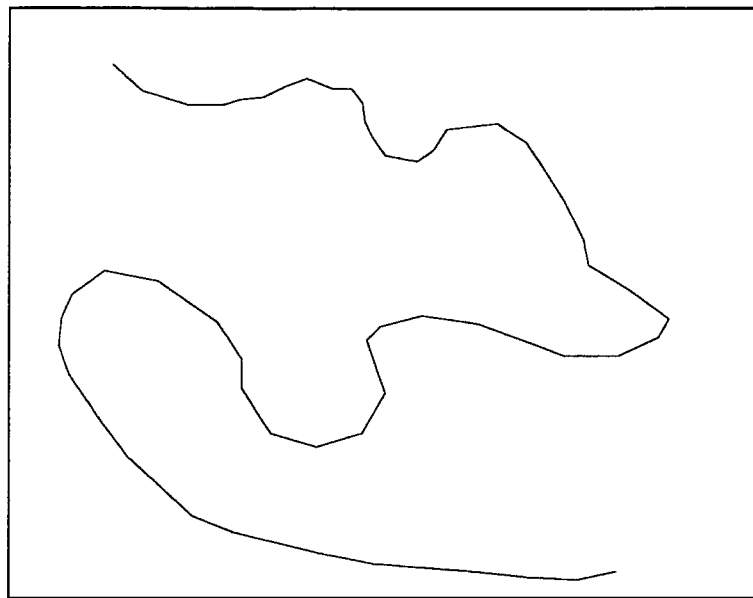


Figure 5. An example of fractal self-affinity. The feature does not have any regular, self-repeating shape. The feature is apparently random, and can be described as fractal Brownian motion (Mandelbrot, 1983).

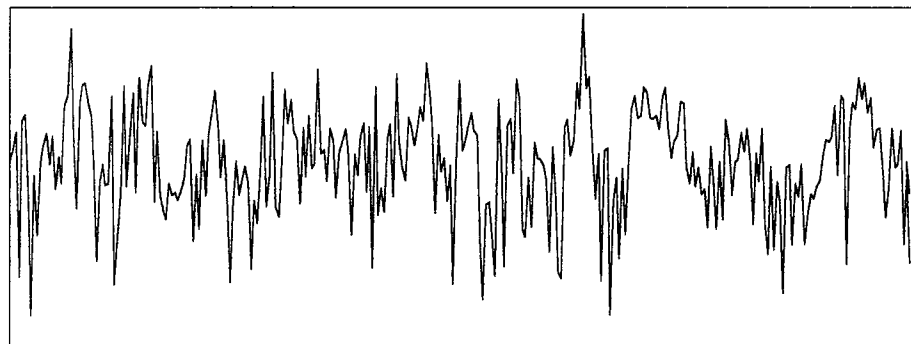


Figure 6. A time series example of fractal self-affinity. This feature exhibits anisotropic magnification. Scaling in the horizontal direction is not equal to intervals in the vertical direction.

In addition to the self-similar and self-affine groups, fractals can also be described as being either deterministic or statistically self-similar or statistically self-affine. Deterministic self-similarity is the previously described feature regarding self-similarity, a feature simply being a magnification of itself. Statistical self-similarity is not as rigid regarding the shapes of the features. Instead, an object is said to be statistically self-similar if the probability distribution of its occurrence is consistent through space or time (Rodriguez-Iturbe and Rinaldo, 1997; Kulatilake et al., 1998)

Important in the fractal dimension calculation of a feature is determining whether the feature is self-similar or self-affine. The techniques for determining the fractal dimension are specific to the type of fractal. For example, techniques for determining the fractal dimension of self-similar fractals can be inappropriate for determining the fractal dimension of self-affine fractals (Kulatilake et al., 1998). Self-similar techniques include the divider method, box method, and the perimeter-area method. Self-affine techniques include the rescaled range method, the roughness-length method, the variogram method, and the power spectral density method (Malinverno, 1990; Kulatilake and Um, 1999; Malamud and Turcotte, 1999).

Roughness-Length Method Used in This Study

A time series is a type of self-affine fractal, and the roughness-length method is a technique to determine the fractal dimension of self-affine fractals (Malinverno, 1990; Kulatilake and Um, 1999). The usefulness of the roughness-length method is its simplicity and accuracy. It can also be used when the intervals between measurements are not uniform. This feature might not be meaningful to tree-ring studies when there is annual resolution, but this feature could be useful if data are missing for particular years.

Earlier studies in the field of fractals used techniques like the 'box counting' or 'divider' methods to describe self-affine fractals. These methods work for self-similar fractals, and will only work effectively for self-affine fractals if the box size or divider length approaches the crossover length, the length at which the horizontal and vertical ranges of the series are equal (Malinverno, 1990). Because of the very small size of the crossover length, it is rarely attained with box or divider methods. Consequently, much of the early work defining the fractal dimension of self-affine fractals using self-similar techniques was inaccurate. Subsequent methods developed specifically to handle the anisotropic scale issues inherent

in self-affine fractals have been developed. These techniques include the spectral, rescaled range, variogram, and the roughness-length methods. The roughness-length method has been shown to be as accurate as the spectral method to describe self-affinity, although the spectral method is more widely used (Malinverno, 1990). Because of the relative simplicity and accuracy, the roughness-length method will be used in this study; a complete description is described later.

Autocorrelation and Self-Affine Fractals

Autocorrelation is a measure of the self-similarity or persistence of a single time series (Davis, 1986). A sequence is compared to itself at successive positions (lags) and the degree of similarity between corresponding intervals is determined. Typically, in tree-ring studies, the number of lags does not exceed 20% of the length of the series (Fritts, 1976). Lags of 20 years are commonly used to describe this 'short-term' persistence in dendrochronological studies. The short-term persistence encompasses climatic factor lags, such as precipitation and drought, that affect tree growth.

Autoregressive-moving average (ARMA) modeling is used to examine the persistence in a time series up to a specified

number of lags, commonly from 1 to 20 (Cook et al., 1990; Box and Jenkins, 1976; Fritts, 1976). In contrast to short-term persistence, self-affine fractals describe the overall, or long-term persistence, of the entire length of a time series (Mandelbrot, 1983).

The scientific community has long investigated rivers and tree-rings. During these investigations, new analytical tools and approaches have been developed and discovered. New mathematical concepts describing natural features have been introduced (e.g. fractals). While some facets of dendrochronology are continually being investigated (e.g. climate), other aspects have been neglected (e.g. substrate). The research presented herein will provide insight into the relationship between tree-rings, substrate, and streamflow, and present the application of fractals to dendrochronological studies.

CHAPTER 2. METHODS

Field

Species Selection

Piñon was the species selected to compare the effects of substrate on streamflow reconstruction. Piñon grows abundantly throughout the Paria River basin on at least three different substrates. Six tree-ring chronologies were developed for this analysis (Fig. 2; Appendix A).

Sampling Site Criteria

To compare the response related to differing substrates, other variables should remain constant while the substrate changes. By controlling the species and elevation, the effects of substrate will be addressed. Other variables also play a role in tree growth; temperature, actual precipitation at the site, evapotranspiration, nutrient supply, insect infestations, and disease are examples. During sampling, trees with physical evidence of lightning strikes, disease, fire damage, or insect infestations were avoided. Assessment of variables other than substrate is beyond the scope of this study.

Piñon trees grow on sandstone in the southern portion of the basin, on alluvial fan and deltaic deposits in the upper basin, and on shale in the central basin. The sites (SK1,

SK2, DSM, RVD, CB, and HCL) are all between 1,800 and 2,200 meters in elevation. Sites DSM and RVD were sampled in May 2000. Sites HCL and CB were sampled in May 2001. Sites SK1 and SK2 were sampled in July 2001.

Laboratory

Sample Preparation and Chronology Development

Samples were prepared and mounted according to procedures described by Stokes and Smiley (1996). Cores were crossdated using skeleton plots, and crossdating was verified by Laboratory of Tree-Ring Research personnel. Ring widths were then measured to within +/- 0.01 mm. Approximately 10% of the samples were independently remeasured for verification. To provide consistency and to maximize sample depth across all of the sites, the chronologies were truncated from 1700 to 1998. After truncating the chronologies before 1700, 61% of the chronologies spanned the entire period from 1700 to 1998. The shortest series is 50 years in length, and the remaining series are at least 150 years in length.

Data Analysis

Chronology Assessment

Crossdating of the tree-ring series was checked using COFECHA (Holmes et al., 1986). COFECHA is a computer program used to identify possible dating errors based on tree-ring measurements. After crossdating was checked, growth trend was removed, and standard and residual chronologies were developed using ARSTAN (Holmes et al., 1986). ARSTAN (autoregressive standardization) is a computer program that removes growth trend from a series of tree-ring measurements to create a chronology. A cubic spline with a 50% frequency response at half the series length was used to remove growth trend from all core measurements.

A standard chronology was created by removing differential growth trend among trees. Removal of the growth trend was necessary to create a stationary time series, one that maintains constant mean, variance, and autocorrelation through time (Cook et al., 1990; Fritts, 1976; Box and Jenkins, 1976). Growth trend was removed by fitting a curve to tree-ring widths, and then dividing the actual ring width by the expected value of the fitted curve (Fig. 7). A residual chronology was created similarly, but with persistence modeled and removed via ARMA modeling.

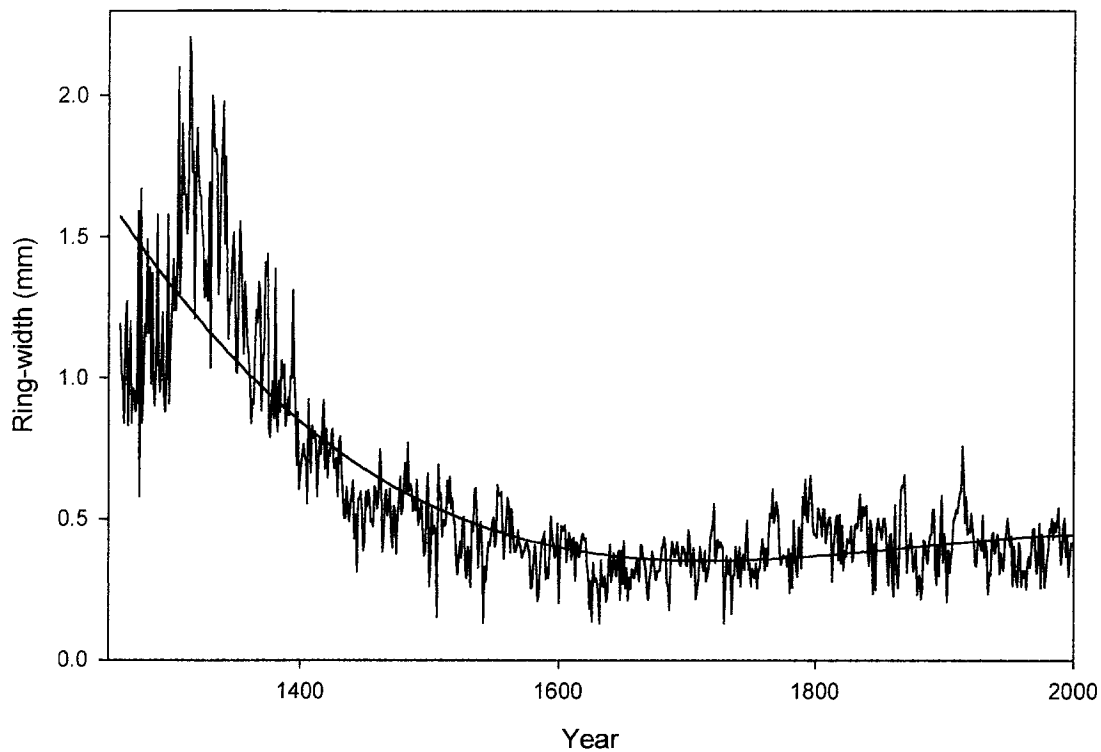


Figure 7. Removing growth-trend from tree-ring measurements.
The example above uses a cubic smoothing spline to
detrend the ring-width measurements.

Chronology confidence was assessed by examining the mean sensitivity (MS), Expressed Population Signal (EPS), the signal-to-noise ratio (SNR) (Wigley et al., 1984; Briffa and Jones, 1990), and cross-correlations between sites. Mean sensitivity measures the relative difference between adjacent ring widths (Fritts, 1976). The EPS compares the actual chronology with an infinitely large, perfect chronology. The signal-to-noise ratio is an indicator of the strength of the common signal of a set of tree-ring series (Wigley et al., 1984). Mean sensitivity of a series is calculated by taking the absolute value of:

$$MS = (1/n-1) \sum [2(x_{t+1} - x_t) / (x_{t+1} + x_t)]$$

where n = the number of rings in the series, and x_t = the ring-width at time t.

The EPS statistic is calculated by:

$$EPS = Nr / [1 + ((N-1) \times r)]$$

where r is the mean interseries correlation and N is the number of series averaged. Mean interseries correlation is the average of correlations among the series.

The signal-to-noise ratio is determined by:

$$\text{SNR} = N(\%Y) / [100 - \%Y]$$

where N = the number of chronologies, and $\%Y$ = the percent common variance among the chronologies.

The EPS value ranges from 0 to 1, and is a better descriptor of the chronology signal than mean sensitivity (MS) or the signal to noise ratio (SNR) because the upper limits of MS and SNR are unbounded, and EPS is easier to interpret; as the EPS value approaches 1, the chronology signal is stronger. Persistence in the tree-ring and hydrologic series was examined using the autocorrelation function.

Fractal Analysis: Roughness-Length Method

To compare the Hurst exponent (H), the fractal dimension (D_f), and the y-intercept (A) between the tree-ring and the hydrologic series, the annual and partitioned hydrologic series were converted to z-scores (subtract the mean and divide by the standard deviation for each value) to create a dimensionless series comparable to the tree-ring chronologies. The Hurst exponent, fractal dimension, and the y-intercept were determined for each tree-ring site and for

the discharge record for the calibration period (1924-1997) and for each tree-ring chronology (1700-1998). Initial observation of the fractal dimension (D_f) and Hurst exponent (H) revealed that for all tree-ring sites, except site DSM, the site fractal dimensions and the Hurst exponents of the tree-ring series exceeded those of the hydrologic series for the same time interval.

The fractal dimension of a series was determined by calculating a sequence of root-mean-square (RMS) values for various window lengths (ω) using the following relationship (Malinverno ,1990):

$$\text{RMS } (\omega) = 1/n_w \sum [1/m_i - 2 \sum (z_j - z)^2]^{1/2}$$

where n_w = number of windows of length ω , m_i = the number of points in the window, z_j = are the residuals from the local trend, and z = mean residual in the i th window. Malinverno suggested using window lengths up to 20% of the series length, down to a minimum window with 10 data points. Kulatilake and Um (1999) found that using window lengths between 2.5% and 10% of the series length provide accurate determinations of the fractal dimension. This study followed the recommendations of Kulatilake and Um (1999).

After the RMS for each window length was determined, a log-log plot of window length and RMS was created by plotting:

$$\log \sigma(\omega) \text{ versus } \log (\omega)$$

where $\log \sigma(\omega)$ is the average standard deviation determined for a window length (ω). The resulting linear relationship:

$$\log \sigma(\omega) = \log A + H \log (\omega)$$

is then used to determine the constant (A) and the Hurst exponent (H). The slope of the best fit line is the Hurst exponent; the fractal dimension is then determined by subtracting the Hurst exponent from 2: $D_f = 2 - H$ (Tab. 3; Fig. 8).

Table 3. Determination of fractal parameters for site DSM for the common period 1924-1998: Hurst exponent (H), y-intercept (A), and the fractal dimension (D_f).

<u>log (ω)</u>	<u>log $\sigma (\omega)$</u>	<u>H</u>	<u>A</u>	<u>Df</u>
0.477121	-0.585303	0.261	0.178	1.739
0.550303	-0.663709			
0.635484	-0.613788			
0.714665	-0.545037			
0.793846	-0.502085			
0.873028	-0.495157			
0.952209	-0.542309			

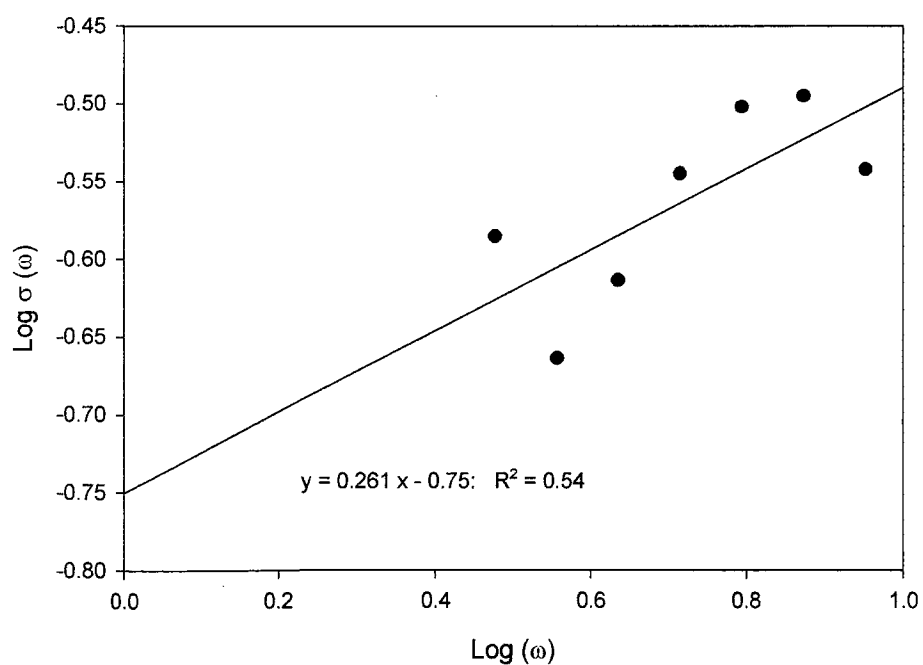


Figure 8. Determining the fractal dimension, y-intercept, and the Hurst exponent for site DSM by plotting $\log (\omega)$ vs. $\log \sigma (\omega)$.

The constant (A) is the y-intercept of the plot and is important in describing the characteristics of the plot; the y-intercept reflects the amplitude of the feature. Determination of the fractal parameters for site DSM and the annual discharge show different y-intercepts and slopes for the data (Fig. 9). The difference in the constant (A) is the difference between the amplitudes of the tree-ring series and the hydrologic series, -0.751 and -0.231, respectively.

The ratio of the amplitudes can be used as a scaling factor to adjust the tree-ring series amplitude to align with the amplitude of the hydrologic series by multiplying the tree-ring indices by the ratio of the amplitudes, but scaling a series by a constant will not affect the regression, and subsequently the reconstruction correlation, between the variables (Bland and Altman, 1986). Because changing the amplitudes will have no effect on the reconstruction correlation, modification of the amplitudes is not necessary. The amplitudes do provide insight into the degree of difference of the variables and are useful when comparing the spread of the data.

The slopes of the lines, 0.198 for the annual discharge and 0.261 for site DSM, are the Hurst exponents and describe the overall persistence in each series. The higher value

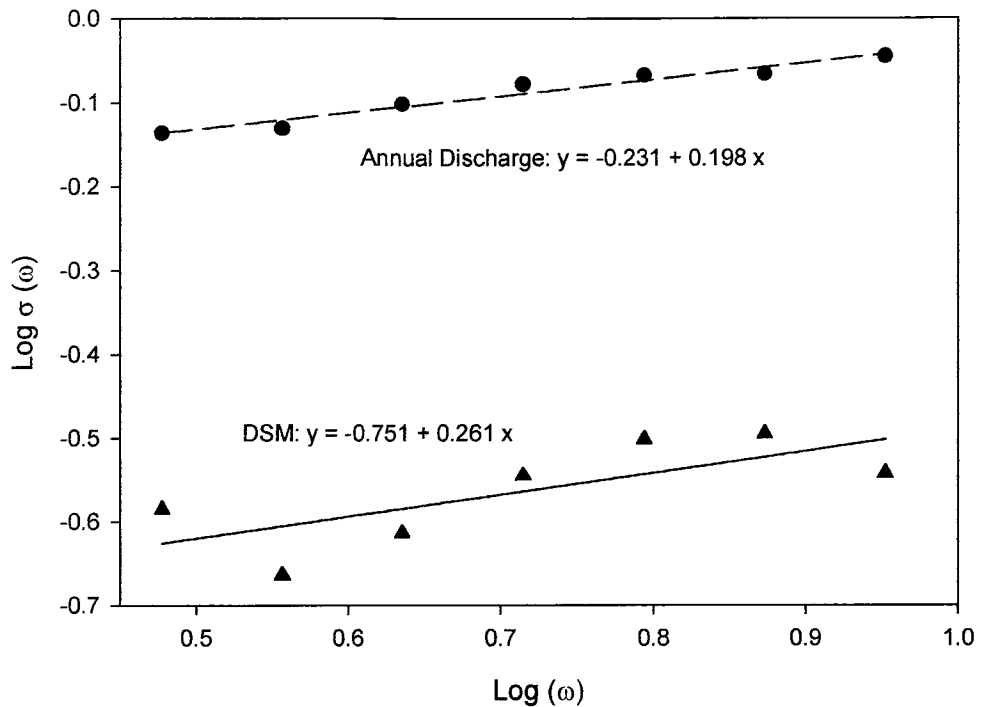


Figure 9. Determination of fractal parameters for mean annual discharge and site DSM tree-ring indices. The slopes of the lines are the Hurst exponents, and the y-intercepts are the amplitudes (A) of each series. For the annual discharge, $R^2 = 0.95$, and for site DSM indices, $R^2 = 0.54$.

for Site DSM (0.261) indicates that the persistence for site DSM is greater than that of the hydrologic series. To align the two series to the same persistence requires that the tree-ring indices be modified to align with the hydrologic series.

Barefoot et al. (1974) used an exponential weighted smoothing technique to detrend tree-ring growth. The smoothing technique is a variation of a weighted moving average. The modified smoothing portion of the equation used is:

$$i = \alpha (i_t) + (1 - \alpha) (i_{t-1})$$

with i = the estimated value for an increment, α = a weighting factor derived from the fractal parameters, i_t = actual value for year t , and i_{t-1} = mean for the period preceding i , which in this case is the value for the preceding year. For example, if an index value is 1.2, the weighting factor (α) is 0.732, $1 - \alpha = 0.268$, the preceding value is 1.1, the estimated value for year t (i) is:

$$i = (0.732)(1.2) + (0.268)(1.1) = 1.17$$

The mean value for a year (i) can be the average for any period preceding the current year. Barefoot et al. (1974) used the entire length of record preceding the current year. As a longer period is used to calculate the average, the smoothing effects become more pronounced. This study uses

the previous year as the average because of the relatively minor smoothing needed to adjust the difference in the Hurst exponents.

The remainder of the Barefoot technique process involves a lag correction factor for removing trend, but inclusion of the detrending factor here is not necessary because the tree-ring indices used in the present study have been detrended. Barefoot et al. (1974) encountered problems determining the weighting factor (α), and through trial-and-error calculated factors ranging from 0.2 to 0.02. Their technique successfully detrended ring-width measurements for climate studies in England. This study uses the ratios of the Hurst exponents as the weighting factors (α) in the above equation to adjust the persistence of the tree-ring series to align with the persistence of the hydrologic series. The ratios are scaling factors between the slopes of the lines (the Hurst exponents) and can be used to adjust the slope of one line to match the other (Cleaveland and Stahle, 1989; Loaiciga et al., 1993).

The fractal parameters are determined for two scenarios: 1) The common period between the tree-ring series and the hydrologic series, and 2) The total length of the chronologies. The first analysis is to compare the relationships of the fractal parameters for purposes of

chronology modification. The second analysis is to compare the chronologies with each other and with substrate.

Water Year Partitions

The total discharge for a year is based on the water year, October 1 through September 30. The water year was partitioned into three sub-periods. Two water year partitions were based on examination of the precipitation distribution for the Paria River basin (Fig. 2). The first partition, from October 1 through March 31 (Winter 1), accounts for approximately 50% of the total annual precipitation. The second partition, from October 1 through May 31 (Winter 2) accounts for approximately 62% of the mean annual precipitation. The third partition, from November 10 to April 17 (Winter 3), is defined by suspended sediment load as reported by Graf et al. (1991). Summer water year partitions were determined by precipitation distribution and by suspended sediment discharge, and are defined as: 1) Summer 1 = April 1 through September 30, 2) Summer 2 = June 1 through September 30, and 3) Summer 3 = July 4 through September 3.

Exploratory analyses were conducted to assess the viability of the different water year partitions and the tree-ring indices with respect to dendrochronologic reconstruction. In essence, the questions are how do precipitation and discharge relate to each other and to the tree-ring indices? Evaluation of these relationships helps develop a basis proceeding with the calibration and verification of reconstructions (Fig. 10). For example, if there is no relationship between mean annual discharge and mean annual precipitation, can a meaningful relationship be expected between discharge and the tree-ring record?

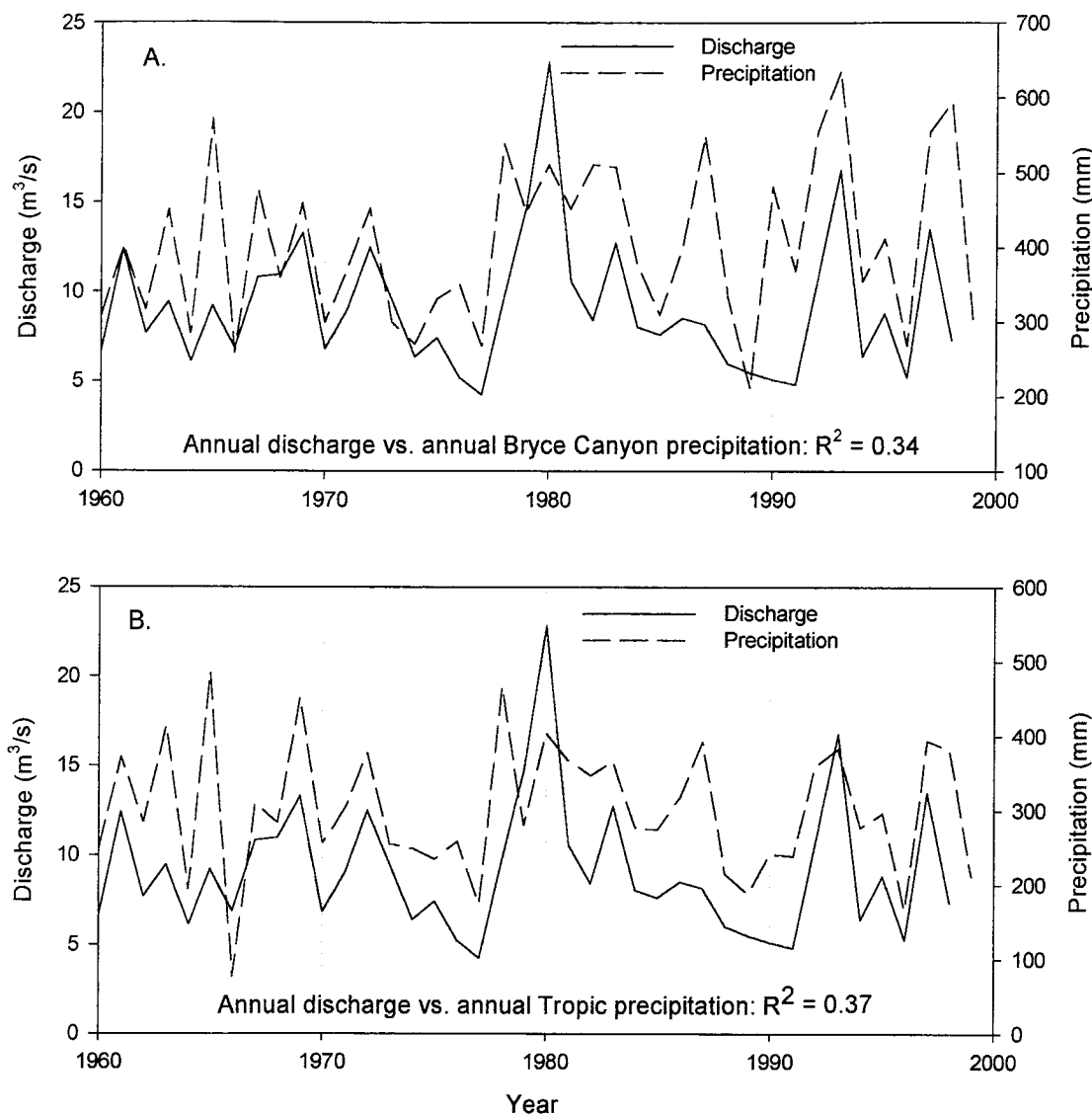


Figure 10. Annual discharge and annual precipitation for two sites in the Paria River basin. Plot A is Bryce Canyon National Park. Plot B is Tropic. Discharge is from the U.S.G.S. gauge at Lee's Ferry. Note the similarity of peaks and troughs for both locations.

Correlation between annual discharge and precipitation is higher for the Tropic station than for Bryce Canyon ($R^2 = 0.37$ vs. $R^2 = 0.34$, respectively) (Fig. 10). The Winter 2 partition (October 1 to May 31), shows a higher correlation with the Bryce Canyon station data than with the Tropic data ($R^2 = 0.47$ vs. $R^2 = 0.43$, respectively) (Fig. 11). These latter values indicate that over 50% of the discharge is unexplained by precipitation. Allowing for storage and evapotranspiration losses, these values are reasonable. Therefore, a meaningful relationship between tree-ring widths and discharge can be expected.

There is minimal to no difference between discharge and the standard and residual indices ($R^2 = 0.06$ vs. $R^2 = 0.07$ for the calibration period, and $R^2 = 0.21$ for the precipitation record) (Fig. 12). The residual indices are created by modeling and removing persistence in the tree-ring series. By removing the persistence, part of the climatic signal recorded as positive or negative lag with respect to the tree-ring signal, is also removed, resulting in lower correlation than with the standard indices. For this analysis, the standard and residual indices of all sites were averaged and plotted for comparison.

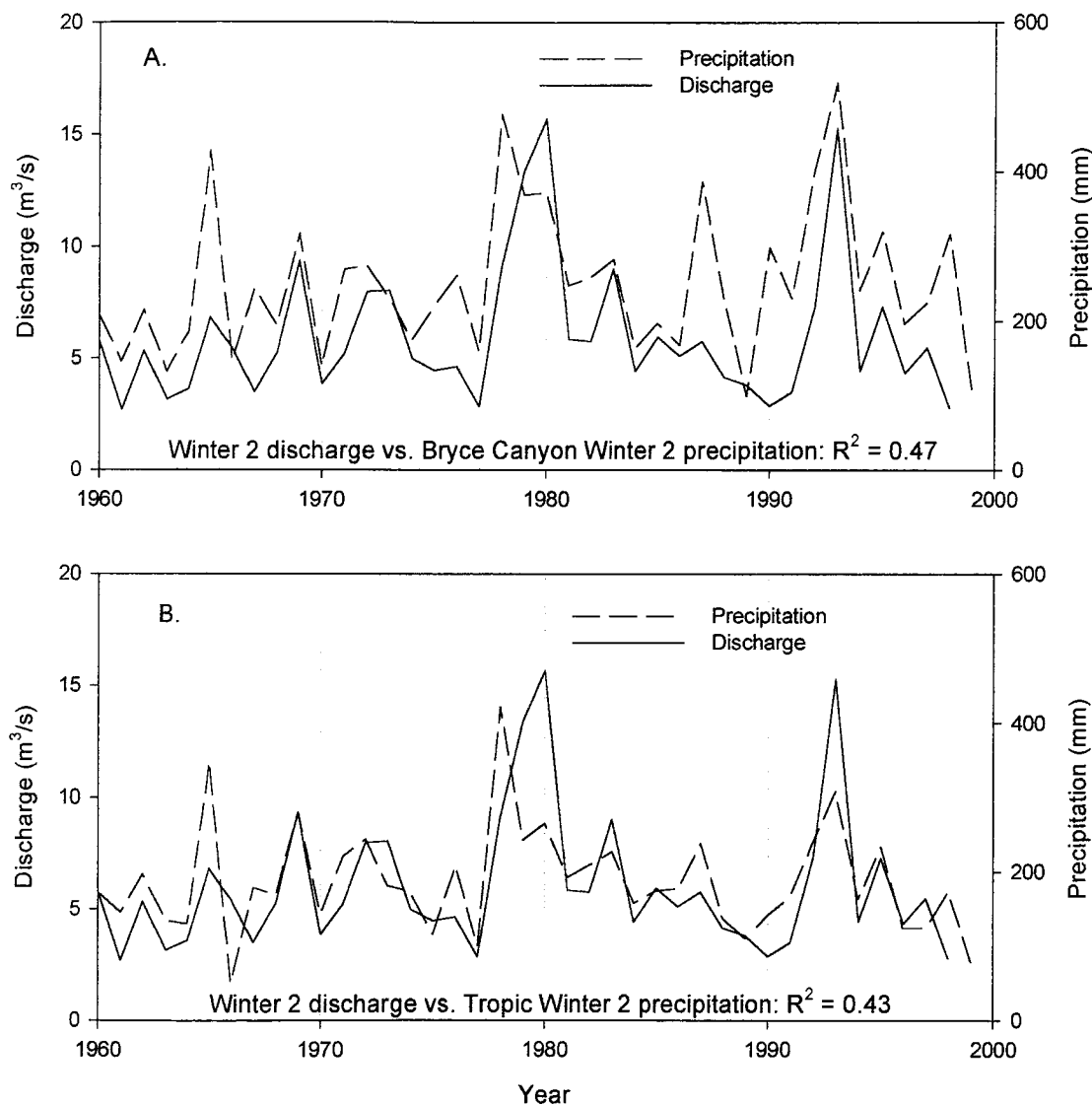


Figure 11. Winter 2 discharge and precipitation at Bryce Canyon (A) and at Tropic (B). The Winter 2 partition is from October 1 to May 31. Precipitation record is from 1960 to 1998.

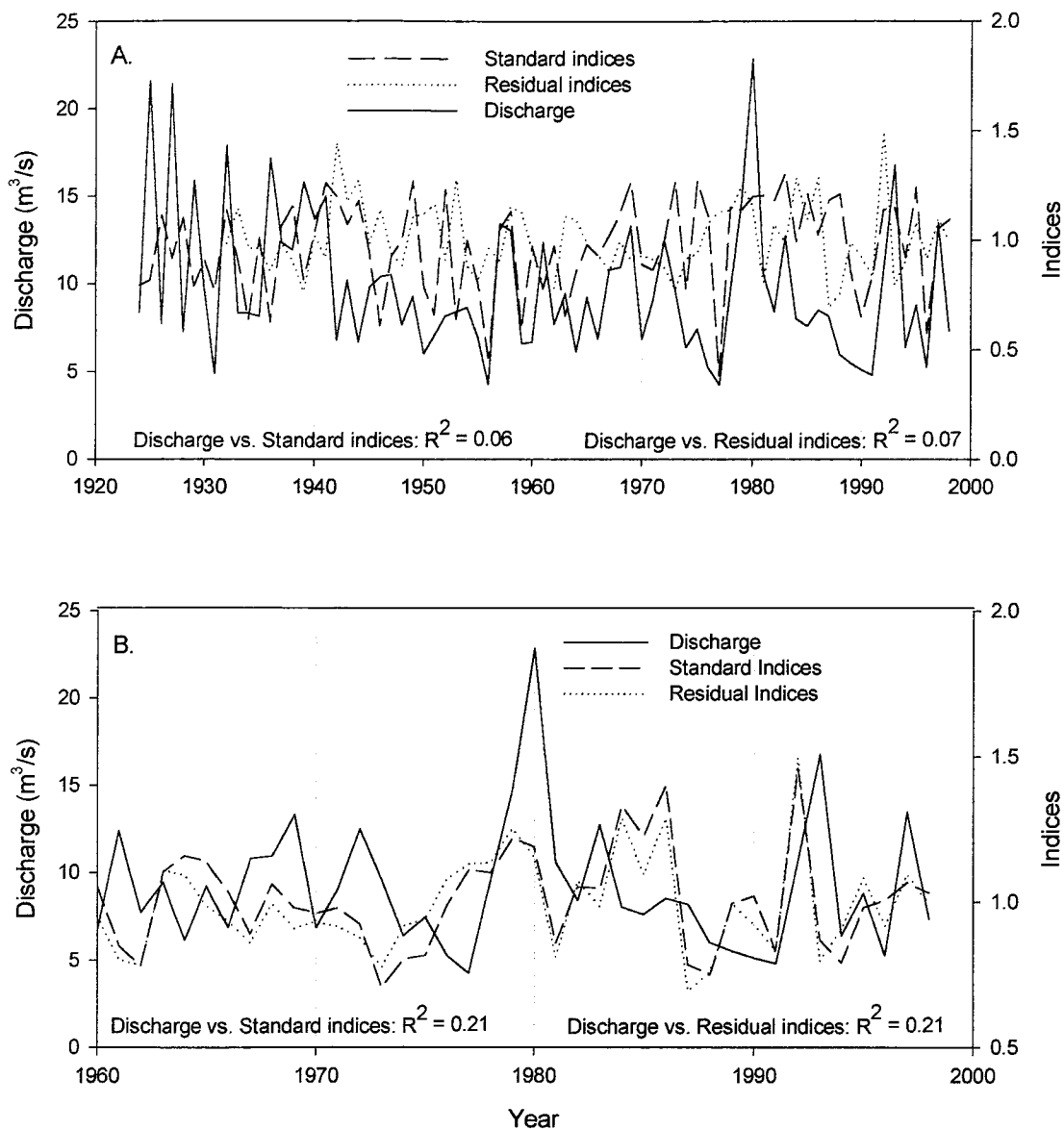


Figure 12. Annual discharge and standard and residual indices. Note that the coefficients of determination are low for both indices (A). When the indices are compared with discharge for the time span of the precipitation record (1960–1998), the R^2 values increase to 0.21 for the standard and residual indices (B). Indices are the mean values of all sites.

Streamflow Reconstructions

Multiple linear regression was used to test each chronology (the predictors) individually, and in concert with each other, to estimate past streamflow (the predictand). The standard and residual indices were used to estimate streamflow. The chronologies were segregated by substrate: CB and HCL are on alluvial fan deposits, DSM and RVD on sandstone, and SK1 and SK2 on shale. The coefficients of determination were adjusted to account for the loss of degrees of freedom due to the addition of predictors (Weisberg, 1985). The validity of each model was determined by examining the estimated model coefficients, the residuals from modeling, the root-mean-square-error (RMSE) of calibration and verification, and the reduction of error (RE) statistic of calibration and verification.

Each model was verified using the PRESS statistic (Weisberg, 1985). The PRESS statistic measures the accuracy of the regression model by the magnitude of the total sum of squares of the predicted residuals ($\sum \hat{e}_{(i)}^2$). The lowest sum of squares of the predicted residuals indicates the most accurate model. The PRESS method estimates the model by first excluding one observation, using the model to estimate the excluded observation, and repeating the procedure for all observations. An advantage of using the PRESS statistic

is that the entire length of the calibration series is used, as opposed to using only part of the calibration series as is done with a split-sample approach.

Predictors were added to the model until the model coefficients were not significantly different from zero at the 0.95 confidence interval. Modeling was then performed again up to the number of predictors at which the coefficients were not significantly different from zero.

The residuals from the modeling process were then examined for randomness, normal distribution, and autocorrelation (Figs. 13-14). The root-mean square error (RMSE) of validation and calibration were examined to assure that minimum RMSE had been achieved. The reduction of error (RE) statistic, a test of the skill of the model, was examined for the most positive value (Fritts, 1976). The reduction of error can range from negative infinity to +1.0. Positive values indicate that the model possesses predictive capability, with values approaching 1.0 indicating a model with more predictive skill (Fritts et al., 1990).

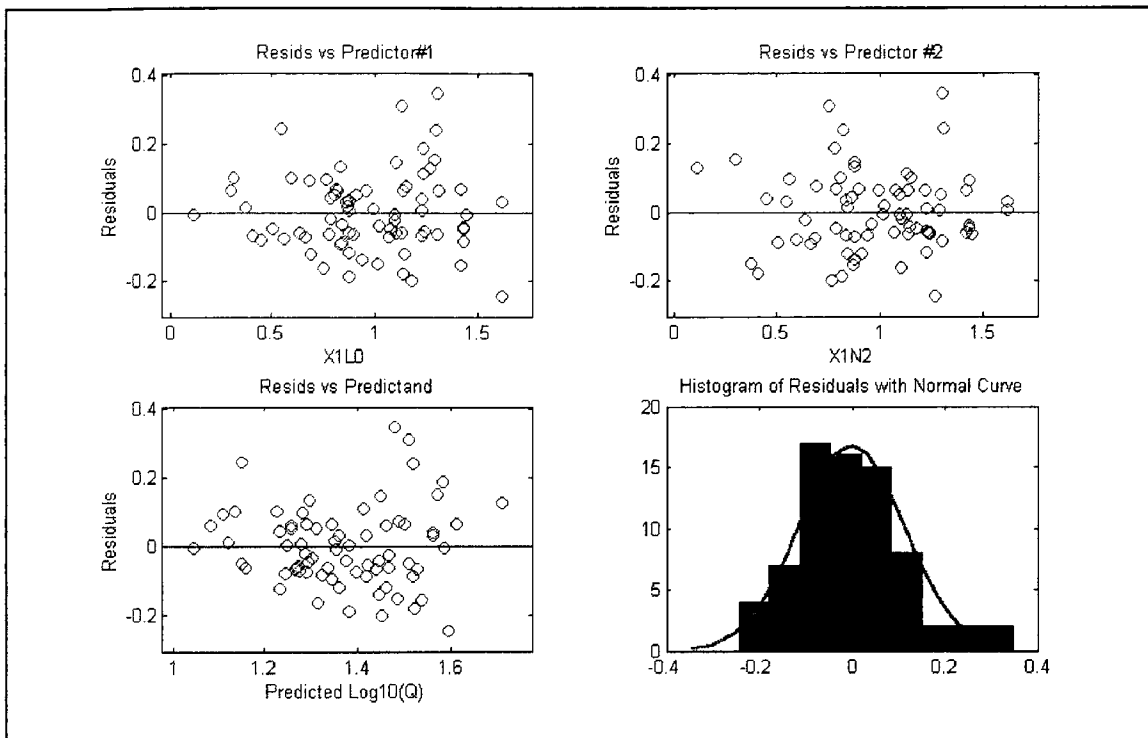


Figure 13. Scatter plots and histogram of the residuals of modeling sites CB and HCL against discharge. In all of the scatter plots, the residuals vs. the predictors and predictand exhibit random distributions. The upper two diagrams show the residuals versus the predictors at lag 0 ($X1LO$) and at negative lag 2 ($X1N2$). The histogram of the residuals is approximately normally distributed.

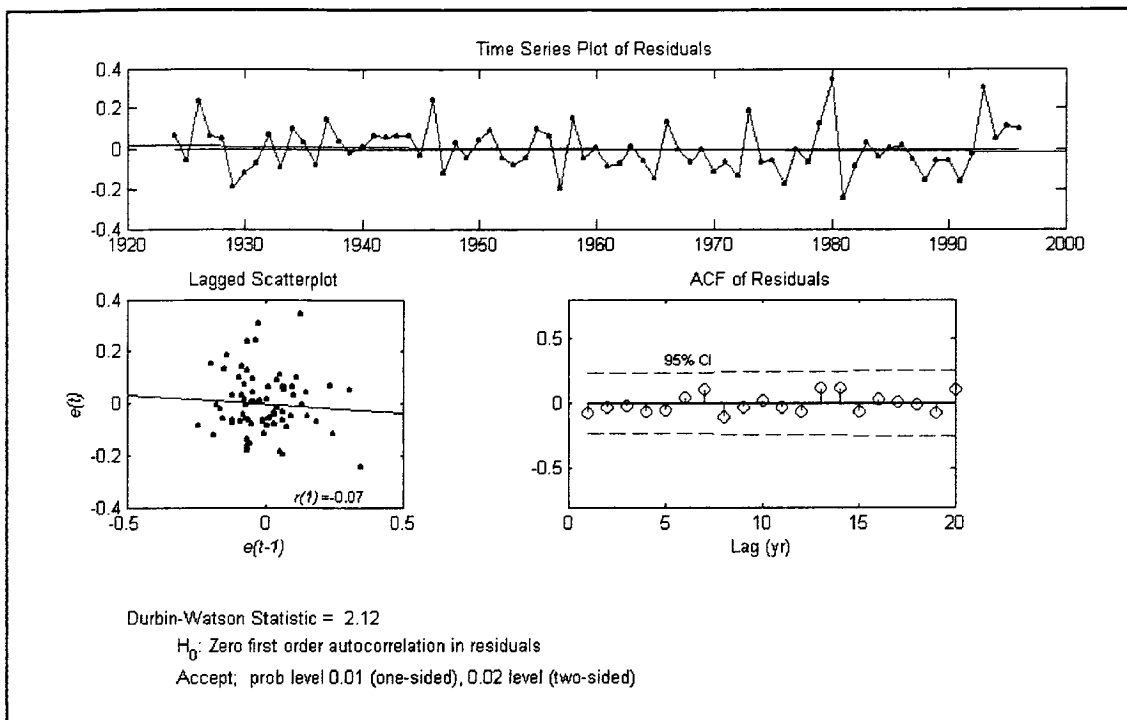


Figure 14. Time series plot, lagged scatter plot, and plot of the autocorrelation function (ACF) of the residuals (e) from sites CB and HCL. The time series plot and the lagged scatter plot do not exhibit persistence, and the ACF shows no autocorrelation at the 95% confidence level. The lagged scatter plot shows the residuals from time $e(t)$ versus the residuals at time $e(t-1)$.

CHAPTER 3. RESULTS

Chronology Assessment

The tree-ring chronology statistics illustrate the quality of the chronologies (Tab. 4). The mean between-tree correlation values range from 0.76 to 0.83. These values indicate a strong relationship between the cores/trees used to develop the chronologies. The expressed population signal (EPS) values (at the minimum sample depths) from 0.91 to 0.96 for the chronologies indicate that the samples used for chronology development closely represent a hypothetical population chronology. The mean sensitivity (MS) values range from 0.31 to 0.45; standard deviations (SD) range from 0.30 to 0.36; the signal-to-noise ratios (SNR) range from 9.9 to 23.8.

Table 4. Summary of chronology statistics for the common period (1700–1998).

Site	Mean Intraseries Correlation	Sample Depth (cores)	MS	SD	SNR	EPS
CB	0.83	10	0.38	0.35	19.96	0.95
HCL	0.82	7	0.42	0.36	12.9	0.93
DSM	0.82	14	0.41	0.36	23.8	0.96
RVD	0.80	11	0.45	0.36	20.0	0.95
SK1	0.79	9	0.31	0.30	10.2	0.91
SK2	0.76	8	0.31	0.31	9.9	0.91

Mean sensitivity (MS) has long been a standard for assessing the quality of a chronology (Fritts, 1976). Mean sensitivity does have a problem in that there is no upper bound for the value (Briffa and Jones, 1990; Strackee and Jansma, 1992). The MS values are related to the variance and first order autocorrelation of a time series. A high MS value can result from a large variance and/or small first order autocorrelation. Therefore, MS values can approach infinity (Strackee and Jansma, 1992). Interpretation of a limitless parameter is ambiguous. The highest MS values in the Paria basin (>0.40) are apparently caused by the greater number of missing rings in those chronologies creating greater variability between rings (Tab. 4). The relatively narrow range of MS in the Paria basin, approximately 0.31 to 0.45, does suggest consistency across the basin for all sites and chronologies. The range of mean sensitivity values encompasses the mean of the mean sensitivity value (0.41) for *Pinus edulis* for western states (Fritts and Shatz, 1975).

Elevated signal-to-noise ratios (SNR) can result from increasing the number of trees used to create a chronology (Briffa and Jones, 1990). The highest signal-to-noise ratios (sites DSM and RVD, Tab. 4) are generally associated with the sites with the most trees used for chronology

development. Exceptions include site HCL with a sample depth of 7 and an SNR of 12.96. There is no consistent trend regarding number of trees and higher SNRs in this basin.

The expressed population signal (EPS) for all sites at minimum sample depths exceeds 0.91 (Tab. 4). The high EPS values indicate that the developed chronologies adequately represent a hypothetical population.

The narrow range of standard deviation values (0.30 to 0.36, Tab. 4) also supports the similarity between sites. The moderately high standard deviations of these sites could result from the arid environment contributing to more locally absent rings.

Cross-correlation

Cross-correlation is a measure of the relationship between multiple time series. Values can range from -1 to +1, with values approaching 1 indicating a strong relationship between the series (Davis, 1986). Cross-correlation values at lag 0 (zero) for this study range from 0.78 to 0.87 (Tab. 5).

Table 5. Between-site chronology correlation matrix.

Site	CB	HCL	DSM	RVD	SK1
HCL	0.87				
DSM	0.81	0.82			
RVD	0.80	0.80	0.85		
SK1	0.82	0.79	0.78	0.81	
SK2	0.78	0.80	0.83	0.79	0.85

The highest correlation values all occur with substrate pairs - CB/HCL, DSM/RVD, and SK1/SK2 (Tab. 5). This grouping seems plausible because a high degree of correlation would be expected in similar environments. More noteworthy are the lowest correlations. The lower values are associated with differing substrates - CB/SK2, and DSM/SK1, alluvial fan/shale and sandstone/shale, respectively.

Autocorrelation Assessment

Autocorrelation was determined for the standardized indices of each chronology and for the hydrologic series. Site CB exceeds the 95% confidence limits up to third order, second order for site SK2, and first order for sites HCL, DSM, and SK1. Site RVD displays no autocorrelation at the 95% confidence level. The autocorrelation coefficients for

the annual and water year partitions all fall within the 95% confidence limits All of the sites except RVD show first order autocorrelation, and sites CB and SK2 display third and second order autocorrelation, respectively (Tab. 6).

Table 6. Summary of autocorrelation coefficients for standardized tree-ring indices and hydrologic series. An (*) indicates that the coefficients exceed the 95% confidence limits.

Autocorrelation Order

Site	1°	2°	3°	4°	5°	6°
CB	0.283*	0.197*	0.248*	0.136	0.028	0.045
HCL	0.245*	0.112	0.126	0.029	0.003	0.048
DSM	0.243*	0.130	0.085	0.030	-0.030	-0.022
RVD	0.099	0.105	0.155	0.043	-0.004	0.108
SK1	0.345*	0.153	0.068	-0.024	0.008	0.032
SK2	0.385*	0.222*	0.109	0.022	0.033	0.034
Discharge						
Annual	0.130	0.030	0.041	-0.009	0.014	-0.002
Winter 1	0.082	-0.139	-0.078	-0.024	-0.067	0.172
Summer 1	0.001	0.257	0.130	0.140	0.076	-0.019
Winter 2	0.102	-0.140	-0.077	0.003	-0.081	0.148
Summer 2	-0.012	0.256	0.176	0.153	0.043	-0.005
Winter 3	0.211	-0.070	0.014	0.065	-0.088	0.025
Summer 3	0.038	0.198	0.038	0.264	-0.031	0.032

The low-order autocorrelation on the sites might reflect the precipitation distribution. Little snow falls on the lower basin elevations. Most of the precipitation falls as spatially and temporally sporadic summer thunderstorms. The

lack of consistent moisture for tree growth can reduce autocorrelation in arid environments (Fritts, 1976).

The annual and partitioned water year of discharge display no autocorrelation. The lack of autocorrelation in a hydrologic series is often presumed (sometimes incorrectly) in hydrologic studies. The presumption might lead to incorrect inferences. Statistically, the lack of autocorrelation in these series is refreshing because the autocorrelation of the hydrologic series does not need to be removed before the reconstruction process.

Streamflow Reconstructions

One-hundred and five permutations of streamflow reconstructions were performed using the standard and residual chronologies of the sites (Tab. 7) (Appendix B). The mean adjusted coefficients of determination (R_a^2) for the standard indices are equal to or higher than the means for the residual indices for all partitions except Winter 3 and Summer 3. The highest adjusted coefficients of determination (R_a^2) show that the Winter 2 partition provides the highest R_a^2 values, with the paired sites CB/HCL providing the highest R_a^2 values for the reconstructions (Fig. 15). The overall mean of the Winter 2

partition ($R_a^2 = 0.46$) reconstruction is greater than the Winter 1 and Winter 3 partitions (both $R_a^2 = 0.40$).

Table 7. Adjusted coefficients of determination (R^2_e) of discharge reconstructions: standard indices (Sx) and residual indices (Rx).

Reconstruction Period

Site	Annual	W1	S1	W2	S2	W3	S3
CB Sx	0.22	0.42	0.04	0.46	0.02	0.40	0.04
HCL Sx	0.24	0.46	0.02	0.54	0.02	0.45	0.04
DSM Sx	0.11	0.35	0.03	0.43	0.06	0.42	0.12
RVD Sx	0.18	0.45	0.03	0.48	0.05	0.39	0.08
SK1 Sx	0.23	0.38	0.05	0.43	0.02	0.43	0.02
SK2 Sx	0.25	0.42	0.04	0.45	0.01	0.45	0.02
CB Rx	0.17	0.42	0.02	0.47	0.02	0.41	0.08
HCL Rx	0.23	0.48	0.01	0.54	0.02	0.44	0.06
DSM Rx	0.12	0.39	0.02	0.45	0.06	0.46	0.14
RVD Rx	0.18	0.45	0.03	0.48	0.02	0.46	0.11
SK1 Rx	0.17	0.37	0.03	0.41	0.02	0.44	0.03
SK2 Rx	0.17	0.37	0.01	0.43	0.01	0.46	0.03
CB/HCL Sx	0.27	0.50	0.04	0.59	0.02	0.47	0.08
DSM/RVD Sx	0.18	0.46	0.04	0.52	0.06	0.46	0.13
SK1/SK2 Sx	0.25	0.42	0.06	0.45	0.02	0.45	0.03
Mean	0.20	0.40	0.05	0.46	0.04	0.40	0.07
Mean Sx	0.21	0.39	0.05	0.44	0.04	0.38	0.06
Mean Rx	0.17	0.39	0.03	0.44	0.04	0.40	0.08
Mean Pairs	0.03	0.45	0.06	0.51	0.06	0.43	0.08

W1 = Winter 1, W2 = Winter 2, W3 = Winter 3, S1 = Summer 1, S2 = Summer 2, and S3 = Summer 3 partitions.

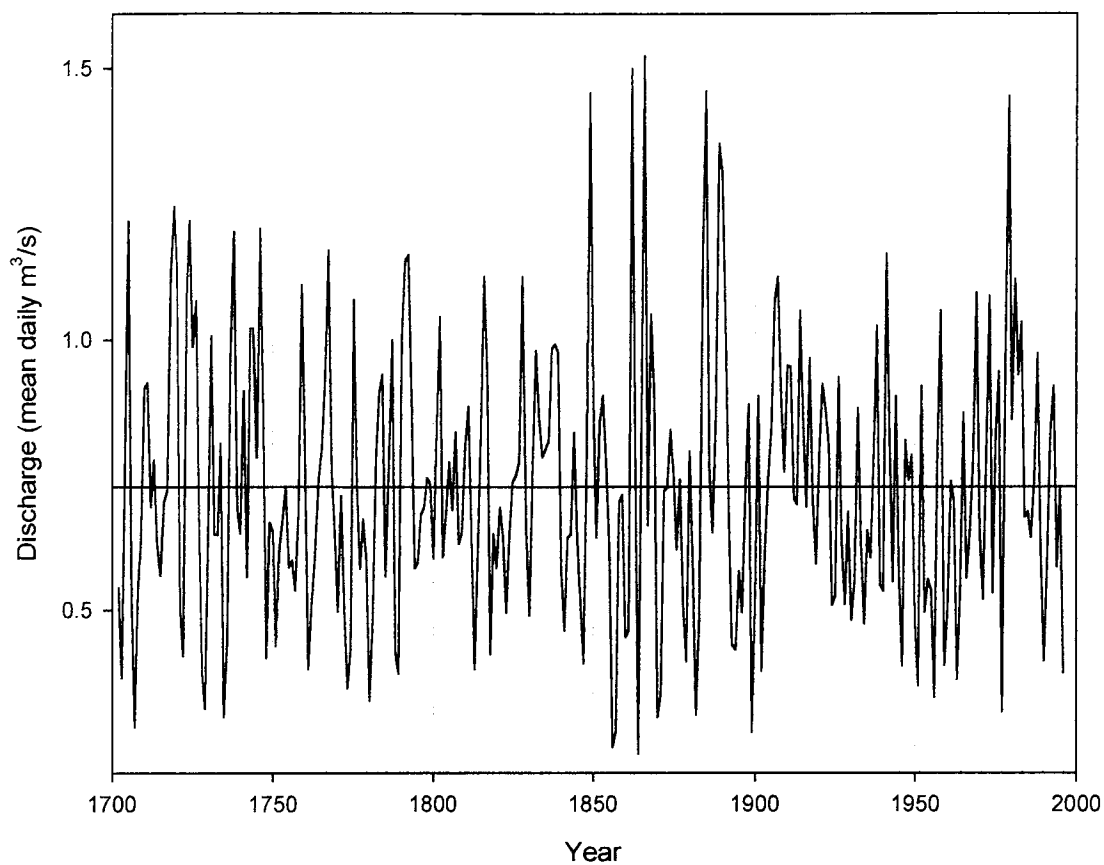


Figure 15. Winter 2 (October 1 to May 31) discharge reconstruction using sites CB (Coal Bench) and HCL (Lower Henderson Canyon). Units are mean daily discharge in cubic meters per second.

The standard index annual reconstructions range from $R_a^2 = 0.11$ for site DSM to 0.25 for site SK2. Combining the pairs of sites by substrate improves the coefficient of determination for sites CB and HCL, $R_a^2 = 0.27$ up from 0.22 and 0.24. Combining sites DSM and RVD did not improve the single site R_a^2 value of 0.18 from site RVD. Sites SK1 and SK2 also did not show improvement over the single site SK2 $R_a^2 = 0.25$.

The winter reconstructions are more promising. The single site reconstruction R_a^2 values range from 0.35 for site DSM for the Winter 1 partition up to 0.54 for site HCL for the Winter 2 partition (Tab. 7). The means of the winter partition R_a^2 values are 0.40 for the Winter 1 and Winter 3 partitions, and 0.45 for the Winter 2 partition. When the substrate pairs are combined to reconstruct streamflow using multiple linear regression, R_a^2 for sites CB/HCL reaches 0.59 for the Winter 2 partition, followed by 0.52 for sites DSM/RVD, and 0.45 for sites SK1/SK2. The Winter 2 partition, accounting for approximately 93% of the annual precipitation, provides the highest reconstruction R_a^2 values.

The mean R_a^2 values for all summer partitions are below 0.07. Ninety-one percent of the summer reconstructions fall below $R_a^2 = 0.10$. From a practical viewpoint, none of the

summer partition reconstructions are reliable; the highest adjusted coefficient of determination (R_a^2), is 0.14 for site DSM and the Summer 3 partition (Tab. 7). The low values indicate that there is little or no correlation between the indices and streamflow for those periods.

Error in stream gauge discharge can range from less than 3% to greater than 10%, depending on characteristics peculiar to each channel (N. Andrews, 2002, U.S.G.S., pers. comm.). The sand bed channels near the gauging station used in this study can cause discharge record errors greater than 10%. The summer reconstruction R_a^2 values fall below potential gauging station error. A reasonable expectation is that the variance explained by reconstruction should exceed the error possible in the instrumental data. Therefore, the reconstruction data needs to exceed the possible error in the gauged record to be meaningful.

Reconstruction Validation

Streamflow reconstructions were validated by examining the reduction of error statistic, standard error of the estimate, root-mean-square-error, and the Durbin-Watson test for first order autocorrelation (Tab. 8). All reduction of error statistics (RE) are greater than zero, indicating that all models exhibit skill in the predictions. Site CB/HCL

displays the highest RE (0.56), and the highest R_a^2 value (0.59). The differences between the standard error of the estimates (SE) and the root mean square errors (RMSEv) are all less than 0.008. The small differences indicate validation within the models.

The Durbin-Watson statistic (DW) is a test for first order autocorrelation (Kendall and Ord, 1990). The null hypothesis (H_0) is that there is no first order autocorrelation of residuals from the reconstruction process. In all cases, the null hypothesis is accepted, indicating that there is no first order autocorrelation in the residuals. Residuals were also visually examined for randomness and normal distribution (Figs 13-14).

Table 8. Reconstruction validation summary for sites CB/HCL. R_a^2 = adjusted coefficient of determination; RE = reduction of error statistic; SE = standard error of the estimate; RMSEv = root mean square error of validation; DW H_0 = Durbin-Watson zero first order autocorrelation in residuals.

Validation Statistics						
Annual	Years	R_a^2	RE	SE	RMSEv	DW H_0
CB/HCL	1702-1997	0.27	0.17	0.1455	0.1531	Accept
Winter 2						
CB/HCL	1702-1997	0.59	0.56	0.1176	0.1200	Accept

Substrate Analysis

Clay content and permeability is highest for sites SK1 and SK2, ranging from 40-50% clay content and 0.15 to 5.0 centimeters per hour permeability (Tab. 1, Fig. 16). Sites DSM and RVD are located on sandstone residuum. Compared to alluvial fan and shale substrates, clay content is low, 5 - 25%, and permeability is high, 5.0 to 15.0 centimeters per hour. Sites CB and HCL are intermediate between the other two sites with clay content from 18-27%, and permeability from 1.5 to 5.0 centimeters per hour.

Substrate appears to play a role in the streamflow reconstructions. The extremes of the infiltration rates of sandstone and shale, 5.08-15.24 cm/hr and 0.15-0.51 cm/hr, respectively, bracket the infiltration rate of 1.52-5.08 cm/hr for the alluvial fan deposits (Tab. 1; Fig. 16).

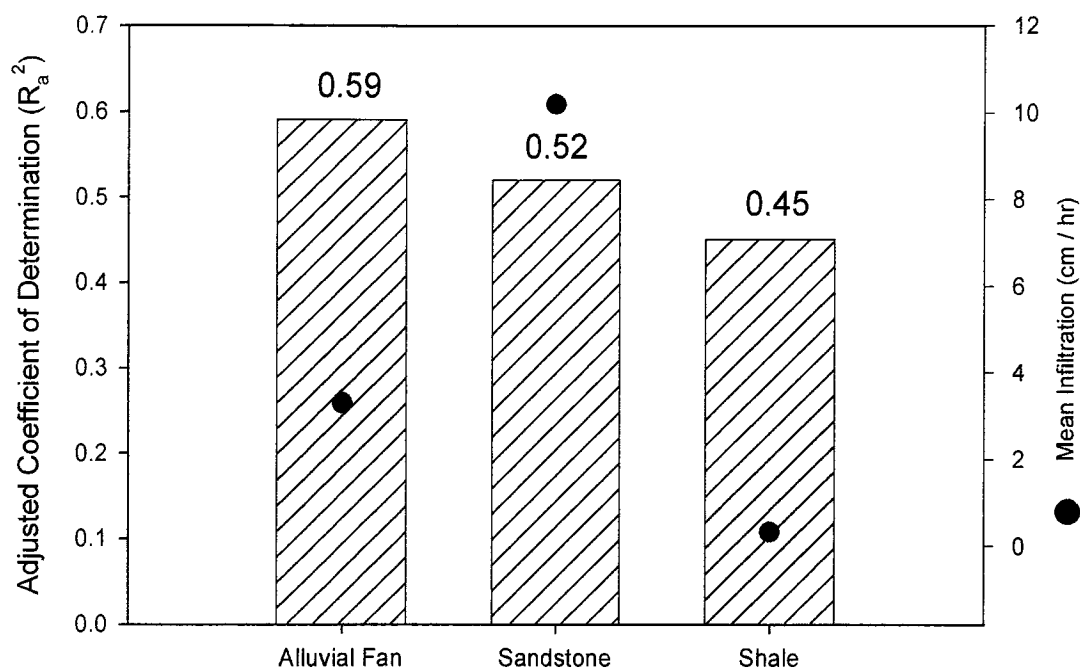


Figure 16. Substrate versus the adjusted coefficient of determination (hatched bars) for the Winter 2 discharge reconstruction with mean infiltration (filled circles).

Statistical Significance of Reconstructions

Sites located on the alluvial fan deposits (CB and HCL) consistently provide the highest coefficient of determination values for all of the winter partition reconstructions (Tab. 7). The highest reconstruction values are from the Winter 2 partition; $R_a^2 = 0.59$ for the alluvial fan deposits (CB and HCL), followed by $R_a^2 = 0.52$ for the sandstone substrate (DSM and RVD), and $R_a^2 = 0.45$ for the shale substrate (SK1 and SK2) (Fig. 16).

A t-test is utilized to evaluate the statistical difference between correlation coefficients of each substrate and the reconstructed discharge series for each combination of substrates: alluvial fan and sandstone, alluvial fan and shale, and sandstone and shale. The correlation coefficient of each reconstruction is transformed to a z-function as described by Sokal and Rohlf (1973):

$$z = \frac{1}{2} \ln (1+r/1-r)$$

Correlation coefficients can be skewed and a t-test assumes a normal distribution. A z-transform is used, therefore, because the z-distribution is normally distributed (Sokal and Rohlf, 1973). The t-test compares

differences in the probability distribution of two variables to determine if they are from the same population.

To measure the difference between the correlation coefficients of two variables, the null hypothesis is that the probability of the occurrence of one value is equal to the probability of the second value: $H_0: p_1 = p_2$, and the alternate hypothesis is $H_a: p_1 \neq p_2$. The t-value is calculated for each pair of correlation coefficients being evaluated, and the value is then compared to t-tables to accept or reject the null hypothesis (Sokal and Rohlf, 1973). The following formula determines the calculated t_s -value:

$$t_s = (z_1 - z_2) / [(1/n_1-3) + (1/n_2-3)]^{1/2}$$

where t_s is the t-value of the samples, z_1 and z_2 are the z-transforms, and n_1 , and n_2 are the number of data points in each sample. In these series, $n = 74$, the number of years in the calibration period. In all combinations of substrates, the calculated t_s -values exceed the table t-values, supporting rejection of the null hypothesis. The differences in correlation coefficients are statistically significant at the 95% confidence level ($\alpha=0.05$) (Tab. 9).

Table 9. Substrate correlation coefficient (r) between tree-rings and discharge series. Table t-values are at the 95% confidence level with 71 degrees of freedom.

Substrate

	Alluvial fan (1)	Sandstone (2)	Shale (3)
r	0.77	0.72	0.67
z	1.02033	0.90764	0.81074
$t_s(1-2)$	0.67141		
$t_s(2-3)$		0.57734	
$t_s(1-3)$			1.24875
t_{Table}	0.43875	0.43624	0.78833

Fractal Analysis

Fractal analysis is a technique to examine the persistence of a time series using the fractal dimension and the Hurst exponent. The fractal analyses were performed on the annual and Winter 2 discharge partitions because the Winter 2 partition provided the highest R_a^2 value, and the annual partition provided a yearlong view of the discharge.

The persistence of a time series can be weak or strong, and can be short- or long-term (Malamud and Turcotte, 1999). For 2-dimensional space, fractal dimensions will range from 0 to 2, with values approaching 2 indicating a greater space

filling capacity, or greater randomness, of that feature (Mandelbrot, 1983). All of the tree-ring fractal dimensions are relatively high (on a scale from 1 to 2), ranging from 1.73 to 1.93 (Tab. 10). For the common period, the lowest fractal dimension of the series is 1.739 for site DSM and the highest is 1.939 for site HCL. Translating the fractal dimensions to the Hurst exponent is straightforward: 2 minus the fractal dimension equals the Hurst exponent. A Hurst exponent of 0.5 (fractal dimension = 1.5) represents a random series. Hurst values greater than 0.5 are positively correlated (as differentiated from uncorrelated) and represent persistence, with higher values indicating greater persistence (Malamud and Turcotte, 1999).

For the calibration period (1924 to 1998), the fractal dimensions of the hydrologic series, 1.802 for the annual series, and 1.819 for the Winter 2 partition, are lower than all tree-ring sites except DSM. For the length of the chronologies, all tree-ring fractal dimensions are also greater than those of the hydrologic series (Tab. 10). The fractal dimension for the chronology lengths are more consistent than for the common period.

In fractal terms, the tree-ring series exhibit greater space-filling capacity than the discharge record. This feature translates into the tree-ring series having more

randomness, or less persistence, than discharge. To equalize the randomness (and persistence) between the tree-ring series and the hydrologic record, a fractal transformation is in order.

Table 10. Fractal dimensions (Df) and Hurst exponents (H) of the tree-ring and hydrologic series.

Site	<u>Calibration period</u>		<u>Chronology length</u>	
	(1924-1998)	(1700-1998)	Df	H
CB	1.855	0.115	1.884	0.116
HCL	1.939	0.061	1.927	0.073
DSM	1.739	0.261	1.908	0.092
RVD	1.909	0.091	1.946	0.054
SK1	1.906	0.095	1.876	0.124
SK2	1.842	0.158	1.862	0.138
Annual Discharge	1.802	0.198		
Oct 1 - May 31 Discharge	1.819	0.181		

Fractal Transformations

The purpose of this fractal transform is to smooth the tree-ring series to attain similar Hurst exponents, and subsequently similar fractal dimensions, as the hydrologic series ($H = 0.198$ for the annual series, and $H = 0.181$ for the Winter 2 partition). The exception is site DSM, where the fractal dimension of the tree-ring record is less than the hydrologic record. In this case, the tree-ring chronology needs to be accentuated to align with the hydrologic record. The weighting factor for site DSM, being greater than 1, performs the accentuation by weighting the current value more than previous values. Fractal transforms following the Barefoot et al. (1974) technique were performed on all tree-ring indices (Tab. 11; Fig. 17). The ' α ' value is the ratio between the Hurst exponent of the hydrologic series and the Hurst exponent of each tree-ring standardized index series.

Table 11. Fractal parameters used to smooth each tree-ring series. The α value is derived from the Hurst exponents of the tree-ring series and the hydrologic series.

Site	H	Annual		Winter 2	
		α	1 - α	α	1 - α
CB	0.145	0.732	0.268	0.801	0.199
HCL	0.061	0.309	0.691	0.337	0.663
DSM	0.261	1.318	0.318	1.442	0.442
RVD	0.091	0.460	0.540	0.503	0.497
SK1	0.095	0.480	0.520	0.525	0.475
SK2	0.158	0.798	0.202	0.873	0.127
Annual Discharge	0.198				
Winter 2 Discharge	0.181				

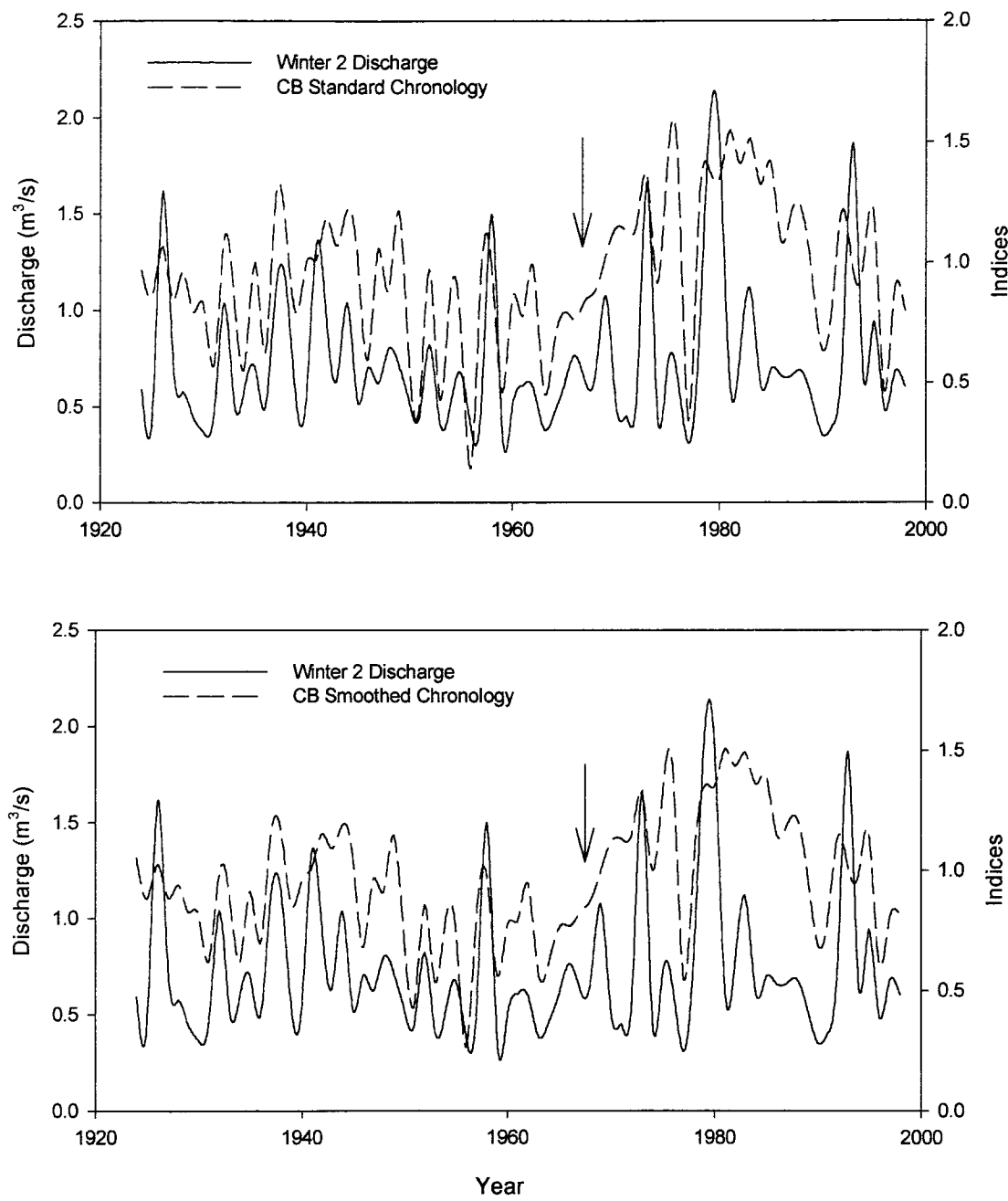


Figure 17. Smoothing results for site CB standard chronology. The upper plot shows the unsmoothed data, and the lower plot shows the smoothed data. The arrows indicate an area where the limited amount of smoothing is visible.

After the tree-ring series were adjusted using the Hurst ratios, the Hurst exponent (H) and fractal dimension (D_f) of each tree-ring series were re-calculated using the same roughness-length technique described previously (Tab. 12).

Table 12. Fractal parameters of the modified tree-ring series.

Site	Annual		Winter 2	
	H	Df	H	Df
CB	0.196	1.804	0.226	1.770
HCL	0.210	1.800	0.222	1.780
DSM	0.379	1.620	0.423	1.580
RVD	0.220	1.780	0.236	1.760
SK1	0.329	1.670	0.322	1.680
SK2	0.238	1.760	0.204	1.800

One-half of the sites display Hurst values that were closer to the desired Hurst value (0.198) than before the smoothing process, while the other half display values more distant.

For the annual calculation, the smoothing process resulted in a very close approximation to the annual Hurst exponent (0.196 vs. 0.198) for site CB. Sites HCL, RVD, and SK2 also showed improvements toward the desired Hurst

exponent of 0.198. Sites DSM and SK1 showed an exaggerated adjustment well beyond the desired Hurst exponent of 0.198.

The Winter 2 calculations show a similar trend in that all sites surpass the desired Hurst exponent of 0.182 as a result of smoothing. Sites CB, HCL, RVD, and SK2 most closely approximate the desired result with Hurst exponents of 0.226, 0.222, 0.236, and 0.204, respectively. The Hurst exponents for sites DSM and SK1 are 0.322 and 0.423, respectively.

The fractal dimensions of the common period analysis (1924 to 1998) and the length of the chronologies used in this study (1700 to 1998). The fractal dimension for the chronology lengths are more consistent than for the common period (Tab. 8).

Fractal Transform Reconstructions

After each tree-ring series was modified with the fractal-based smoothing technique, multiple linear regression was again used to estimate streamflow (Tabs. 13-14; Appendix C). The fractal modification of the tree-ring series improved R_a^2 in most cases for the annual series, and decreased R_a^2 values for sites HCL, DSM-RVD, and SK1-SK2. For the Winter 2 reconstructions, only 2 sites, CB and DSM, show improvement, sites HCL and RVD show a

decrease, and sites SK1 and SK2 display no change. The paired sites CB-HCL and DSM-RVD show a decrease, and sites SK1-SK2 show no change (Tab. 15).

Table 13. Annual streamflow reconstruction and validation statistics of fractally modified tree-ring chronologies. The coefficient of determination is adjusted for addition of predictors (R_a^2). The number in parentheses after the R_a^2 is the number of predictors used in the reconstruction.

Site	R_a^2	SE	RMSEv	RE
CB	0.23 (2)	0.150	0.155	0.150
HCL	0.24 (2)	0.148	0.154	0.160
DSM	0.15 (2)	0.157	0.164	0.060
RVD	0.16 (2)	0.156	0.161	0.080
SK1	0.22 (2)	0.151	0.160	0.090
SK2	0.28 (2)	0.145	0.155	0.150
CB-HCL	0.29 (2)	0.144	0.153	0.170
DSM-RVD	0.16 (2)	0.156	0.161	0.080
SK1-SK2	0.24 (2)	0.148	0.162	0.070

SE = standard error of the estimate; RMSEv = root mean square error of validation; RE = reduction of error statistic;

Table 14. Winter 2 streamflow reconstruction and validation statistics of fractally modified tree-ring chronologies. The coefficient of determination is adjusted for addition of predictors (R_a^2). The number in parentheses after the R_a^2 is the number of predictors used in the reconstruction.

Validation Statistics

Site	R_a^2	SE	RMSEv	RE
CB	0.47 (2)	0.134	0.133	0.460
HCL	0.49 (3)	0.131	0.135	0.440
DSM	0.46 (2)	0.135	0.138	0.420
RVD	0.47 (2)	0.133	0.136	0.430
SK1	0.43 (2)	0.139	0.141	0.390
SK2	0.45 (2)	0.137	0.144	0.370
CB-HCL	0.57 (4)	0.121	0.123	0.540
DSM-RVD	0.46 (2)	0.135	0.138	0.420
SK1-SK2	0.45 (2)	0.137	0.144	0.370

The highest R_a^2 values for the annual reconstructions are from sites CB-HCL (0.29). In all cases, the reduction of error statistic is positive, and the Durbin-Watson test of no first-order autocorrelation of the reconstruction residuals was accepted.

The highest R_a^2 values for Winter 2 reconstructions are from CB-HCL (0.568). Again, in all cases, the reduction of error statistic is positive, and the Durbin-Watson test of

no first-order autocorrelation of the reconstruction residuals was accepted.

Table 15. Discharge Reconstruction Summary (R_a^2) for the Annual (October 1 - September 30) and Winter 2 (October 1 - May 31) partition.

Site	<u>Fractal Series</u>		<u>Original Series</u>	
	Annual	Oct - May	Annual	Oct - May
CB	0.23	0.47	0.22	0.46
HCL	0.24	0.49	0.24	0.54
DSM	0.15	0.46	0.11	0.43
RVD	0.16	0.47	0.18	0.48
SK1	0.22	0.43	0.23	0.43
SK2	0.28	0.45	0.25	0.45
CB-HCL	0.29	0.57	0.27	0.59
DSM-RVD	0.16	0.46	0.18	0.52
SK1-SK2	0.24	0.45	0.25	0.45

CHAPTER 4. DISCUSSION

Chronology Confidence

The intraseries correlations (0.76 to 0.83) reflect the crossdating across the entire basin. Plots and measurements of tree-ring samples visually support the crossdating between trees (Appendix A). Particular index years (e.g., 1686, 1729, 1735, 1864, 1894, 1902, and 1956) are common to all sites at all elevations. The cross-correlation coefficients (0.78 to 0.87) among the sites indicate the similarity of the chronologies and a common climatic signal throughout the basin.

The common signal throughout the basin lends credence to using the chronologies to compare the effects of substrate because the climate appears to affect the basin equally across the length and width of the basin, and at the range of elevations of the sites.

Streamflow Reconstructions and Meteorology

The common tree-ring signal across the entire basin indicates that the spatio-temporal distribution of precipitation does not hamper streamflow reconstructions. The two meteorological stations in the upper basin apparently reflect the general precipitation pattern across the entire basin.

The distribution of the adjusted coefficients of determination (R_a^2) values with respect to the water year partitions display some striking similarities (Tab. 7). All of the cool-season partitions show moderate values, ranging from 0.37 to 0.59. All of the warm season partitions show relatively low values, ranging from 0.01 to 0.14. The actual length of the warm- or cool-season partition does not appear to adversely influence discharge reconstructions. The consistent cool-season reconstructions could reflect winter and spring precipitation storage within the basin providing available moisture for both tree growth and discharge measurements.

The consistent warm-season reconstructions could result from evapotranspiration removing water from the basin, thereby reducing available moisture for tree growth and discharge measurements. Additionally, the sporadic, late summer thunderstorms would increase discharge measurements, but the moisture would not be recorded in current-year tree-ring growth.

The adjusted coefficients of determination (R_a^2) values for the standard indices deserve some consideration. When the 6 individual sites are grouped by substrate (CB and HCL, DSM and RVD, SK1 and SK2), the R_a^2 values are similar (0.22 and 0.25, 0.11 and 0.15, 0.23 and 0.26, respectively). The

sites of the pairs are separated by several miles. The similarity of R_a^2 values between pairs on the same substrate at distant sites suggests that substrate plays a role in tree growth, and consequently in streamflow reconstruction.

Visual examination of the reconstruction plots and the mean monthly discharge record reveals a possible explanation for the low summer reconstruction adjusted coefficients of determination (Fig. 3; Tab. 7; Appendix B). Looking at the period from approximately 1900 to 1925, all of the summer reconstructions except HCL Summer 2, CB/HCL Summer 2, and Summer 3, and SK1/SK2 Summer 3 are below the mean reconstructed discharge. Reviewing the mean monthly discharge shows anomalously high discharge during August and September. The high discharge can be attributed to localized summer thunderstorms. Correlation of tree-ring indices and discharge during this period is not realistic because the tree-rings would not record a brief, intense precipitation event late in the growing season, but the discharge event would be recorded. Therefore, during a relatively dry year when a tree would have a narrow ring, the summer partition of discharge would infer otherwise, resulting in negligible correlations.

The exceptions, HCL Summer 2, CB/HCL Summer 2, and Summer 3, and SK1/SK2 Summer 3, might be attributed to 2 scenarios:

1) Precipitation events during the spring and summer could have occurred on or around these sites, and the tree-ring record reflects the precipitation events and the discharge record, or 2) The mean monthly discharge record is the average of each month for the period of record (1924 - 1998). During particular years when minimal, intense, late summer thunderstorms did not occur, the tree-ring record at these sites would be more representative of the summer discharge partitions, but by averaging the entire discharge record, the discharge record for those years would be inflated, again resulting in negligible correlations. These scenarios could be addressed by examining the daily precipitation record for the basin, but this task would be daunting, given the paucity of meteorological stations in the lower basin.

Are the differences in reconstruction results due primarily to substrate characteristics, or do they differ just by chance? Do the spatially variable precipitation patterns provide more moisture to the alluvial fan deposits, thereby creating a more realistic relationship between tree growth and discharge? Unless a fairly dense network of meteorological stations is established throughout a basin, this problem is not easily addressed.

Is the rate of snowmelt equal throughout the basin? Vegetation changes from mixed conifer on the plateaus to piñon-juniper in the lower basin. Species and density changes affect interception and incident radiation on a snowpack, suggesting differential snowmelt (Brooks et al., 1997; Skau, 1964). Different rates of snowmelt can differentially provide more or less water to a particular substrate. If infiltration capacity is surpassed, less moisture will be available for tree growth, and the resulting chronology would not represent the actual amount of precipitation for a site. The north-south orientation of the basin would appear to minimize the effects of differential solar radiation influx, but density of vegetative cover will cause differences in snow accumulation and snowmelt. Careful examination of tree-ring sites is necessary to address this issue, but the problem of spatially variable precipitation still exists.

Substrate Analysis

Substrate affects the amount of moisture available for tree growth. The clay content and permeability are factors that affect infiltration and the available water capacity of a soil (Birkeland, 1984; Brooks et al., 1997; Ritter et al., 2002). In a study of rooting depth and soil types in Ohio,

Fritts and Holowaychuck (1959) found that an increase in clay content restricted rooting depth of trees. Fritts and Holowaychuck (1959) concluded that radial growth was related to soil type and soil moisture. An increase in clay content reduces the porosity and available water content of the soils. A decrease in clay content will increase porosity and permeability. If a soil has low clay content, as in the sandstone residuum, available water capacity can be reduced by increased percolation removing the water from the system. Either extreme can have a similar effect on the tree-ring chronology by not recording a precipitation event. The range of soil clay content in this study (Tab. 1) is reflected in tree growth and subsequent tree-ring chronologies. With sporadic summer thunderstorms in mind, if rainfall exceeds infiltration capacity, Hortonian overland flow will commence (Brooks et al., 1997; Ritter et al., 2002). The high clay content and low soil permeability of sites SK1 and SK2 fit this category. Excess runoff results in less water being retained by the soil for tree growth. At the other extreme, the soils of sites DSM and RVD, being developed from sandstone residuum, have high permeability and low clay content. Water entering the soil quickly infiltrates the upper layers of soil and passes through to groundwater. This scenario also reduces available water for

tree growth. The intermediate sites, CB and HCL, have soils developed from alluvial fan deposits. Being intermediate between shale and sandstone in clay content and permeability, these sites have greater moisture retention capability, and are more amenable to tree growth , resulting in a chronology more representative of precipitation and streamflow.

Fractal Analysis

Fractal analysis of time series is a technique that provides a simple, easily understandable description of the overall persistence of tree-ring chronologies and hydrologic records. Autoregressive-moving average (ARMA) modeling often concentrates on short-term persistence (from 1 to 20 years), and the technique is effective in modeling, and when necessary, removing the short-term persistence. Often, ARMA modeling accounts for persistence in 1, 2, or 3 lags, resulting in, for example, AR(1), AR(2), or AR(3) models. As the number of lags increase, so does the complexity of the model. When examining the entire length of a chronology (e.g., 300 years in this study) an ARMA(300) model would become a bit cumbersome to interpret. Imagine the complexity when dealing with millennial length series. The ability to describe the long-term persistence of a series

with a single number is advantageous when comparing multiple series.

The long-term persistence (fractal dimension) of the common period sequences is more variable than the persistence for the entire length of the chronologies in this study (Tab. 10). Site DSM illustrates the change in fractal dimension from the calibration period to the chronology length in relation to the fractal dimension of the hydrologic record. This anomaly raises concern that the persistence of the tree-ring record is inconsistent over time. More specifically, the fractal dimension is dependent on the period of record being examined, at least at site DSM. What could cause this anomaly? Site specific idiosyncrasies not revealed by conventional examination of the tree-ring record could be the culprits.

A process that remains in equilibrium around a constant mean level is termed stationary (Box and Jenkins, 1976). The inconsistencies of the fractal dimensions between different periods within these series represent a new option to assess non-stationarity in a time series. The inconsistency illustrates that the fractal dimension is dependent on the length of record being examined in this study. If the fractal dimensions of different segments of a series are identical, there would be no differences in persistence of

the segments. The presence of a difference in the fractal dimensions suggests inconsistencies in the long-term persistence, and a lack of stationarity.

The common period between the environmental variable and the gauged record is normally used for calibration and verification for reconstruction purposes. If the fractal dimensions of different segment lengths suggest non-stationarity, perhaps a more realistic approach would be to use the long-term fractal dimension of the tree-ring indices in the transformation calculations.

Sites CB and HCL are more consistent through time than sites RVD, DSM, SK1 and SK2 (Tab. 10). The fractal dimensions of sites CB and HCL display less variability between the calibration period and the chronology length than the other sites. Two scenarios might help explain these phenomena. One is that the substrate plays a role in tree growth, and the substrate at sites CB and HCL provides a more stable environment for consistent, long-term growth. The second option could be one of a statistical nature. The longer period of the chronologies might be more representative of the actual long-term persistence of the series. By increasing the number of data points, the law of large numbers provides a more realistic view of the data. The shorter common period is only a subset of the total

length under investigation. Idiosyncrasies within the shorter subset become pronounced with fewer data points. Should the fractal dimensions of the chronology lengths instead of the common period be used for calibration with the hydrologic series? Possibly, but this procedure seems impractical when the hydrologic series is relatively short compared to the tree-ring chronologies. This is a common situation when dealing with streamflow reconstructions. An alternative approach would be to modify the hydrologic series' fractal dimension to the long-term fractal dimension of the tree-ring record, and then re-perform the reconstructions with redefined fractal modifiers. This procedure might appear to be working backwards because the roles of predictors and predictand are reversed, but it provides an opportunity to apply fractals from another viewpoint.

This study relies on the differences of fractal dimensions among the tree-ring series and the hydrologic series as an analytical tool. The range of fractal dimensions for all series for the calibration period, 1.793 to 1.939, poses the question of statistical significance. The descriptive nature of the values indicate that the series are different with respect to persistence, but are these values statistically different? Currently, practices

to assess the accuracy of self-affine fractal dimensions derived using the roughness-length method have been developed (Kulatilake and Um, 1999), and these practices were incorporated in determining the fractal dimensions used for my analyses. A fractal dimension referred to as accurate does not imply statistical significance when compared to other fractal dimensions. Further research beyond the scope of this study is required to ascertain the statistical difference among fractal parameters.

Fractal Transformations

The fractal transforms represent an initial attempt to equalize the fractal parameters of different series. The narrow range of fractal parameters (Tab. 10) actually makes this task difficult (Fig. 17). How much smoothing is too much, or how much is not enough, are questions not easily addressed. The ratios between the Hurst exponents of the series are a logical approach because the Hurst exponent is a descriptor of the long-term persistence inherent within each series. The ratios then become scaling factors between the series. The fractal approach to transforms provides a definitive scalar between series, thereby eliminating the question of how much to modify a series.

Barefoot et al. (1974) used the mean of the entire length of the preceding data values to estimate the weighting factor (α). Initial attempts to smooth the data in this manner resulted in 'over-smoothing' the data in this study, meaning that too much persistence was removed, and the Hurst exponents diverged away from the desired Hurst exponent of the hydrologic series. Trial and error of different segment lengths found that using the previous data value approximated the Hurst exponent somewhat better than other lengths. This is effectively a two year weighted average using the Hurst ratios of the series as the weights. Other segment lengths used in experimentation were the entire preceding segment, and 3, 5, 10, and 20 year segments. Longer segment lengths (even three years) smoothed the data too aggressively. Intuitively, this seems antithetical. The means of longer segments are more representative of the long-term persistence, so a longer data segment would be more representative of the present predicted value, and to use this value to estimate the α value seems plausible. The results indicate otherwise.

Another point to address is why some Hurst values are overestimated and some underestimated when using the same technique on the series. Perhaps characteristics peculiar to each series affect the amount of smoothing. If this is

the case, no single technique is appropriate for a blanket modification. Each series would need to be assessed individually, and this approach would increase time and computer usage substantially. Conjecture at this level points to nuances of fractals that need to be studied more thoroughly.

Fractal Transformation Reconstructions

The results of the fractal reconstructions are initially disappointing. The hypothesis that fractal modification of the tree-ring series would improve reconstructions failed. These results suggest two possibilities: 1) the relationship between the long-term persistence (the Hurst exponent or the fractal dimension) of the tree-ring and hydrologic series is inconsequential regarding streamflow reconstructions in this basin, or 2) the subtle alignment in this study does affect the reconstructions, and the resultant reconstructions are actually more representative of the relationship between the variables because the series are more aligned. During chronology development using ARSTAN, low order autocorrelation is modeled and removed to create the residual indices. If the low order autocorrelation affects the chronology, the long-term persistence should also affect chronology development, even minutely so. Following this

reasoning, Option 1 can be discarded. Intuitively, Option 2 seems more realistic than Option 1 because both series are more aligned. Presuming Option 2 is true, the reconstructions, even though the R_a^2 values are slightly lower, represent a more realistic relationship between the variables.

Spatial Variability of Sites

Additional sources of error introduced into the streamflow reconstructions in this study can be gleaned from Figure 2. The location of the meteorological stations are in the upper portion of the basin, and the tree-ring sites are located in the upper and mid-basin. The Bryce Canyon station is located on the Paunsaugunt Plateau, well above the Tropic station located in the valley. How representative are these stations of the entire basin? Without a network of meteorological stations throughout the basin, this question is difficult to address.

The spatial distribution of the tree-ring sampling sites could also introduce error. Sites CB and HCL are located near the upper basin, just below the cliffs of Aquarius Plateau. Sites DSM, RVD, SK1, and SK2 are located in the mid-basin, away from any nearby topographic protuberances. Do orographic effects of Aquarius Plateau introduce greater

rainfall or increased snowmelt to sites CB and HCL, while the remaining sites do not benefit? Site selection also attempted to minimize elevation differences among the sites, but the range of elevation, 1,800 to 2,200 meters, could be enough to introduce precipitation differences, especially when considering the locations of sites CB and HCL.

CHAPTER 5. CONCLUSIONS

Several factors influence tree growth and chronology development. This study has successfully compared geologic substrates with respect to tree-ring chronology development and streamflow reconstructions using multiple linear regression. The alluvial fan deposits generally provide the highest coefficient of determination values for streamflow reconstruction.

This study is the first application of fractal analysis in a dendrochronological, process-based approach to streamflow reconstruction. The smoothing technique used is based on properties inherent within each series, and provides a more practical approach than arbitrary, external smoothing operations, such as three or five year running averages. In this study, fractally derived smoothing failed to improve the amount of variance explained in the streamflow reconstructions. In spite of this shortcoming, the fractal analyses provide some thought provoking concepts:

1. By equalizing the fractal parameters of two series with each other, a higher coefficient of determination would be expected. As this was not the case, the fractal-based smoothing brings to light inconsistencies within each series

not previously addressed, for example, by using ARMA modeling.

2. Fractal examination of tree-ring indices provides insight into the long-term persistence of a time series, and consequently into the stationarity of a series. Visual examination of each tree-ring series can reveal segments that exhibit local trends. By partitioning the series into segments based on visual examination and comparing the fractal dimension of each segment with the fractal dimension of the entire length, an accurate picture of the behavior of long-term persistence will be ascertained. Fractal dimensions can provide an analytical tool complementary to ARMA modeling.

Future fractal forays should include comparison of the different self-affine techniques applied to the same time series. Techniques such as roughness-length, variogram, rescaled range, and power spectral density could be compared. This approach would help define which technique(s) provides optimum results in dendrochronological studies.

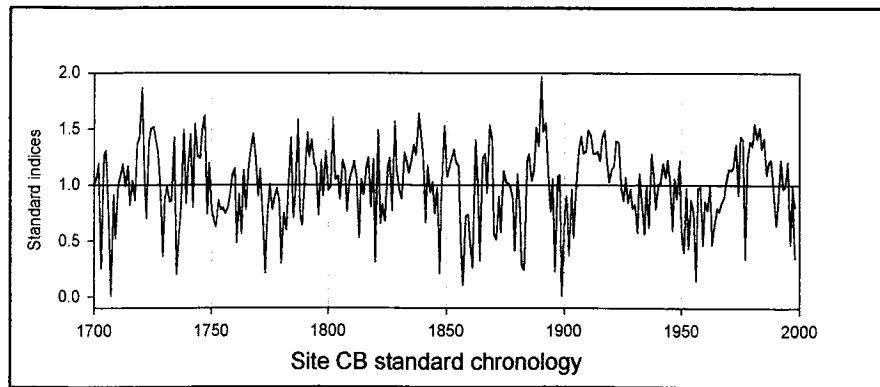
This study provides a foundation to expand the substrate/species component of dendrochronological reconstructions. Future work on this topic should include more species and substrate comparisons. This study area

provides abundant piñon on various substrates throughout the basin at lower elevations. To expand this work, a basin with multiple species and substrates with similar aspect and elevations is required. Isolated pockets of ponderosa pine grow primarily on sandstone residuum at lower elevations within the basin, so substrate comparison using ponderosa pine is not practical. At higher elevations, abundant ponderosa pine grows on carbonate substrate, but the elevation, aspect, and precipitation regimes are not consistent with the lower elevation sites. A major problem to overcome is finding suitable sites with sufficient species to conduct investigations. The paragon basin remains elusive.

APPENDIX A. TREE-RING CHRONOLOGIES:
STANDARD INDICES AND PLOTS.

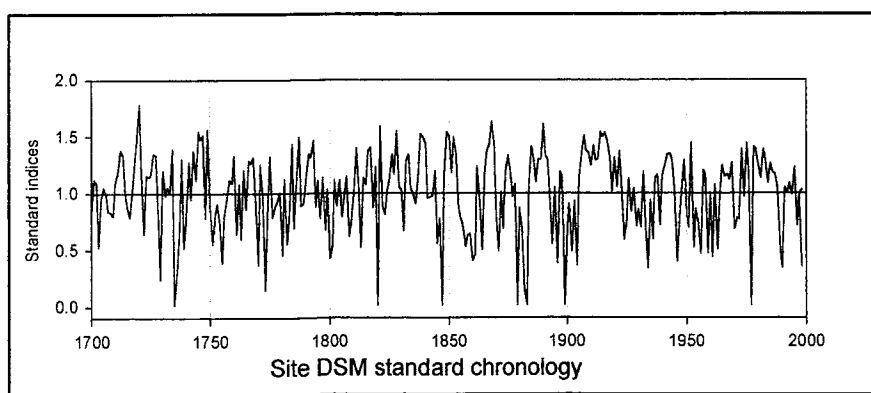
Site: Coal Bench (CB)

Year	0	1	2	3	4	5	6	7	8	9
1700	100	107	119	26	127	130	76	1	91	52
1710	100	110	118	99	117	82	104	86	136	143
1720	186	117	70	139	150	151	139	130	99	36
1730	88	98	85	86	143	21	49	81	149	84
1740	116	145	80	155	126	124	150	162	74	120
1750	79	68	62	86	78	80	75	81	90	110
1760	115	48	92	56	113	78	117	131	146	125
1770	90	114	74	22	70	100	78	88	97	86
1780	30	74	60	97	142	71	91	158	71	64
1790	105	147	125	140	119	115	73	122	90	130
1800	96	99	160	105	108	87	122	113	76	106
1810	113	121	106	53	105	91	117	125	80	123
1820	31	149	65	83	67	115	124	77	157	114
1830	96	88	129	123	111	123	136	127	164	147
1840	126	67	117	94	102	75	98	21	100	153
1850	107	113	123	132	120	117	43	11	72	74
1860	49	26	140	97	32	124	128	93	154	140
1870	56	51	90	58	112	103	101	98	88	42
1880	110	79	28	24	123	128	104	114	151	135
1890	196	148	155	110	76	105	23	107	109	1
1900	75	90	37	96	53	101	134	143	128	130
1910	149	145	128	128	130	121	143	148	120	103
1920	113	117	139	138	97	86	106	84	97	79
1930	82	57	110	84	56	100	62	128	113	79
1940	100	101	119	107	122	102	59	105	88	122
1950	60	40	97	43	87	74	15	97	98	46
1960	86	78	99	47	66	79	76	84	88	103
1970	114	113	116	136	91	143	140	34	121	139
1980	134	155	141	151	132	142	109	121	122	95
1990	64	82	122	97	99	120	47	89	80	100
2000	34									



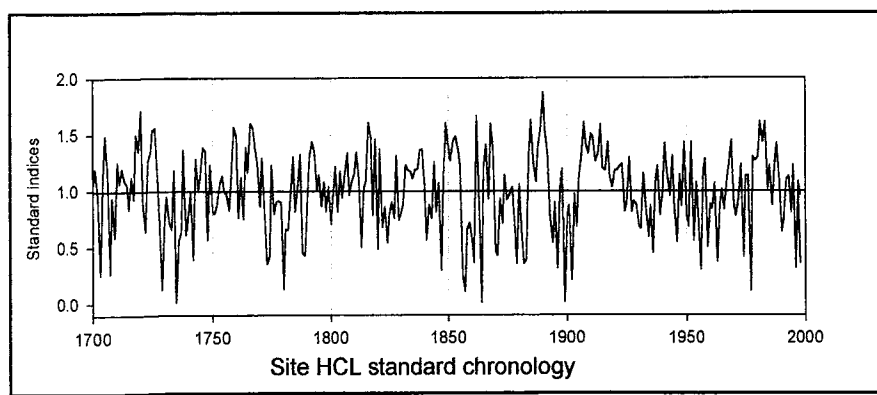
Site: Deer Springs Mesa (DSM)

Year	0	1	2	3	4	5	6	7	8	9
1700	81	111	109	52	96	106	102	86	83	81
1710	109	119	139	134	102	88	79	98	125	150
1720	178	119	65	116	114	116	134	132	89	23
1730	119	97	105	99	137	2	27	62	129	51
1740	80	125	94	135	110	153	146	150	77	154
1750	88	54	80	89	74	38	79	94	112	111
1760	135	66	107	59	119	87	131	128	134	92
1770	37	126	95	14	75	134	80	89	92	101
1780	46	113	56	81	141	69	109	147	90	90
1790	114	134	132	147	89	112	77	114	67	103
1800	42	54	111	89	112	80	97	116	63	74
1810	100	138	102	53	113	108	139	141	89	123
1820	2	157	90	82	103	115	136	119	157	108
1830	103	68	127	133	105	100	90	117	151	148
1840	141	95	97	98	119	56	77	2	115	153
1850	150	117	149	134	87	78	69	53	63	65
1860	41	47	124	98	52	117	136	143	163	141
1870	82	50	102	69	119	134	119	97	108	2
1880	87	69	15	2	105	141	128	109	129	131
1890	161	134	128	88	55	104	38	118	116	2
1900	70	90	48	93	37	111	134	149	138	135
1910	124	142	128	129	154	150	153	146	132	104
1920	132	107	137	108	60	78	114	84	104	72
1930	87	71	120	75	34	93	60	112	116	71
1940	114	123	133	134	130	102	40	70	101	130
1950	82	70	144	54	86	74	48	119	116	48
1960	101	44	107	50	104	123	115	116	111	126
1970	68	77	77	140	98	145	121	2	141	139
1980	125	114	138	130	110	126	119	118	103	51
1990	33	103	101	110	99	122	71	99	103	



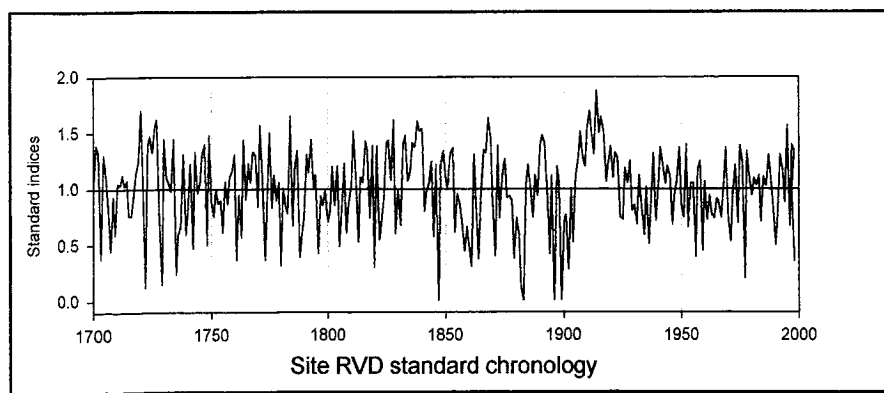
Site: Henderson Canyon Lower (HCL)

Year	0	1	2	3	4	5	6	7	8	9
1700	105	119	96	26	114	149	115	27	94	59
1710	125	107	120	109	106	84	112	92	150	135
1720	171	90	64	126	134	153	155	111	71	13
1730	80	95	72	66	118	2	56	64	136	61
1740	81	99	39	129	101	113	138	135	57	124
1750	83	80	88	106	114	100	97	83	113	157
1760	149	76	112	75	139	117	160	156	139	125
1770	86	129	83	36	43	123	79	91	91	90
1780	13	66	66	96	130	82	103	132	45	43
1790	93	129	144	134	100	115	86	108	82	103
1800	70	93	121	81	117	94	114	134	96	108
1810	116	134	112	50	102	109	161	147	78	146
1820	48	137	68	86	54	79	90	76	132	74
1830	81	88	123	118	117	111	119	119	137	137
1840	105	56	88	76	125	81	107	30	110	160
1850	139	127	145	148	137	123	25	11	66	72
1860	56	37	166	90	2	119	141	93	160	136
1870	47	43	93	71	114	92	97	103	76	35
1880	106	69	36	40	133	163	125	108	139	155
1890	187	154	133	75	54	90	32	103	119	2
1900	78	87	21	97	69	111	130	161	141	133
1910	151	148	126	132	159	120	118	143	112	104
1920	118	118	122	124	82	90	129	81	91	88
1930	69	66	115	84	59	87	45	110	122	78
1940	99	142	114	96	131	84	55	114	86	143
1950	79	68	143	56	108	77	30	118	129	50
1960	88	84	107	37	88	102	84	110	123	145
1970	88	78	94	123	41	113	114	12	130	127
1980	130	162	143	162	102	122	87	124	142	110
1990	64	75	110	113	81	123	32	108	96	



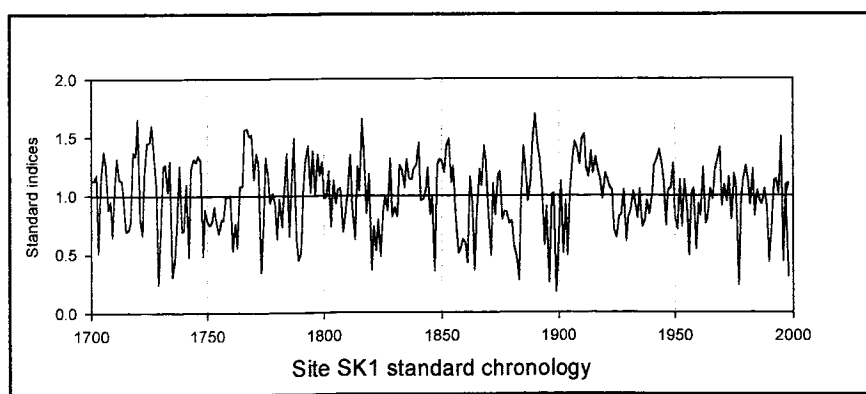
Site: Round Valley Draw (RVD)

Year	0	1	2	3	4	5	6	7	8	9
1700	102	138	132	39	130	118	88	45	93	60
1710	105	103	112	103	107	76	76	97	113	124
1720	170	107	13	139	146	132	156	162	72	15
1730	145	110	104	98	144	24	59	67	131	59
1740	79	122	47	133	96	105	131	140	50	147
1750	89	75	100	87	90	62	107	87	111	115
1760	131	37	95	57	144	91	123	106	133	130
1770	84	157	112	37	84	150	83	112	90	105
1780	32	100	84	78	165	67	117	134	39	57
1790	76	131	114	144	101	112	43	94	86	99
1800	71	82	120	86	121	49	82	123	61	90
1810	103	152	114	53	110	106	143	135	74	139
1820	30	138	54	70	91	141	143	108	161	60
1830	100	68	141	147	107	116	141	137	160	152
1840	153	81	97	105	124	58	122	1	120	134
1850	107	102	132	136	61	95	86	71	45	66
1860	50	31	131	74	37	99	134	133	163	145
1870	88	40	139	74	112	127	92	94	90	38
1880	74	59	14	1	104	122	101	75	112	94
1890	139	147	141	99	42	112	1	120	105	1
1900	70	77	28	100	52	111	127	151	129	121
1910	154	170	146	131	188	150	164	151	107	122
1920	138	110	132	128	75	73	119	105	125	81
1930	86	68	112	84	60	101	51	97	132	72
1940	103	137	122	105	121	113	68	94	108	137
1950	87	75	140	66	105	105	40	117	125	45
1960	107	72	94	78	74	91	88	74	107	137
1970	75	54	97	121	70	139	125	20	134	110
1980	94	110	103	112	71	111	103	130	114	85
1990	50	76	130	116	88	156	67	139	134	



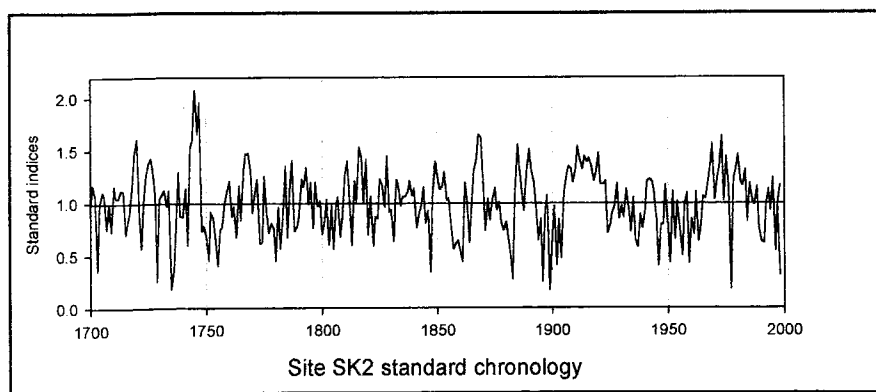
Site: Skutumpah Road Site 1 (SK1)

Year	0	1	2	3	4	5	6	7	8	9
1700	102	138	132	39	130	118	88	45	93	60
1710	105	103	112	103	107	76	76	97	113	124
1720	170	107	13	139	146	132	156	162	72	15
1730	145	110	104	98	144	24	59	67	131	59
1740	79	122	47	133	96	105	131	140	50	147
1750	89	75	100	87	90	62	107	87	111	115
1760	131	37	95	57	144	91	123	106	133	130
1770	84	157	112	37	84	150	83	112	90	105
1780	32	100	84	78	165	67	117	134	39	57
1790	76	131	114	144	101	112	43	94	86	99
1800	71	82	120	86	121	49	82	123	61	90
1810	103	152	114	53	110	106	143	135	74	139
1820	30	138	54	70	91	141	143	108	161	60
1830	100	68	141	147	107	116	141	137	160	152
1840	153	81	97	105	124	58	122	1	120	134
1850	107	102	132	136	61	95	86	71	45	66
1860	50	31	131	74	37	99	134	133	163	145
1870	88	40	139	74	112	127	92	94	90	38
1880	74	59	14	1	104	122	101	75	112	94
1890	139	147	141	99	42	112	1	120	105	1
1900	70	77	28	100	52	111	127	151	129	121
1910	154	170	146	131	188	150	164	151	107	122
1920	138	110	132	128	75	73	119	105	125	81
1930	86	68	112	84	60	101	51	97	132	72
1940	103	137	122	105	121	113	68	94	108	137
1950	87	75	140	66	105	105	40	117	125	45
1960	107	72	94	78	74	91	88	74	107	137
1970	75	54	97	121	70	139	125	20	134	110
1980	94	110	103	112	71	111	103	130	114	85
1990	50	76	130	116	88	156	67	139	134	



Site: Skutumpah Road site 2 (SK2)

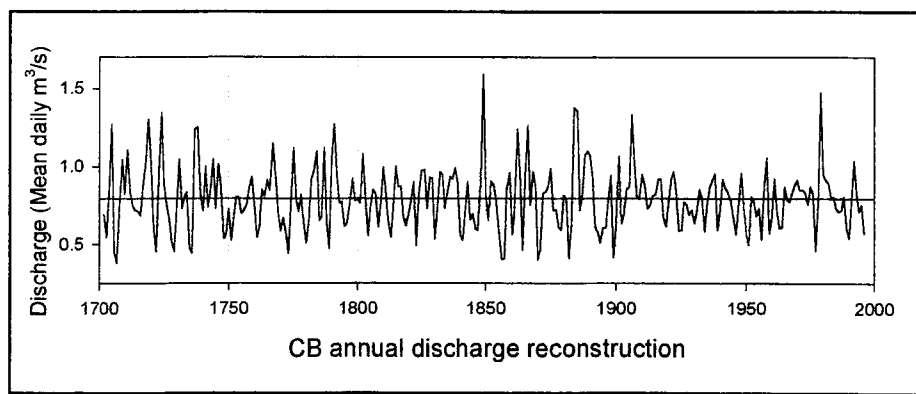
Year	0	1	2	3	4	5	6	7	8	9
1700	97	117	107	36	98	110	107	76	99	73
1710	116	105	104	112	112	70	81	92	121	149
1720	161	90	58	106	126	138	143	132	105	26
1730	104	109	113	97	112	19	37	76	129	88
1740	87	114	60	154	160	208	166	196	74	78
1750	69	45	92	86	68	41	75	77	100	111
1760	121	87	96	68	117	84	130	147	148	132
1770	91	111	123	62	62	126	89	71	81	76
1780	46	96	57	88	135	67	117	141	73	77
1790	88	123	116	134	99	120	76	119	97	102
1800	70	84	104	60	98	56	96	106	68	94
1810	127	140	99	60	121	102	153	144	101	142
1820	70	105	59	87	85	123	117	97	145	92
1830	94	64	122	117	97	106	106	111	121	107
1840	114	76	90	97	115	81	93	35	106	139
1850	126	113	116	130	102	104	79	56	61	64
1860	53	44	119	104	62	102	131	142	164	162
1870	116	73	104	84	103	115	91	101	81	74
1880	82	67	48	28	112	156	135	109	93	128
1890	152	131	120	100	65	85	25	93	107	17
1900	69	97	41	84	48	108	122	135	133	119
1910	131	154	141	132	145	139	143	136	121	129
1920	148	118	118	121	72	79	91	97	118	85
1930	97	86	113	94	73	105	65	58	89	76
1940	90	121	123	120	111	85	40	79	81	117
1950	76	44	111	66	102	75	50	98	109	43
1960	85	71	111	64	76	106	104	118	136	157
1970	103	124	134	164	102	144	113	18	123	131
1980	146	120	117	132	83	118	102	98	116	76
1990	64	62	99	113	93	124	55	100	116	



APPENDIX B. STREAMFLOW RECONSTRUCTIONS

SITE CB: Annual reconstructed discharge.
 Units are mean daily cubic meters per second (m^3/s) $\times 100$.

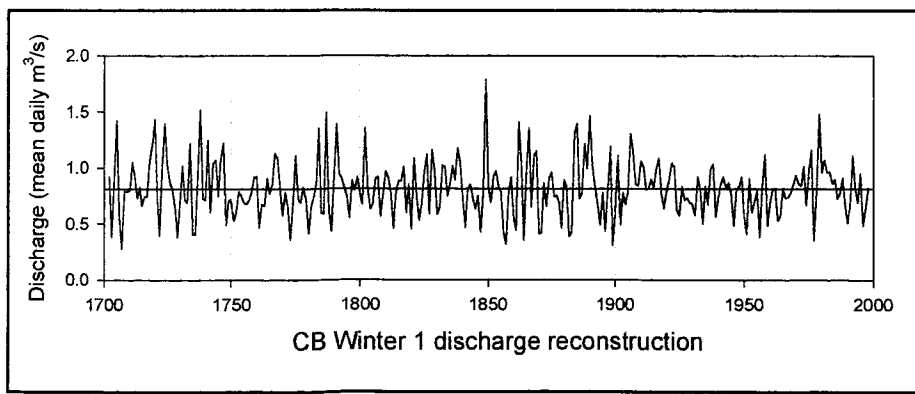
Year	0	1	2	3	4	5	6	7	8	9
1702			69	54	86	127	45	38	74	104
1710	83	111	84	75	72	71	69	87	102	130
1720	102	61	46	98	134	89	77	67	52	46
1730	72	104	73	81	84	48	44	124	125	82
1740	71	100	74	85	104	73	101	86	54	57
1750	73	53	69	81	80	70	72	76	86	93
1760	76	55	60	85	81	91	85	115	94	71
1770	59	67	58	44	76	112	79	71	82	63
1780	51	66	92	98	110	65	68	112	63	47
1790	105	127	95	77	77	62	64	77	92	78
1800	79	76	108	81	55	74	85	83	61	76
1810	99	84	65	54	74	100	87	87	67	62
1820	69	79	90	49	82	98	98	73	93	92
1830	53	72	97	95	73	83	93	92	99	90
1840	56	52	72	90	66	70	60	59	90	159
1850	82	65	91	89	78	60	40	41	85	96
1860	56	68	124	95	46	95	126	75	96	87
1870	40	47	83	84	87	99	72	72	61	59
1880	81	78	41	63	138	136	72	81	107	110
1890	107	94	61	58	51	61	60	79	94	42
1900	63	106	63	70	86	87	133	103	80	81
1910	95	88	73	75	81	82	92	92	67	62
1920	77	92	96	84	59	59	77	76	69	72
1930	64	71	85	80	58	76	87	91	95	59
1940	72	92	86	84	78	67	56	75	96	75
1950	57	50	81	77	68	73	53	87	105	57
1960	68	92	71	61	61	87	79	77	83	88
1970	91	85	85	84	76	87	83	46	76	148
1980	94	91	90	80	81	73	71	72	81	60
1990	54	77	104	83	71	75	57	61		



SITE CB: Winter 1 reconstructed discharge.

Units are mean daily cubic meters per second (m^3/s) $\times 100$.

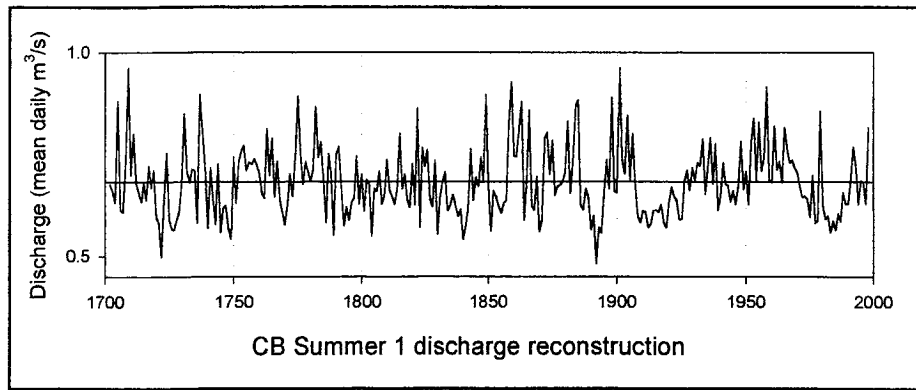
Year	0	1	2	3	4	5	6	7	8	9
1702			92	38	90	142	55	27	79	79
1710	80	105	92	73	83	66	74	74	105	121
1720	143	74	40	102	139	103	88	80	64	38
1730	70	102	71	69	122	40	40	93	152	73
1740	71	124	60	104	107	75	108	122	49	70
1750	72	53	61	79	75	69	68	71	79	92
1760	92	46	67	66	91	77	85	113	108	84
1770	58	78	64	36	66	110	73	69	83	72
1780	42	65	74	85	136	60	59	149	62	43
1790	92	139	95	90	82	74	55	88	80	92
1800	78	67	135	81	63	67	91	92	57	77
1810	97	91	77	46	79	88	88	101	60	85
1820	45	109	77	53	67	96	112	59	116	97
1830	58	65	102	101	75	86	102	89	117	104
1840	73	46	81	85	73	63	75	42	78	179
1850	82	69	92	97	83	78	42	32	78	91
1860	55	45	141	105	35	97	135	65	111	115
1870	41	42	86	66	91	96	74	75	69	46
1880	89	83	39	43	131	139	72	77	121	99
1890	146	102	83	68	49	77	43	81	119	31
1900	59	110	49	78	67	79	130	114	86	84
1910	106	101	80	81	89	83	99	109	76	64
1920	80	89	104	101	63	58	83	71	73	69
1930	67	58	92	81	50	83	67	99	103	56
1940	73	86	92	82	87	77	49	80	83	92
1950	57	41	90	61	70	79	38	84	112	48
1960	68	81	81	53	57	81	73	74	77	85
1970	93	86	84	101	67	97	116	35	78	148
1980	96	107	96	96	86	89	73	77	91	67
1990	50	67	111	81	69	94	48	64	82	



SITE CB: Summer 1 reconstructed discharge.

Units are mean daily cubic meters per second (m^3/s) $\times 100$.

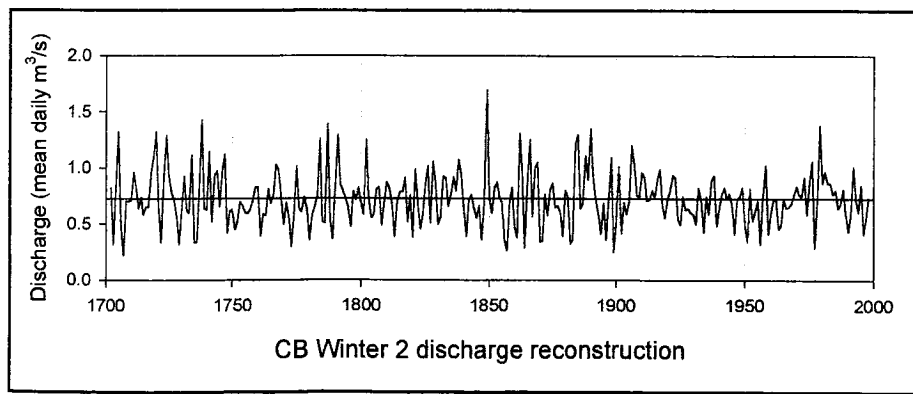
Year	0	1	2	3	4	5	6	7	8	9
1702			68	66	63	88	62	61	74	96
1710	70	80	68	65	63	68	64	72	67	71
1720	60	58	50	64	75	59	57	57	59	61
1730	68	85	71	68	71	71	58	90	81	72
1740	57	72	64	58	73	56	62	62	57	54
1750	74	63	73	76	77	71	73	73	74	72
1760	70	65	64	81	70	79	65	73	64	61
1770	58	62	70	65	74	89	75	68	73	71
1780	68	71	87	74	78	68	58	75	70	55
1790	75	77	67	57	62	59	63	64	74	63
1800	70	61	69	68	55	67	66	71	63	65
1810	74	66	65	63	66	80	67	70	64	62
1820	73	63	86	57	77	72	76	64	62	73
1830	55	64	69	71	61	62	65	63	60	62
1840	54	57	62	76	64	69	67	74	68	90
1850	68	56	66	65	62	61	63	64	83	93
1860	75	74	81	88	59	69	86	62	61	70
1870	56	59	79	80	70	79	65	67	67	68
1880	71	83	65	73	87	88	63	61	67	64
1890	57	60	48	57	56	65	74	67	89	66
1900	66	96	74	70	85	69	80	68	60	58
1910	61	61	57	58	61	61	61	63	58	57
1920	63	67	65	64	59	59	68	71	66	72
1930	69	73	72	79	65	72	79	68	77	61
1940	65	73	68	67	63	66	63	67	78	66
1950	71	63	78	84	68	83	71	74	91	69
1960	68	82	71	73	68	82	76	73	74	72
1970	70	67	64	65	64	60	70	58	59	86
1980	63	59	60	56	59	57	60	58	66	63
1990	63	69	77	72	63	69	68	63	82	



SITE CB: Winter 2 reconstructed discharge.

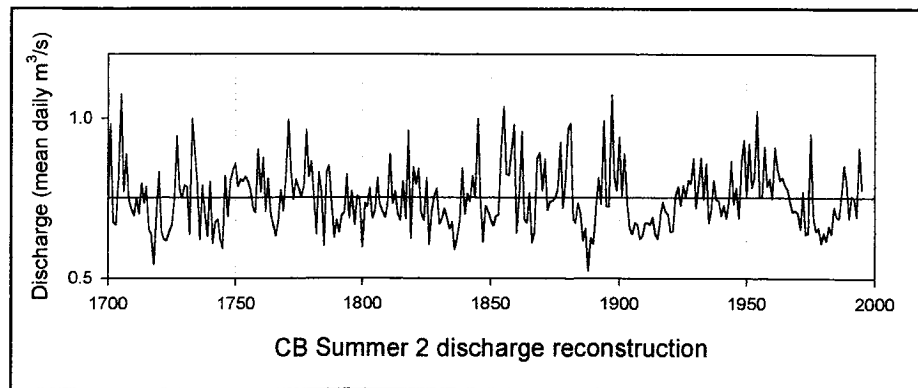
Units are mean daily cubic meters per second (m^3/s) $\times 100$.

Year	0	1	2	3	4	5	6	7	8	9
1702			82	32	81	132	47	22	70	70
1710	71	96	82	64	73	58	65	65	96	111
1720	133	65	33	92	129	93	78	71	56	32
1730	61	92	63	60	111	34	34	84	142	64
1740	63	114	52	94	97	66	98	112	42	61
1750	63	45	53	70	67	60	60	63	70	83
1760	83	39	59	58	81	68	76	103	98	75
1770	50	69	56	30	58	101	64	61	74	63
1780	35	57	65	76	126	52	51	139	54	36
1790	83	129	85	80	73	65	48	79	71	82
1800	69	58	125	72	55	59	81	83	49	68
1810	88	82	68	39	70	79	79	91	52	75
1820	38	99	68	46	59	87	102	51	105	88
1830	50	57	92	91	66	76	92	79	107	94
1840	64	39	72	76	64	55	66	36	69	169
1850	73	60	83	87	74	69	36	26	69	82
1860	48	38	131	96	29	88	125	57	100	105
1870	34	35	77	58	81	86	65	66	60	39
1880	80	74	33	36	121	130	64	69	111	90
1890	136	92	73	60	41	69	36	71	109	25
1900	51	101	42	69	59	70	120	104	76	74
1910	96	91	71	72	80	73	89	99	67	55
1920	71	80	94	91	55	50	74	63	64	60
1930	59	50	82	72	43	74	59	89	93	49
1940	64	77	82	73	77	68	41	71	74	82
1950	49	34	81	53	61	71	32	75	102	41
1960	60	72	72	46	49	73	64	65	69	76
1970	83	77	74	91	58	87	106	29	69	138
1980	86	96	86	86	77	80	64	68	81	59
1990	43	59	101	72	61	85	41	55	73	



SITE CB: Summer 2 reconstructed discharge.
 Units are mean daily cubic meters per second (m^3/s) $\times 100.$

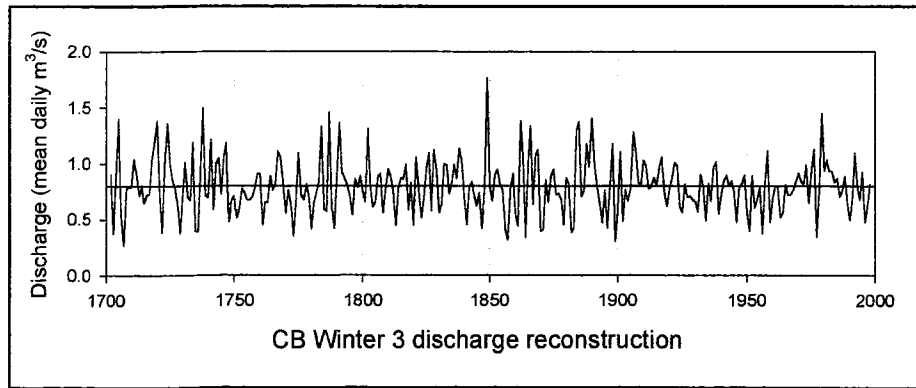
Year	0	1	2	3	4	5	6	7	8	9
1698									75	73
1700	70	98	68	67	81	107	77	89	75	72
1710	70	75	70	80	74	79	65	64	54	70
1720	83	65	62	62	65	67	75	94	78	75
1730	79	79	64	100	90	80	62	79	70	63
1740	80	61	68	68	62	59	82	69	81	84
1750	86	79	81	80	82	80	77	72	71	90
1760	77	88	71	81	70	67	63	68	77	71
1770	82	100	83	74	81	78	76	79	96	82
1780	86	75	64	83	77	60	83	85	73	63
1790	68	64	70	71	82	69	77	67	76	75
1800	60	73	72	78	69	71	81	73	71	69
1810	73	89	73	77	70	68	80	69	96	62
1820	85	79	84	70	68	81	61	71	76	78
1830	67	69	72	69	65	68	59	63	68	84
1840	70	76	74	82	75	100	74	61	73	71
1850	68	66	69	70	92	104	83	82	90	98
1860	64	76	96	68	67	77	61	64	88	89
1870	77	87	71	74	74	75	78	92	72	81
1880	97	98	69	67	73	71	62	66	52	63
1890	61	72	81	73	99	73	72	107	82	77
1900	94	76	89	74	66	64	67	67	62	63
1910	67	67	67	69	64	62	69	74	71	70
1920	65	65	76	79	73	79	76	81	80	87
1930	72	79	88	75	86	67	71	81	74	74
1940	70	73	69	74	87	73	78	69	86	93
1950	75	92	78	82	102	76	75	91	79	81
1960	75	91	85	81	81	79	78	74	71	71
1970	70	65	77	64	64	95	69	65	66	61
1980	64	62	66	64	72	69	69	76	85	80
1990	69	76	75	69	91	78	80			



SITE CB: Winter 3 reconstructed discharge.

Units are mean daily cubic meters per second (m^3/s) $\times 100$.

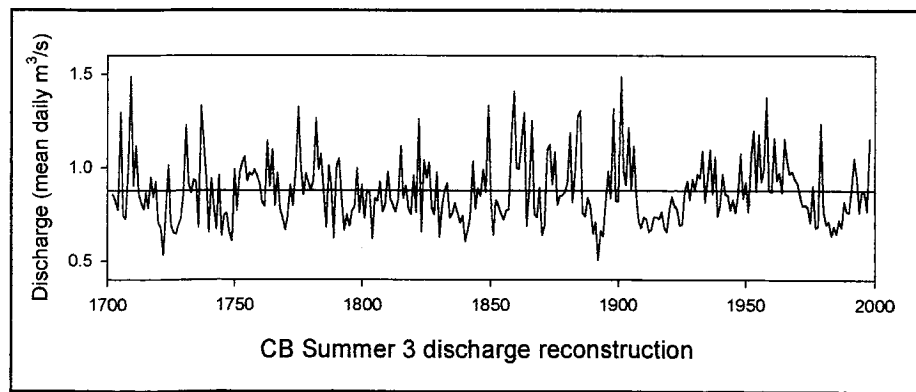
Year	0	1	2	3	4	5	6	7	8	9
1702			90	38	88	141	54	27	78	79
1710	79	104	90	71	81	65	72	73	103	119
1720	138	72	39	99	136	100	85	78	63	37
1730	68	101	70	67	119	40	39	93	149	72
1740	69	122	59	100	105	72	104	118	48	67
1750	71	52	60	78	74	68	67	70	78	90
1760	91	46	66	65	89	76	83	111	105	82
1770	56	76	63	35	65	110	72	68	81	71
1780	41	65	73	83	133	59	57	146	61	42
1790	91	136	92	87	80	72	54	86	79	89
1800	76	65	132	80	62	66	89	90	55	75
1810	95	89	75	45	77	87	86	99	59	82
1820	45	105	77	52	67	94	110	58	112	96
1830	56	64	100	99	73	83	99	87	114	101
1840	71	45	79	84	71	62	73	42	77	176
1850	81	67	90	94	81	76	42	32	77	91
1860	54	44	138	104	34	95	133	64	107	112
1870	40	41	85	65	89	94	72	73	67	46
1880	87	82	38	43	129	138	71	76	117	97
1890	141	99	79	66	47	76	42	79	117	30
1900	58	110	49	76	67	78	128	111	83	81
1910	103	98	78	79	87	80	96	105	74	62
1920	78	87	101	98	61	56	81	70	71	68
1930	66	57	90	80	49	82	66	97	101	55
1940	71	85	90	80	84	75	48	79	82	90
1950	56	40	89	60	68	79	38	83	111	48
1960	67	80	80	52	56	81	72	72	76	84
1970	91	84	82	98	65	94	113	34	76	145
1980	93	103	93	93	83	87	71	75	89	65
1990	50	66	109	80	67	92	47	62	81	



SITE CB: Summer 3 reconstructed discharge.

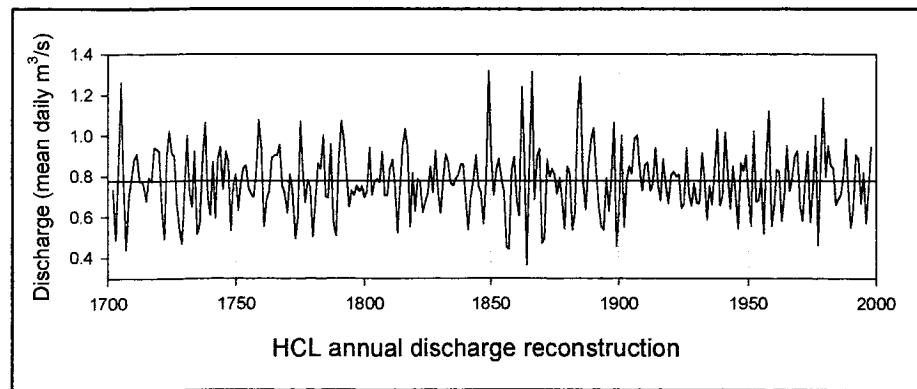
Units are mean daily cubic meters per second (m^3/s) $\times 100$.

Year	0	1	2	3	4	5	6	7	8	9
1702			86	83	77	130	74	73	98	149
1710	90	112	86	81	78	87	78	95	84	93
1720	70	68	53	78	101	69	65	65	69	73
1730	87	122	92	87	93	93	68	133	114	95
1740	65	94	79	67	96	64	74	76	65	61
1750	99	77	97	103	106	93	97	96	99	96
1760	91	81	79	114	90	109	80	97	78	72
1770	67	75	91	80	99	132	101	86	97	92
1780	88	93	126	99	107	87	68	101	90	62
1790	101	105	84	66	75	69	77	79	100	76
1800	91	73	88	87	62	84	82	92	76	80
1810	98	83	80	76	83	112	84	90	78	75
1820	96	76	126	66	104	94	103	79	75	98
1830	63	80	88	92	73	76	81	76	71	74
1840	60	66	75	103	78	89	85	99	87	133
1850	86	64	83	80	76	72	77	78	117	141
1860	100	99	114	129	69	88	125	75	74	89
1870	64	69	109	112	91	108	80	85	85	87
1880	92	119	81	97	128	130	76	74	84	79
1890	65	71	50	66	63	81	98	84	132	83
1900	82	149	99	91	122	88	111	86	71	68
1910	73	73	66	67	73	74	73	76	68	66
1920	77	85	80	78	69	70	88	93	83	94
1930	88	96	95	109	81	94	109	86	106	74
1940	80	97	86	85	77	83	76	85	108	83
1950	92	76	107	120	87	118	92	99	138	88
1960	87	116	93	97	87	115	104	96	98	94
1970	92	85	79	80	79	70	90	68	69	124
1980	77	70	71	64	69	65	72	68	82	77
1990	76	89	105	95	76	88	87	77	115	



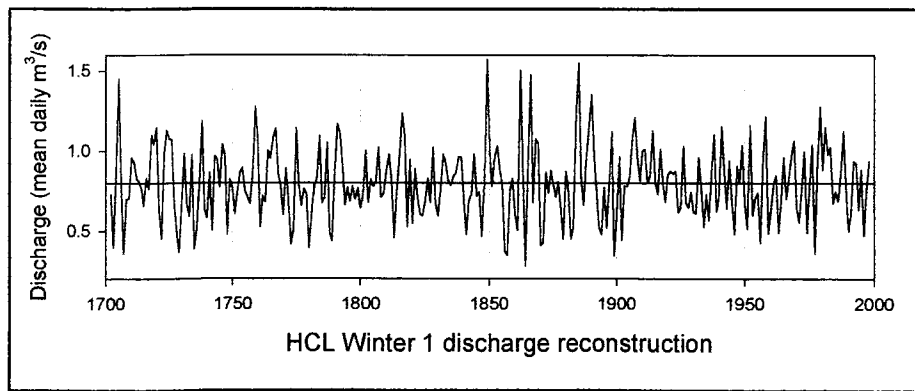
SITE HCL: Annual reconstructed discharge.
 Units are mean daily cubic meters per second (m^3/s) $\times 100$.

Year	0	1	2	3	4	5	6	7	8	9
1702			73	49	83	126	78	44	70	79
1710	88	91	77	78	73	68	79	77	94	94
1720	92	64	50	90	102	91	90	67	54	47
1730	73	100	72	65	92	52	57	89	106	71
1740	61	87	59	88	94	74	92	87	53	76
1750	81	63	76	84	85	74	71	70	82	108
1760	93	55	68	73	89	90	90	96	76	71
1770	62	81	73	50	60	107	84	67	78	75
1780	50	66	86	84	100	70	70	96	57	51
1790	89	107	98	82	65	73	71	76	73	75
1800	70	73	94	71	77	79	77	92	71	71
1810	84	88	77	52	74	95	103	94	55	81
1820	63	79	77	62	67	72	85	72	92	73
1830	62	78	91	87	77	76	79	81	86	86
1840	69	54	70	78	90	75	72	57	78	132
1850	90	71	84	89	79	72	46	45	83	90
1860	68	61	124	90	37	87	132	69	90	94
1870	47	50	88	80	84	81	71	79	68	54
1880	85	81	54	62	112	129	77	64	85	98
1890	104	83	67	56	54	79	63	80	106	46
1900	64	100	55	78	85	81	99	100	85	73
1910	86	87	73	76	94	76	68	89	76	67
1920	80	82	80	81	64	66	94	72	66	76
1930	67	67	91	79	59	76	66	84	103	66
1940	70	102	82	64	85	71	54	87	83	90
1950	72	56	102	68	68	79	52	90	112	56
1960	65	83	82	58	70	95	73	80	90	92
1970	66	58	77	92	58	75	100	46	85	118
1980	80	95	86	84	66	69	71	80	99	74
1990	55	65	91	89	67	82	57	73	94	



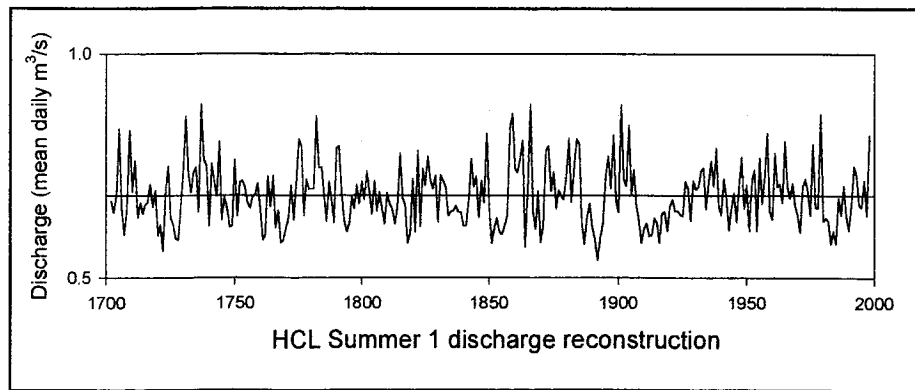
SITE HCL: Winter 1 reconstructed discharge.
 Units are mean daily cubic meters per second (m^3/s) $\times 100$.

Year	0	1	2	3	4	5	6	7	8	9
1702			73	40	87	145	82	36	70	71
1710	96	93	83	81	75	66	83	76	110	104
1720	115	63	45	98	113	108	107	70	50	37
1730	68	98	67	60	98	39	51	80	119	63
1740	58	87	50	97	95	77	104	98	48	82
1750	77	60	74	86	89	75	71	67	86	127
1760	108	52	72	68	100	95	109	114	86	78
1770	60	89	70	42	51	114	79	66	76	73
1780	39	61	78	83	110	67	71	105	49	44
1790	87	117	111	91	66	77	69	78	70	77
1800	64	72	100	68	82	78	81	102	71	73
1810	88	98	80	46	75	97	124	109	53	94
1820	54	89	70	61	59	68	83	68	102	68
1830	59	76	98	92	81	79	84	86	96	96
1840	70	48	69	73	98	72	74	47	81	157
1850	101	78	96	103	89	79	37	35	75	83
1860	61	51	150	88	28	92	148	68	108	104
1870	41	43	87	74	88	79	71	81	64	45
1880	87	75	45	53	124	155	84	66	96	115
1890	135	98	74	52	48	77	52	81	112	35
1900	60	96	44	78	78	84	108	121	96	81
1910	100	101	80	85	113	81	73	101	79	68
1920	85	88	86	87	62	65	103	68	65	74
1930	62	61	96	75	53	73	57	87	110	62
1940	71	115	86	64	94	69	48	91	80	103
1950	68	51	116	60	71	74	43	96	122	49
1960	63	80	85	49	68	96	70	83	97	106
1970	64	55	76	99	49	79	104	36	93	128
1980	88	115	98	102	67	75	69	86	112	77
1990	50	61	93	92	64	88	47	76	93	



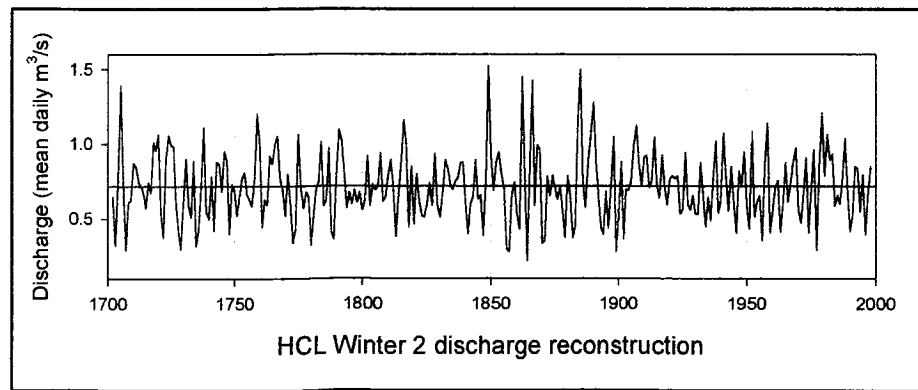
SITE HCL: Summer 1 reconstructed discharge.
 Units are mean daily cubic meters per second (m^3/s) $\times 100.$

Year	0	1	2	3	4	5	6	7	8	9
1702			67	65	69	83	66	60	65	83
1710	69	76	64	67	64	66	67	71	66	70
1720	59	62	56	70	75	63	62	59	58	66
1730	74	86	73	69	73	75	65	89	77	75
1740	62	76	72	68	80	63	68	66	61	62
1750	76	64	71	72	70	67	66	68	69	71
1760	66	58	60	73	66	73	61	65	58	58
1770	61	64	71	63	71	81	79	64	72	70
1780	70	70	86	75	75	69	63	71	67	62
1790	79	79	69	63	60	62	68	65	71	67
1800	71	67	74	69	64	72	65	69	65	62
1810	69	67	65	62	66	78	68	66	58	60
1820	72	60	78	62	74	71	77	72	70	73
1830	63	73	72	70	64	65	65	66	65	65
1840	62	62	67	77	70	73	64	72	67	82
1850	66	58	61	63	60	60	62	64	83	87
1860	74	73	77	81	57	70	89	65	61	69
1870	58	62	79	79	69	74	65	70	69	67
1880	73	81	67	74	81	80	62	57	64	67
1890	61	59	54	59	62	73	77	70	82	67
1900	65	89	72	70	84	69	74	66	63	58
1910	61	62	59	60	63	62	58	64	65	61
1920	66	67	65	65	64	64	71	70	63	72
1930	70	70	74	74	65	71	76	70	79	66
1940	64	72	68	61	66	69	63	71	77	65
1950	71	61	72	74	61	77	67	72	82	65
1960	63	78	70	71	67	81	70	68	71	66
1970	64	60	70	72	69	64	80	66	66	87
1980	63	63	63	58	61	58	68	64	70	64
1990	61	66	75	73	66	66	72	64	82	



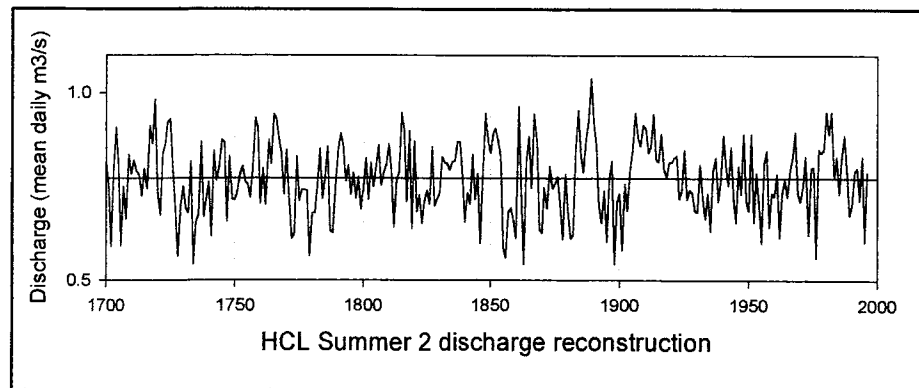
SITE HCL: Winter 2 reconstructed discharge.
 Units are mean daily cubic meters per second (m^3/s) $\times 100$.

Year	0	1	2	3	4	5	6	7	8	9
1702			64	32	78	139	73	29	61	62
1710	87	84	74	72	66	57	74	67	101	96
1720	106	54	38	90	105	99	98	61	42	30
1730	60	90	59	51	89	32	43	72	111	55
1740	50	78	42	88	87	68	95	89	40	73
1750	69	52	65	77	81	66	63	58	77	120
1760	100	44	63	59	92	87	100	105	77	69
1770	52	80	61	34	43	106	70	57	68	64
1780	32	52	70	75	101	59	62	97	41	36
1790	79	109	103	82	57	68	60	69	61	68
1800	56	63	92	59	73	69	72	94	62	64
1810	79	89	71	38	66	89	116	100	44	85
1820	46	80	62	52	51	59	74	59	94	59
1830	51	67	89	84	72	70	75	77	88	88
1840	62	40	60	65	89	63	65	39	72	152
1850	92	69	87	94	80	69	30	28	67	74
1860	52	43	145	79	22	84	142	59	99	96
1870	34	35	78	65	79	71	63	72	55	38
1880	78	66	37	45	116	150	75	57	88	107
1890	128	89	65	44	40	68	44	72	105	28
1900	52	88	36	69	69	75	100	112	87	72
1910	91	92	71	75	104	72	64	92	70	59
1920	76	79	77	78	53	56	94	60	56	65
1930	53	53	88	67	44	64	48	78	102	54
1940	62	107	77	55	85	60	40	82	71	95
1950	59	43	108	52	62	65	35	87	114	41
1960	55	71	76	41	59	87	62	74	88	98
1970	56	47	67	91	41	70	96	29	84	121
1980	79	106	89	93	59	65	60	77	104	68
1990	42	52	85	84	55	79	40	67	85	



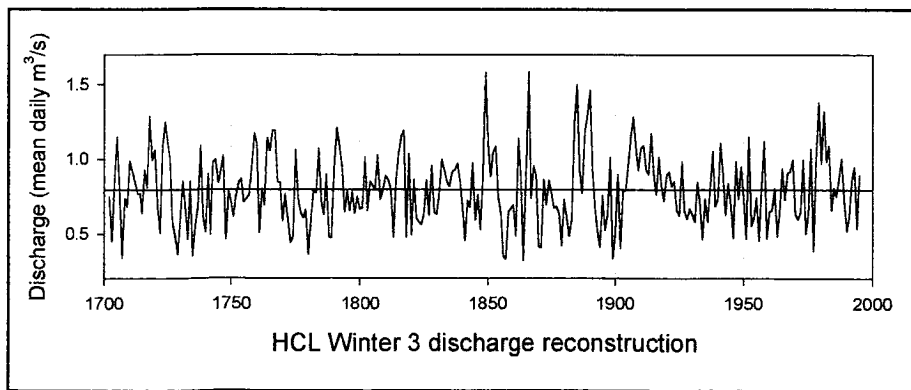
SITE HCL: Summer 2 reconstructed discharge.
 Units are mean daily cubic meters per second (m^3/s) $\times 100.$

Year	0	1	2	3	4	5	6	7	8	9
1699										78
1700	82	76	59	80	91	81	59	75	66	84
1710	78	82	79	78	72	80	74	91	87	98
1720	74	67	84	86	92	93	80	69	56	70
1730	75	69	68	82	54	66	68	87	67	72
1740	76	62	85	77	80	88	87	66	83	72
1750	71	73	78	80	76	76	72	80	93	91
1760	70	80	70	88	81	94	93	88	84	73
1770	85	72	61	63	83	71	74	74	74	57
1780	68	68	76	85	72	77	86	63	63	75
1790	85	89	86	77	81	73	79	72	77	69
1800	75	82	72	81	75	80	86	75	79	81
1810	86	80	64	77	79	95	90	71	90	64
1820	87	68	73	65	71	74	70	86	70	72
1830	73	83	81	81	79	82	82	87	87	78
1840	66	73	70	84	72	78	60	79	94	88
1850	84	89	91	87	83	59	56	68	69	66
1860	61	96	74	54	82	88	75	94	87	64
1870	63	75	69	80	74	76	77	70	61	78
1880	69	61	62	86	95	83	79	88	92	104
1890	92	86	70	65	74	60	77	82	54	71
1900	73	58	76	69	79	85	95	88	86	91
1910	91	84	86	94	82	82	89	80	77	81
1920	81	83	83	72	74	85	72	74	73	69
1930	68	81	72	66	73	63	79	83	71	76
1940	89	80	75	85	72	65	80	73	89	71
1950	68	89	66	79	70	60	81	85	64	73
1960	72	78	62	73	77	72	79	83	90	73
1970	71	75	83	62	80	80	56	85	84	85
1980	95	89	95	77	83	73	83	89	79	67
1990	70	79	80	71	83	60	79	76		



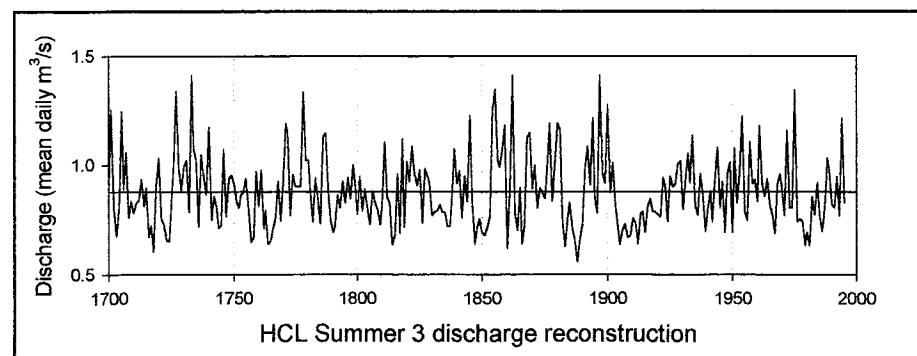
SITE HCL: Winter 3 reconstructed discharge.
 Units are mean daily cubic meters per second (m^3/s) $\times 100.$

Year	0	1	2	3	4	5	6	7	8	9
1702			75	45	88	115	81	34	74	68
1710	99	92	84	77	77	64	92	81	129	100
1720	106	67	51	109	125	110	100	58	48	36
1730	62	86	68	47	85	35	55	69	109	61
1740	51	90	49	98	99	84	92	102	46	79
1750	72	62	75	84	87	71	73	76	96	117
1760	110	50	80	69	114	106	119	119	84	85
1770	58	76	60	44	48	106	74	64	61	66
1780	36	59	79	77	107	72	63	90	48	47
1790	93	121	109	94	65	79	65	78	64	75
1800	66	68	101	66	85	82	80	102	73	80
1810	89	86	80	47	86	104	115	119	48	104
1820	50	86	61	58	56	63	86	62	96	64
1830	63	77	99	93	85	82	91	93	97	86
1840	69	46	72	68	97	59	76	53	88	158
1850	111	89	105	108	75	64	35	33	65	67
1860	69	49	114	88	32	89	159	74	95	89
1870	42	41	86	70	86	78	67	68	64	42
1880	73	62	48	60	124	150	92	77	118	129
1890	146	93	69	52	41	76	52	63	101	34
1900	50	90	40	79	79	96	115	128	108	93
1910	107	109	93	90	117	90	76	101	82	72
1920	89	91	82	85	66	62	98	65	60	67
1930	63	58	85	71	46	73	58	81	105	69
1940	73	111	91	63	84	70	47	98	73	95
1950	74	47	115	55	60	74	46	83	112	47
1960	65	66	80	48	65	93	73	91	92	100
1970	64	59	65	100	50	64	107	39	99	138
1980	98	132	98	109	66	81	75	88	100	72
1990	52	62	86	95	54	89	46			



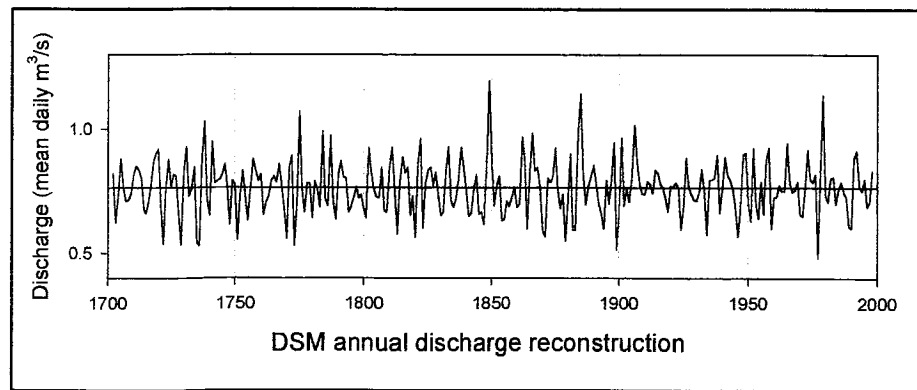
SITE HCL: Summer 3 reconstructed discharge.
 Units are mean daily cubic meters per second (m^3/s) $\times 100$.

Year	0	1	2	3	4	5	6	7	8	9
1698									84	78
1700	88	125	81	67	80	124	89	106	76	83
1710	78	82	84	93	81	90	67	72	60	91
1720	103	75	73	66	65	81	100	134	99	89
1730	99	102	79	141	107	103	72	105	95	87
1740	117	75	86	81	71	72	107	77	94	95
1750	92	84	80	86	88	94	81	65	67	97
1760	81	98	71	79	64	65	71	76	92	74
1770	94	119	115	77	96	90	90	91	133	102
1780	102	88	74	94	85	73	113	115	89	74
1790	69	73	86	80	92	83	94	85	100	89
1800	77	95	79	89	80	73	88	83	80	73
1810	81	111	86	82	64	68	96	69	112	71
1820	101	92	108	96	91	98	74	98	95	92
1830	77	79	79	82	79	78	72	72	84	107
1840	92	97	76	95	83	122	82	64	71	75
1850	69	68	72	77	125	135	102	99	107	118
1860	62	91	141	78	70	89	64	72	112	115
1870	89	100	80	90	87	85	97	119	84	100
1880	119	116	73	63	76	83	71	66	56	66
1890	73	98	108	91	121	85	78	141	96	92
1900	128	88	101	82	74	64	70	73	67	68
1910	76	73	64	78	79	69	81	85	79	79
1920	77	76	94	91	74	95	90	92	101	102
1930	80	94	106	92	114	82	77	96	87	70
1940	80	88	74	93	108	80	92	69	96	101
1950	69	108	83	97	122	79	75	110	92	93
1960	83	118	92	86	94	82	77	69	92	96
1970	89	77	116	81	81	134	74	75	74	63
1980	69	63	85	77	92	76	70	82	103	98
1990	82	81	95	77	121	83	88			



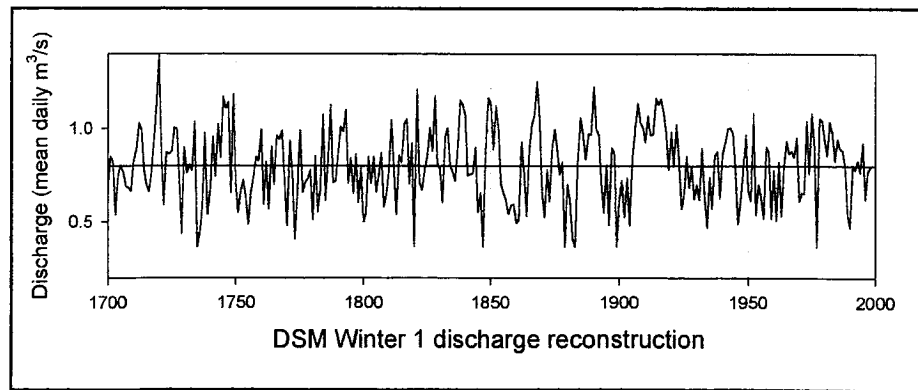
SITE DSM: Annual reconstructed discharge.
 Units are mean daily cubic meters per second (m^3/s) $\times 100.$

Year	0	1	2	3	4	5	6	7	8	9
1702			82	62	73	88	77	71	72	74
1710	82	85	84	80	68	66	70	78	87	90
1720	92	70	54	76	88	77	82	81	66	53
1730	83	93	73	76	85	54	53	88	103	71
1740	65	95	79	79	80	82	86	77	62	79
1750	78	56	73	83	73	63	76	88	83	79
1760	82	66	71	73	79	81	79	86	78	68
1770	56	85	89	53	70	107	76	67	78	78
1780	64	79	76	69	99	72	69	97	71	64
1790	82	87	81	80	67	69	73	77	72	74
1800	68	64	92	83	76	73	72	85	67	67
1810	84	93	76	58	79	89	83	85	65	73
1820	57	87	96	60	78	84	85	77	83	74
1830	65	67	83	93	71	69	72	81	93	85
1840	76	65	66	76	81	66	67	62	85	119
1850	86	69	77	81	63	64	71	69	73	77
1860	69	70	97	87	60	81	98	83	85	77
1870	59	57	80	79	81	92	76	68	74	55
1880	71	90	59	59	98	114	82	70	77	81
1890	85	78	70	66	60	79	70	80	95	52
1900	66	97	69	76	71	80	102	87	78	74
1910	74	79	78	74	84	82	78	77	72	67
1920	77	77	78	77	60	69	89	77	74	72
1930	71	74	84	76	58	79	80	81	90	66
1940	76	89	81	79	76	69	57	68	90	91
1950	71	63	92	70	64	79	66	88	93	60
1960	72	73	77	75	75	94	79	75	76	79
1970	66	65	77	92	80	79	82	48	82	114
1980	73	71	80	81	70	76	79	74	73	61
1990	60	88	91	77	75	80	69	71	83	



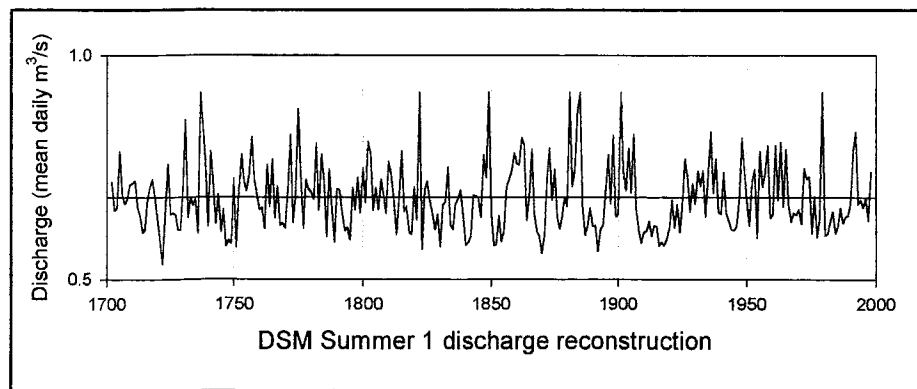
SITE DSM: Winter 1 reconstructed discharge.
 Units are mean daily cubic meters per second (m^3/s) $\times 100$.

Year	0	1	2	3	4	5	6	7	8	9
1700	67	85	83	54	74	80	77	69	68	67
1710	83	89	103	99	78	70	66	76	93	113
1720	140	88	59	87	86	88	100	100	72	44
1730	90	76	81	77	104	37	45	58	97	54
1740	67	95	74	102	84	117	111	114	65	118
1750	71	55	67	72	64	49	66	74	85	83
1760	100	59	82	57	90	70	96	94	99	72
1770	48	94	76	41	64	99	66	71	73	77
1780	51	85	55	67	107	61	83	112	71	72
1790	87	101	98	110	71	84	65	86	60	79
1800	50	55	85	71	85	66	75	87	58	64
1810	78	104	78	54	86	82	103	105	70	92
1820	37	121	71	67	78	86	100	88	117	81
1830	79	60	96	100	81	77	72	89	115	112
1840	107	75	75	76	90	55	65	37	87	116
1850	114	89	112	101	70	66	62	54	59	59
1860	49	52	92	76	53	88	102	107	125	105
1870	67	52	78	61	90	99	89	76	82	37
1880	70	61	41	37	81	105	97	83	97	97
1890	122	100	96	71	55	80	48	89	87	37
1900	62	72	52	73	48	85	101	114	103	101
1910	93	107	96	97	116	113	116	109	98	78
1920	98	80	102	82	57	65	85	68	80	62
1930	70	62	89	64	47	74	57	86	87	63
1940	86	93	100	100	97	78	49	62	78	96
1950	67	61	108	54	70	63	52	90	87	52
1960	78	51	82	53	80	93	87	88	85	95
1970	61	66	65	104	76	108	91	37	105	104
1980	94	86	104	97	83	94	89	88	79	53
1990	47	80	78	83	77	92	62	77	79	



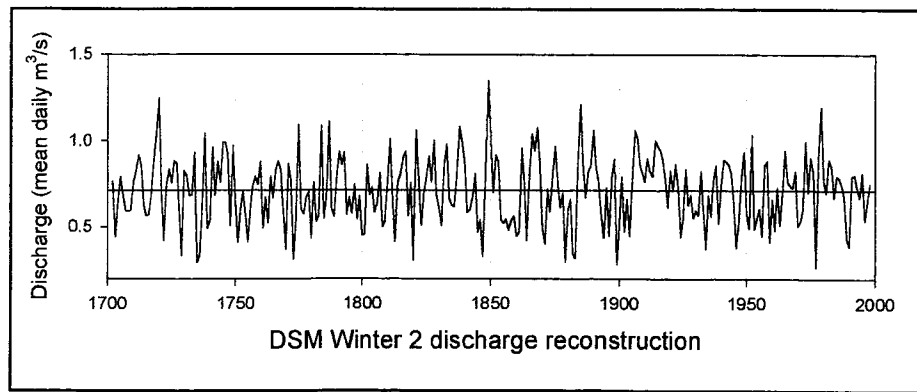
SITE DSM: Summer 1 reconstructed discharge.
 Units are mean daily cubic meters per second (m^3/s) $\times 100$.

Year	0	1	2	3	4	5	6	7	8	9
1702			72	65	66	79	69	67	68	71
1710	71	72	66	64	60	61	68	70	72	68
1720	63	58	53	64	76	65	65	64	61	61
1730	70	86	64	68	67	68	60	92	85	76
1740	62	79	72	62	69	61	65	57	59	58
1750	72	57	70	78	72	70	73	82	72	69
1760	65	66	61	76	66	77	64	71	62	63
1770	61	70	82	63	68	88	73	61	72	70
1780	69	68	80	65	78	72	59	74	66	58
1790	70	70	65	61	62	59	70	65	73	65
1800	75	67	81	78	65	70	65	72	69	65
1810	76	73	68	60	67	79	65	66	61	60
1820	70	63	92	57	70	72	68	65	61	64
1830	57	67	67	75	62	61	67	68	70	64
1840	58	58	59	69	69	68	64	78	73	92
1850	65	58	58	64	58	61	70	72	74	78
1860	76	76	81	80	63	68	79	64	61	59
1870	56	60	72	79	68	74	64	61	64	68
1880	66	92	71	74	88	92	67	60	62	66
1890	62	62	56	61	62	70	78	67	82	64
1900	65	92	74	70	79	69	82	65	61	58
1910	60	61	63	60	62	62	58	58	58	59
1920	62	68	62	67	61	66	77	73	65	71
1930	67	74	71	74	64	73	83	69	77	65
1940	65	74	65	63	61	61	62	67	81	74
1950	68	62	72	74	59	79	71	74	80	64
1960	65	80	68	81	66	79	67	63	65	64
1970	65	62	75	72	73	60	68	59	64	92
1980	60	60	63	65	60	62	66	63	64	64
1990	67	79	83	67	68	66	68	63	74	



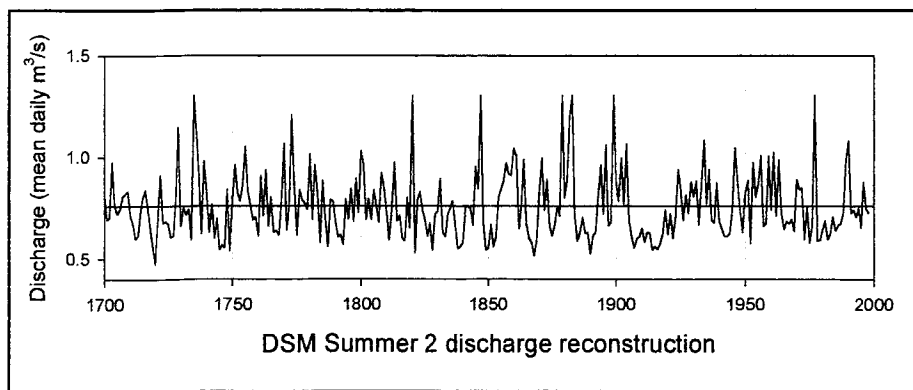
SITE DSM: Winter 2 reconstructed discharge.
 Units are mean daily cubic meters per second (m^3/s) $\times 100.$

Year	0	1	2	3	4	5	6	7	8	9
1702			76	44	64	79	68	59	59	60
1710	76	83	92	86	63	57	57	68	88	105
1720	125	70	42	75	84	76	88	87	58	33
1730	82	80	68	68	93	30	34	63	104	49
1740	54	96	68	87	76	99	99	92	51	97
1750	66	41	60	70	57	42	61	74	79	74
1760	88	49	67	52	79	67	83	88	84	59
1770	37	86	77	31	55	109	60	57	67	70
1780	44	76	53	57	109	55	67	111	61	56
1790	79	94	86	93	57	67	58	75	54	68
1800	45	46	86	69	73	58	64	81	50	53
1810	74	101	69	42	76	81	90	94	56	75
1820	30	106	78	51	70	80	91	76	100	69
1830	61	51	86	98	67	63	62	80	108	99
1840	87	58	60	67	81	47	54	33	81	135
1850	101	70	92	88	54	52	54	48	53	56
1860	45	47	96	75	42	79	104	94	107	87
1870	50	40	72	59	80	97	76	61	70	30
1880	60	66	34	32	87	121	86	67	82	86
1890	106	84	76	57	43	73	45	79	89	28
1900	51	79	47	66	45	77	106	102	87	81
1910	76	90	82	79	100	97	94	89	78	62
1920	83	71	86	72	44	55	83	63	69	55
1930	60	57	82	59	37	68	56	77	86	52
1940	74	89	88	86	81	64	38	53	79	93
1950	58	49	103	49	55	60	45	86	88	42
1960	66	48	72	51	70	94	76	74	73	82
1970	51	53	60	99	70	90	82	27	92	119
1980	77	70	89	85	67	79	78	74	67	43
1990	39	79	80	73	67	81	54	64	75	



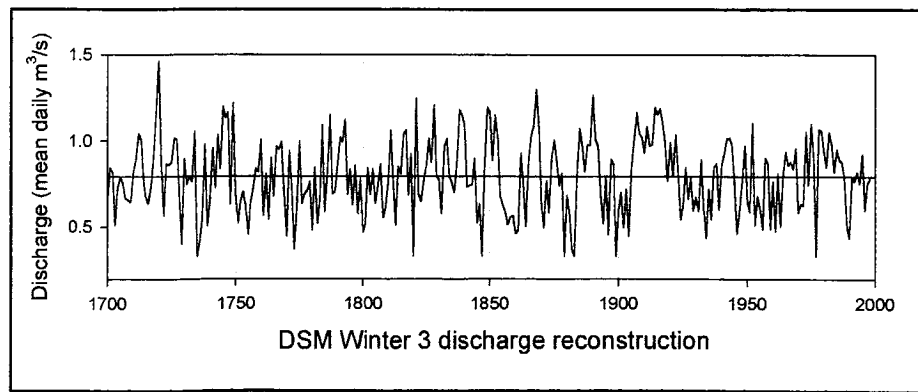
SITE DSM: Summer 2 reconstructed discharge.
 Units are mean daily cubic meters per second (m^3/s) $\times 100.$

Year	0	1	2	3	4	5	6	7	8	9
1700	82	69	71	98	76	72	75	81	82	83
1710	71	67	60	62	74	80	84	76	65	56
1720	48	67	91	68	68	68	61	61	79	115
1730	66	75	72	74	60	130	113	92	63	98
1740	83	64	77	60	70	54	57	56	84	54
1750	79	96	83	78	86	105	84	77	70	71
1760	62	91	71	94	66	80	63	64	62	79
1770	106	64	76	121	86	62	84	79	78	74
1780	101	69	96	83	58	89	70	56	79	79
1790	68	61	62	57	79	70	85	69	90	73
1800	103	97	70	79	70	84	76	68	92	86
1810	74	59	74	98	69	71	60	59	80	65
1820	130	53	79	83	74	69	61	67	54	72
1830	73	90	63	61	72	75	79	67	55	56
1840	58	76	76	75	67	96	84	130	68	55
1850	56	67	56	61	80	84	88	97	92	91
1860	104	101	65	76	99	67	60	58	52	59
1870	83	100	74	89	66	62	67	76	71	130
1880	80	89	120	130	72	59	63	70	63	63
1890	53	61	63	79	96	72	106	67	68	130
1900	88	79	100	77	107	69	61	56	60	61
1910	65	58	63	63	55	56	55	57	62	74
1920	62	72	60	71	94	85	69	81	72	88
1930	81	88	67	86	108	77	94	69	68	87
1940	68	65	61	61	63	74	105	88	74	63
1950	83	89	58	98	80	87	101	66	68	100
1960	74	102	71	99	72	65	68	67	70	64
1970	89	84	85	60	76	58	66	130	59	59
1980	64	69	60	63	71	64	67	67	73	98
1990	108	72	74	71	75	65	88	75	73	



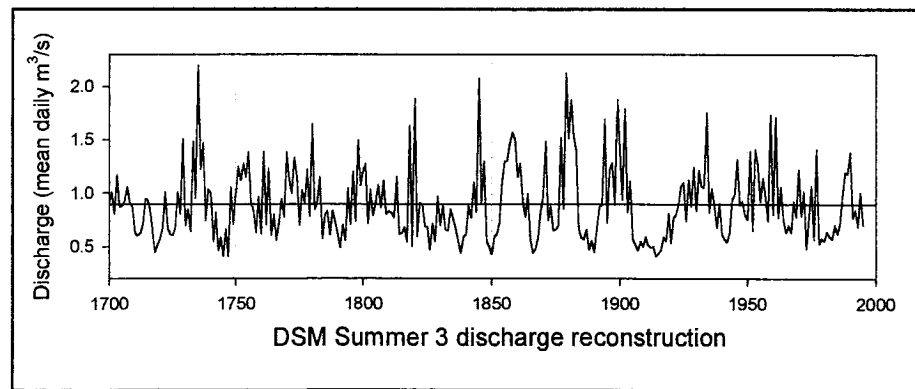
SITE DSM: Winter 3 reconstructed discharge.
 Units are mean daily cubic meters per second (m^3/s) $\times 100.$

Year	0	1	2	3	4	5	6	7	8	9
1700	65	84	82	51	73	79	76	67	66	64
1710	82	89	104	100	76	68	64	74	93	116
1720	146	88	57	87	86	87	102	101	70	40
1730	90	75	80	76	105	33	41	56	98	51
1740	65	96	73	104	84	120	113	116	63	122
1750	70	52	65	70	62	46	64	72	84	82
1760	100	57	81	54	90	68	97	95	100	70
1770	45	94	74	37	61	100	64	69	71	76
1780	48	84	52	65	109	59	82	115	69	70
1790	86	102	99	112	69	84	63	86	58	78
1800	47	52	84	69	84	64	73	87	55	62
1810	76	106	77	51	85	81	104	106	68	92
1820	33	124	70	65	77	85	101	88	121	80
1830	77	58	96	101	80	76	70	89	118	115
1840	109	73	74	75	90	53	63	33	86	119
1850	117	89	115	102	68	63	59	51	56	57
1860	46	49	93	74	50	88	103	109	130	107
1870	64	50	77	59	90	100	89	74	81	33
1880	68	59	38	33	80	107	97	82	98	98
1890	126	101	97	69	52	79	45	89	86	33
1900	60	70	50	72	45	84	102	116	104	102
1910	93	108	97	98	119	115	119	111	98	77
1920	99	79	103	81	54	63	85	66	79	60
1930	68	59	89	62	44	72	54	85	87	60
1940	86	93	101	102	98	77	46	59	77	97
1950	65	59	110	51	68	61	49	90	87	49
1960	76	48	81	50	79	94	86	88	84	96
1970	58	63	63	105	74	110	91	33	107	106
1980	94	85	105	98	82	95	89	88	78	51
1990	44	79	77	82	75	92	60	76	78	



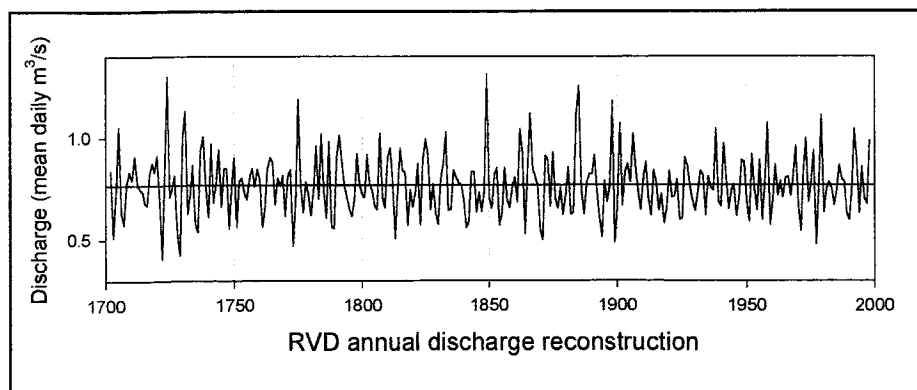
SITE DSM: Summer 3 reconstructed discharge.
 Units are mean daily cubic meters per second (m^3/s) $\times 100.$

Year	0	1	2	3	4	5	6	7	8	9
1700	91	101	81	117	87	88	93	105	91	88
1710	63	60	63	70	94	94	85	64	44	52
1720	57	67	101	67	61	61	68	101	81	151
1730	70	85	64	148	95	220	122	147	74	103
1740	100	55	81	46	58	41	66	41	105	71
1750	101	124	112	128	115	138	91	83	63	96
1760	62	139	70	123	61	80	56	72	94	78
1770	138	113	99	132	115	70	103	91	122	78
1780	164	85	92	115	57	79	83	61	84	73
1790	62	49	70	55	104	71	120	74	150	107
1800	121	127	71	103	78	90	108	86	111	81
1810	83	81	77	115	61	63	68	54	163	50
1820	189	60	91	90	68	69	47	71	54	96
1830	70	88	65	65	85	76	66	55	44	59
1840	61	88	77	110	82	208	91	130	55	50
1850	43	59	62	73	110	130	130	147	157	150
1860	115	128	93	77	99	57	44	47	58	82
1870	97	148	74	88	65	66	70	152	85	212
1880	151	188	153	140	67	58	56	65	47	55
1890	45	70	87	89	169	72	123	128	89	188
1900	141	94	179	82	111	57	52	46	55	50
1910	59	51	49	50	41	44	47	59	55	81
1920	53	77	80	90	106	110	74	112	88	124
1930	84	121	106	105	175	81	104	89	68	90
1940	61	57	54	64	94	98	131	89	93	80
1950	75	139	65	141	126	92	114	98	74	173
1960	80	171	77	106	74	63	70	63	92	77
1970	122	79	101	48	76	106	56	141	53	57
1980	55	63	59	57	70	62	71	98	119	118
1990	138	77	84	68	100	70	102			



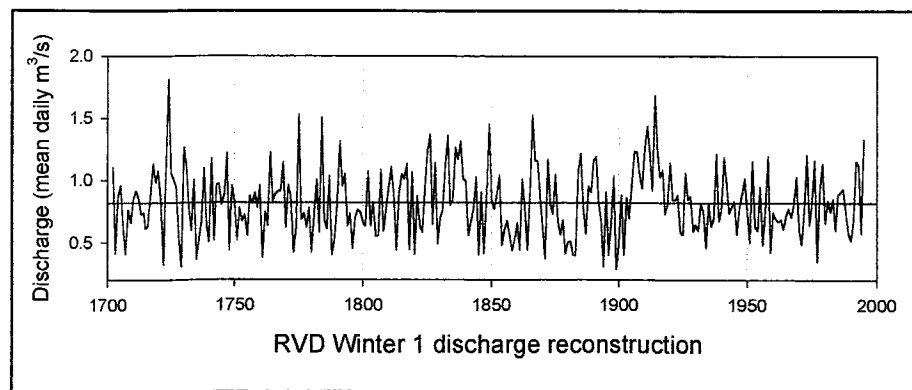
SITE RVD: Annual reconstructed discharge.
 Units are mean daily cubic meters per second (m^3/s) $\times 100.$

Year	0	1	2	3	4	5	6	7	8	9
1702			84	51	72	105	63	57	77	83
1710	79	91	77	75	73	68	67	83	88	83
1720	91	69	41	84	130	71	75	81	53	42
1730	100	113	63	72	87	58	54	94	100	75
1740	61	97	68	77	94	66	85	85	55	75
1750	90	56	79	80	73	70	81	85	76	85
1760	80	56	65	85	90	88	67	80	77	81
1770	62	81	84	47	68	119	76	63	78	73
1780	62	74	96	70	102	74	60	98	56	56
1790	90	101	88	77	71	65	61	70	92	77
1800	72	71	92	78	74	67	65	102	71	66
1810	91	95	78	51	73	95	84	83	57	74
1820	66	73	87	57	89	99	91	65	77	63
1830	57	80	87	103	65	65	84	80	78	77
1840	70	56	59	83	83	64	73	64	74	131
1850	71	65	82	85	57	63	85	69	66	76
1860	81	69	104	93	53	84	112	85	81	77
1870	55	50	91	89	66	93	70	65	75	62
1880	72	86	62	64	112	126	74	63	78	82
1890	82	91	73	61	51	79	69	77	118	49
1900	66	107	67	83	87	78	102	86	74	65
1910	81	88	70	62	84	78	64	72	58	65
1920	84	71	71	79	60	61	90	87	76	69
1930	64	73	84	82	62	81	76	74	104	69
1940	66	97	80	65	74	77	62	70	89	88
1950	70	59	92	75	64	89	60	79	107	57
1960	69	87	72	79	71	80	81	72	82	96
1970	67	54	83	100	69	79	94	48	76	111
1980	64	74	78	75	67	74	87	80	78	63
1990	60	74	104	89	63	86	70	68	98	



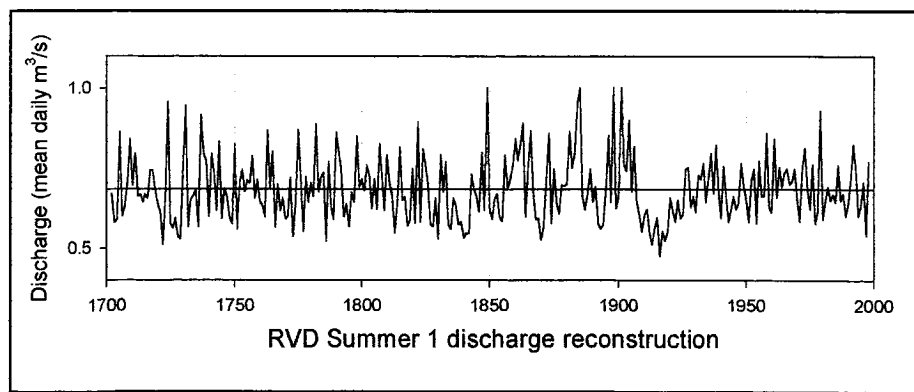
SITE RVD: Winter 1 reconstructed discharge.
 Units are mean daily cubic meters per second (m^3/s) $\times 100$.

Year	0	1	2	3	4	5	6	7	8	9
1702			111	42	87	96	62	41	77	66
1710	86	92	86	73	74	62	63	87	114	99
1720	108	84	32	116	181	106	100	95	57	31
1730	127	111	78	60	100	37	51	67	110	64
1740	50	117	52	97	97	81	89	122	44	96
1750	83	52	78	68	72	56	88	82	90	78
1760	96	38	75	64	122	84	89	91	91	115
1770	63	97	87	42	62	153	69	74	62	78
1780	42	72	100	58	150	69	62	104	40	52
1790	80	131	96	105	64	73	45	70	77	75
1800	66	64	107	63	83	55	56	109	59	75
1810	94	111	89	44	90	105	101	114	44	107
1820	41	87	64	58	94	124	137	65	114	49
1830	70	76	113	136	80	84	126	117	132	102
1840	100	56	67	77	103	40	91	41	87	145
1850	84	77	90	104	48	61	67	56	44	53
1860	66	45	101	78	44	91	152	116	115	87
1870	63	37	116	81	73	104	68	57	68	41
1880	50	51	40	40	107	122	79	57	95	91
1890	116	119	83	67	31	91	40	68	104	29
1900	49	88	40	86	70	97	124	123	104	94
1910	127	144	122	92	169	123	103	108	73	81
1920	115	84	84	88	58	57	106	84	87	59
1930	65	60	81	75	46	82	63	70	121	68
1940	76	119	98	74	79	84	56	77	89	102
1950	75	50	115	64	60	95	48	76	119	42
1960	74	69	67	69	61	72	77	70	80	102
1970	60	48	75	121	64	81	116	35	94	114
1980	66	84	75	85	60	89	91	93	76	58
1990	52	69	115	112	58	133	66			



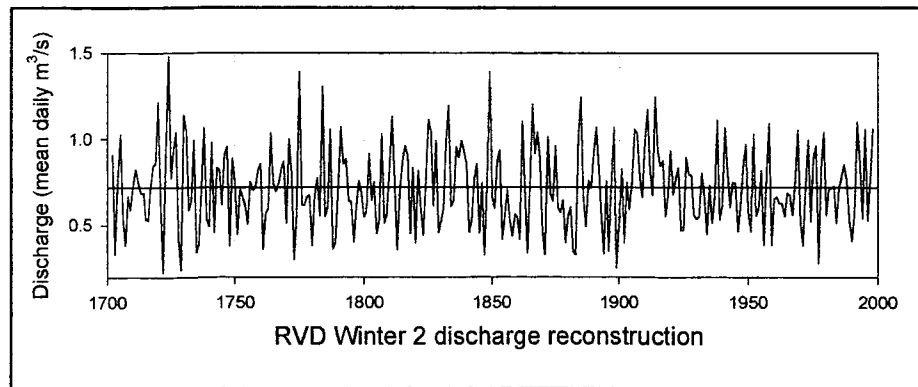
SITE RVD: Summer 1 reconstructed discharge.
 Units are mean daily cubic meters per second (m^3/s) $\times 100.$

Year	0	1	2	3	4	5	6	7	8	9
1702			67	58	59	86	60	63	71	84
1710	70	79	66	67	64	67	66	74	74	68
1720	64	61	51	66	96	58	56	59	54	53
1730	76	95	57	65	66	68	57	92	79	77
1740	60	79	73	62	83	59	69	66	60	58
1750	82	56	71	74	68	71	70	79	66	71
1760	65	63	60	87	69	80	57	70	62	66
1770	59	60	72	54	64	87	72	55	72	64
1780	70	66	89	67	72	74	52	77	63	59
1790	86	80	74	60	64	57	67	64	85	69
1800	71	68	76	73	62	71	62	83	72	62
1810	79	70	67	55	64	81	65	66	57	59
1820	75	58	89	58	81	76	70	57	57	65
1830	53	79	68	77	57	56	65	63	57	58
1840	53	55	55	73	68	66	61	80	62	100
1850	62	59	66	67	60	58	79	69	71	76
1860	84	77	82	89	60	75	87	68	59	59
1870	52	56	71	86	58	75	64	61	70	69
1880	70	87	75	80	95	100	66	62	67	75
1890	64	69	58	56	57	68	85	64	100	62
1900	66	100	76	74	90	67	82	65	61	55
1910	60	62	54	51	56	60	48	55	52	55
1920	66	62	58	65	59	61	75	75	63	66
1930	61	73	71	77	64	72	79	67	82	68
1940	59	76	67	58	62	66	62	64	77	69
1950	65	58	71	75	58	77	66	66	86	63
1960	61	84	66	75	69	74	75	70	71	75
1970	66	58	75	81	68	62	76	58	61	93
1980	59	65	69	65	67	64	76	65	67	60
1990	64	72	82	74	60	63	71	54	77	



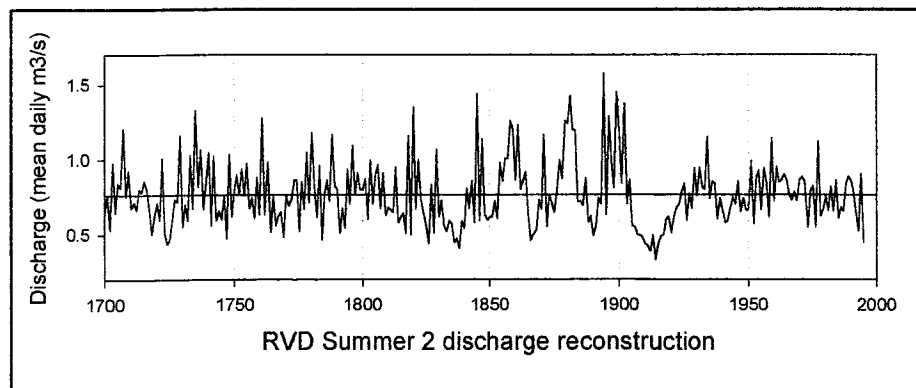
SITE RVD: Winter 2 reconstructed discharge.
 Units are mean daily cubic meters per second (m^3/s) $\times 100$.

Year	0	1	2	3	4	5	6	7	8	9
1702			91	33	78	103	54	38	67	59
1710	73	83	74	69	69	54	53	73	85	86
1720	121	65	23	94	148	77	93	104	42	24
1730	114	105	59	64	100	34	39	69	106	54
1740	49	98	46	84	82	62	91	96	38	89
1750	75	45	71	67	62	51	75	70	73	83
1760	86	36	57	60	103	75	70	75	83	87
1770	51	100	81	30	56	139	62	62	66	68
1780	38	67	78	56	131	55	61	106	36	40
1790	70	107	86	89	64	63	40	61	76	69
1800	55	58	91	64	75	45	53	103	51	56
1810	82	113	76	36	70	87	96	91	45	83
1820	40	81	60	44	76	111	104	62	99	46
1830	52	60	99	119	61	64	95	89	99	93
1840	86	46	53	77	86	45	75	33	74	139
1850	67	60	88	94	42	56	70	53	44	56
1860	54	42	110	71	34	74	120	92	104	89
1870	47	33	101	69	64	96	60	57	64	40
1880	56	60	35	33	101	124	67	49	76	71
1890	92	107	84	55	34	76	35	77	107	26
1900	51	83	40	75	59	75	106	103	79	66
1910	98	117	82	68	124	94	85	88	55	67
1920	93	68	78	84	47	47	89	80	79	56
1930	54	55	80	67	45	73	52	66	111	53
1940	61	106	81	61	75	75	47	61	83	97
1950	58	46	103	55	60	81	39	78	109	38
1960	65	66	63	63	55	69	68	56	76	105
1970	52	38	73	100	52	88	96	28	83	104
1980	56	71	71	72	51	71	79	85	76	52
1990	41	58	110	87	54	106	53	77	106	



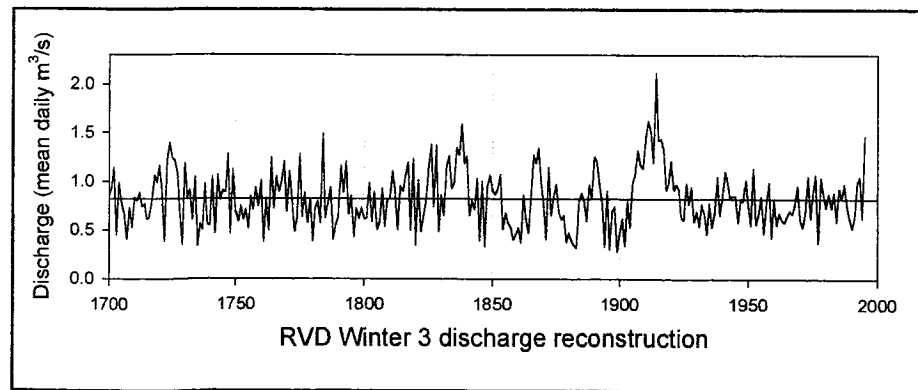
SITE RVD: Summer 2 reconstructed discharge.
 Units are mean daily cubic meters per second (m^3/s) $\times 100$.

Year	0	1	2	3	4	5	6	7	8	9
1700	63	76	53	98	65	84	81	121	75	92
1710	68	71	66	80	78	86	80	68	50	62
1720	71	60	101	51	44	47	60	73	72	116
1730	56	70	59	103	67	133	82	106	67	85
1740	104	56	102	59	66	60	76	48	103	62
1750	79	90	77	94	76	98	67	74	61	88
1760	63	128	63	98	52	76	56	62	65	48
1770	77	69	73	86	87	52	85	67	105	71
1780	118	81	61	96	47	77	86	72	117	83
1790	80	51	67	54	93	70	109	77	91	80
1800	80	87	60	100	70	90	96	67	91	63
1810	68	66	65	95	58	61	64	51	116	50
1820	135	67	100	74	64	56	44	83	51	107
1830	62	73	56	52	59	57	45	47	41	59
1840	54	81	67	86	58	144	59	114	63	60
1850	62	62	72	61	98	86	101	101	126	121
1860	86	123	80	86	92	65	46	50	54	73
1870	67	117	56	77	71	65	80	100	87	126
1880	124	143	120	120	72	72	70	88	58	62
1890	49	56	74	71	158	63	129	100	81	145
1900	119	84	137	70	87	56	56	50	49	48
1910	44	43	39	49	33	44	49	50	60	62
1920	51	62	68	70	79	84	59	77	67	94
1930	76	95	82	80	115	74	86	84	60	74
1940	66	58	59	68	75	70	86	65	74	66
1950	67	99	57	88	93	67	94	84	62	114
1960	73	95	85	87	90	87	77	73	79	72
1970	87	88	86	55	79	82	55	112	62	66
1980	75	66	82	66	87	61	68	66	84	89
1990	87	79	65	53	91	45	77			



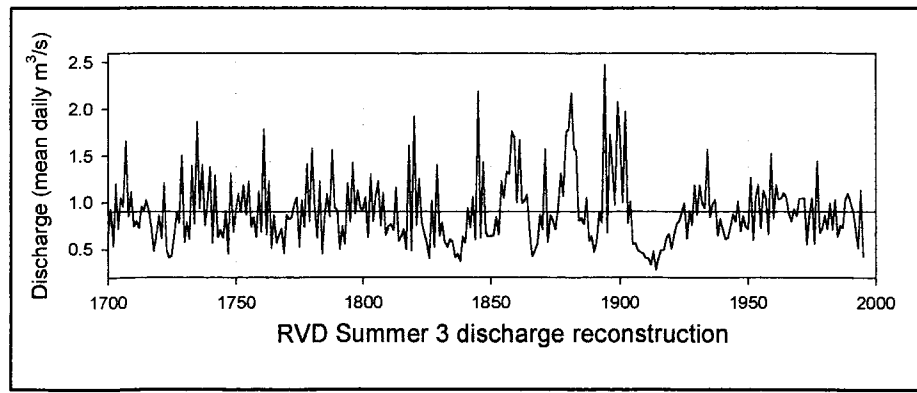
SITE RVD: Winter 3 reconstructed discharge.
 Units are mean daily cubic meters per second (m^3/s) $\times 100.$

Year	0	1	2	3	4	5	6	7	8	9
1700	86	93	114	45	99	78	67	41	73	53
1710	84	80	88	74	77	61	64	80	106	99
1720	116	92	38	122	140	124	121	109	67	36
1730	119	84	91	61	104	34	57	50	97	56
1740	54	104	46	106	81	90	89	128	47	112
1750	69	59	75	61	71	52	85	71	93	74
1760	101	38	83	50	124	72	105	89	100	120
1770	69	110	82	49	63	128	64	88	57	81
1780	38	72	79	57	149	62	76	94	40	56
1790	64	116	88	120	66	85	43	72	62	72
1800	62	62	98	58	89	51	58	93	54	81
1810	83	110	91	50	95	90	107	119	49	123
1820	35	101	49	65	80	115	138	74	137	48
1830	86	65	116	126	93	99	134	127	159	119
1840	126	65	80	71	103	39	100	33	95	106
1850	90	87	93	107	51	68	58	53	40	46
1860	52	37	86	60	47	83	127	119	135	99
1870	76	41	115	65	84	97	70	61	65	38
1880	47	39	34	32	80	88	80	60	96	83
1890	125	120	96	79	34	91	31	70	74	28
1900	47	62	34	79	53	98	108	132	117	114
1910	146	162	152	119	211	142	144	132	91	98
1920	121	91	97	92	64	60	99	77	94	59
1930	69	55	77	67	46	77	53	69	105	65
1940	84	110	100	83	86	85	58	80	80	101
1950	76	55	113	57	68	84	47	78	99	42
1960	80	56	67	61	58	66	70	67	77	95
1970	60	53	68	105	62	88	107	37	104	87
1980	73	87	73	89	59	93	82	98	76	63
1990	52	64	99	105	63	146	62			



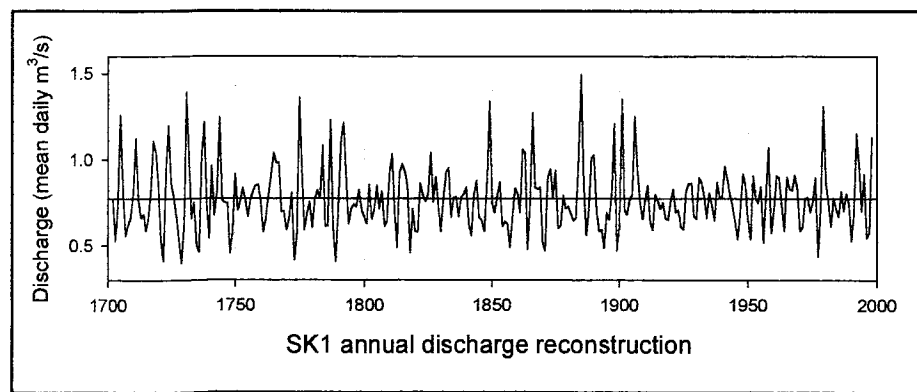
SITE RVD: Summer 3 reconstructed discharge.
 Units are mean daily cubic meters per second (m^3/s) $\times 100$.

Year	0	1	2	3	4	5	6	7	8	9
1700	67	93	54	120	72	104	96	166	86	112
1710	74	80	73	96	92	103	92	73	48	66
1720	86	62	121	50	41	44	65	90	78	150
1730	58	79	61	139	78	186	94	140	76	99
1740	139	57	129	63	71	62	91	45	132	68
1750	91	110	90	118	87	122	74	84	63	112
1760	69	179	66	123	52	86	57	66	72	46
1770	87	82	84	98	105	53	102	74	141	80
1780	157	96	62	122	46	86	109	85	156	95
1790	92	50	74	55	121	79	142	88	113	95
1800	92	106	63	130	80	107	123	75	110	65
1810	74	76	70	116	59	64	71	50	161	49
1820	192	76	126	81	68	58	40	102	52	140
1830	64	79	58	53	61	58	41	45	37	64
1840	57	94	73	106	60	220	62	143	68	64
1850	65	65	85	65	123	105	133	131	176	170
1860	100	168	99	103	108	69	43	49	56	87
1870	71	157	58	86	81	71	95	132	107	175
1880	179	217	158	155	81	84	77	106	59	64
1890	48	59	89	79	248	68	173	137	98	208
1900	167	100	197	78	101	55	57	50	48	46
1910	41	40	33	48	28	41	49	49	62	66
1920	51	65	77	81	90	100	62	91	76	119
1930	87	118	99	94	157	84	99	103	64	82
1940	71	61	62	74	88	79	101	69	86	74
1950	72	127	60	105	119	72	113	105	66	152
1960	83	119	104	105	110	106	88	80	93	86
1970	104	104	104	55	90	104	56	144	67	73
1980	86	72	99	71	103	64	75	73	104	110
1990	101	91	72	52	113	42	86			



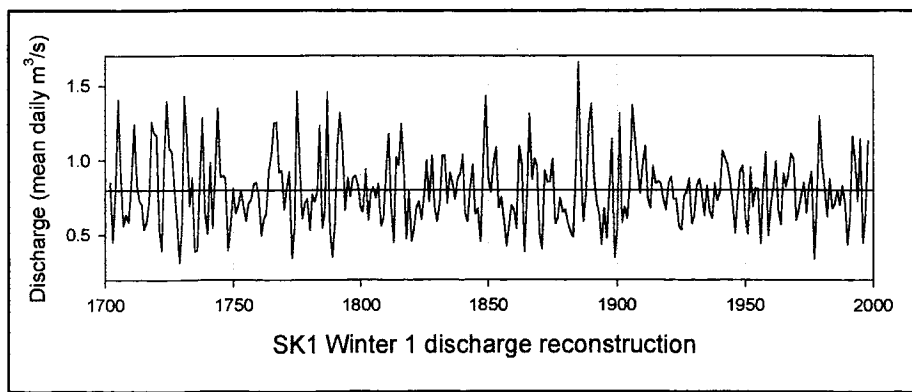
SITE SK1: Annual reconstructed discharge.
 Units are mean daily cubic meters per second (m^3/s) $\times 100$.

Year	0	1	2	3	4	5	6	7	8	9
1702			77	53	72	126	80	56	62	67
1710	81	112	77	66	69	59	65	80	111	105
1720	86	54	41	94	120	87	79	68	54	40
1730	62	139	103	66	75	50	46	101	122	74
1740	54	96	68	81	124	77	75	75	46	58
1750	92	71	76	84	77	67	77	82	85	86
1760	76	58	66	79	91	104	98	98	70	70
1770	59	66	81	42	57	136	94	59	69	76
1780	61	77	82	78	108	62	62	123	60	41
1790	72	111	122	91	63	71	74	72	83	71
1800	67	63	86	65	71	85	71	81	61	65
1810	93	103	70	49	92	98	93	85	46	71
1820	58	58	86	79	76	80	104	76	90	74
1830	58	76	93	95	67	78	78	67	78	80
1840	84	62	56	80	88	67	65	58	88	134
1850	75	69	79	87	62	64	63	49	66	83
1860	80	69	106	104	48	74	127	84	83	84
1870	52	47	90	94	78	94	60	62	79	72
1880	73	69	65	66	101	150	88	56	71	101
1890	103	71	58	59	49	69	65	81	121	47
1900	61	135	71	68	77	80	125	94	76	65
1910	77	85	64	59	80	76	71	75	66	65
1920	76	83	70	71	61	60	82	86	86	67
1930	66	90	87	79	66	81	73	65	87	79
1940	78	96	89	80	74	64	54	70	92	85
1950	65	54	91	78	75	85	52	81	107	58
1960	70	91	90	74	59	90	83	82	91	83
1970	59	61	78	78	70	75	90	44	71	131
1980	88	75	62	78	72	67	81	70	80	75
1990	53	69	115	97	70	91	55	58	113	



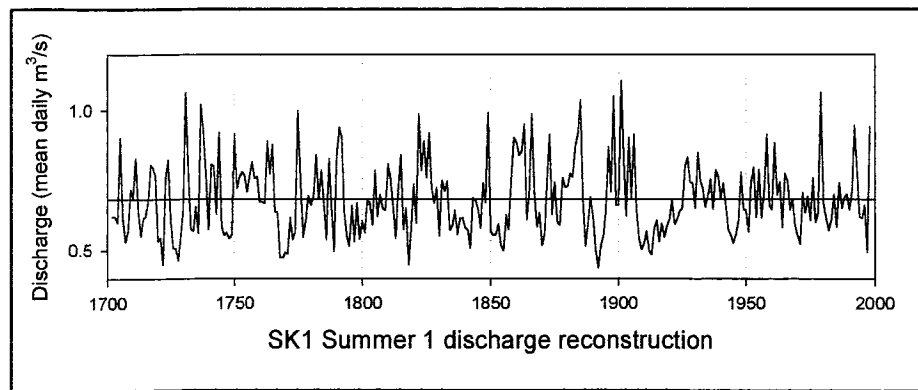
SITE SK1: Winter 1 reconstructed discharge.
 Units are mean daily cubic meters per second (m^3/s) $\times 100.$

Year	0	1	2	3	4	5	6	7	8	9
1702			85	45	79	141	92	57	64	58
1710	85	124	84	73	70	54	59	73	126	118
1720	117	53	40	100	140	108	106	83	60	32
1730	58	143	112	70	88	39	40	87	129	65
1740	51	98	55	90	135	89	90	88	40	58
1750	81	64	70	80	70	60	71	74	84	85
1760	77	49	61	65	93	104	125	125	92	93
1770	67	82	92	34	55	146	100	61	71	74
1780	54	77	72	79	123	55	66	146	54	35
1790	58	110	132	109	67	88	76	88	90	83
1800	69	66	94	60	78	82	75	84	56	62
1810	92	117	69	45	102	97	124	95	47	80
1820	46	54	68	72	60	76	100	72	103	69
1830	59	71	103	103	71	91	85	74	88	91
1840	104	64	59	82	97	64	67	46	99	143
1850	88	79	98	109	68	75	60	42	55	70
1860	67	54	110	97	39	72	132	87	101	97
1870	51	41	93	85	85	101	58	61	75	65
1880	67	58	53	49	95	166	96	59	77	123
1890	138	89	72	65	43	68	48	81	114	35
1900	55	132	58	69	61	82	137	115	94	78
1910	98	109	75	68	96	85	86	85	74	67
1920	85	89	74	74	56	53	76	79	88	58
1930	63	84	87	77	63	83	66	61	85	73
1940	79	107	102	97	87	72	51	74	93	97
1950	63	51	95	69	81	81	44	82	106	50
1960	70	82	99	67	57	91	82	91	104	101
1970	60	67	77	85	65	84	92	34	72	129
1980	98	82	62	88	68	71	80	70	83	72
1990	44	62	116	100	73	114	45	64	113	



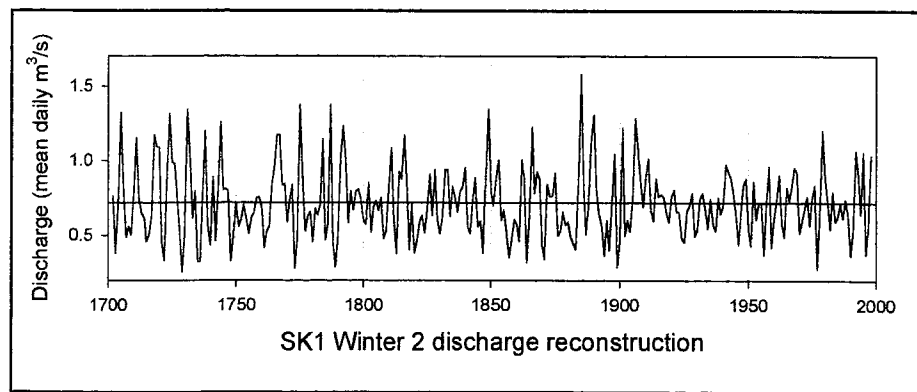
SITE SK1: Summer 1 reconstructed discharge.
 Units are mean daily cubic meters per second (m^3/s) $\times 100$.

Year	0	1	2	3	4	5	6	7	8	9
1702			62	62	60	90	62	53	57	72
1710	69	83	64	55	62	62	67	81	80	77
1720	53	54	45	76	82	60	51	51	47	55
1730	64	106	79	58	57	65	56	102	93	78
1740	57	81	80	63	92	58	55	56	54	56
1750	92	72	77	78	77	71	77	81	76	76
1760	67	67	67	89	77	88	64	64	47	47
1770	49	49	62	54	57	100	76	55	60	70
1780	66	70	84	68	79	66	54	83	65	50
1790	83	94	90	64	55	52	66	53	67	54
1800	60	56	68	67	59	79	62	70	65	64
1810	81	76	66	54	71	84	58	65	45	57
1820	73	60	99	79	89	76	92	72	67	72
1830	55	75	71	75	57	59	64	56	61	62
1840	58	57	51	69	68	65	58	74	67	99
1850	57	55	56	59	52	50	63	58	76	90
1860	89	84	86	95	61	70	99	71	58	64
1870	52	56	75	91	63	74	60	59	76	73
1880	73	77	76	87	92	104	69	52	59	69
1890	62	50	44	52	55	65	87	71	105	67
1900	66	111	83	62	90	69	91	65	55	50
1910	52	57	50	49	58	61	53	59	55	59
1920	61	68	60	61	64	65	80	83	74	74
1930	65	85	75	72	66	70	75	65	79	76
1940	69	74	67	57	56	53	56	61	78	65
1950	64	57	75	80	62	79	62	71	91	66
1960	65	88	70	74	58	77	75	65	68	59
1970	55	52	71	63	69	61	76	60	64	106
1980	67	62	57	61	70	58	74	65	69	70
1990	65	71	95	79	62	62	66	49	94	



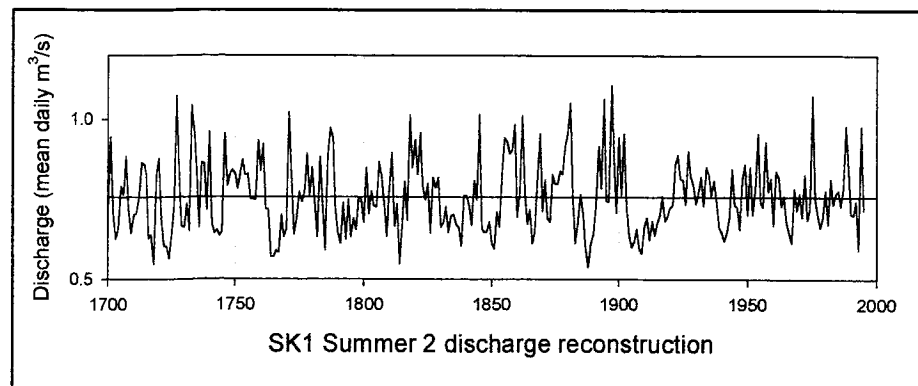
SITE SK1: Winter 2 reconstructed discharge.
 Units are mean daily cubic meters per second (m^3/s) $\times 100$.

Year	0	1	2	3	4	5	6	7	8	9
1702			76	38	70	132	83	49	56	50
1710	76	115	75	65	62	46	50	64	117	109
1720	109	46	33	91	131	99	98	74	52	26
1730	50	134	104	61	79	32	33	77	120	57
1740	43	89	46	81	126	80	81	79	33	50
1750	72	56	61	71	61	51	62	65	75	76
1760	68	42	53	56	84	95	117	117	84	85
1770	59	73	84	28	47	137	91	53	63	66
1780	46	68	63	70	114	47	58	137	46	29
1790	50	101	123	101	58	79	67	79	81	75
1800	60	57	85	52	69	73	66	75	48	53
1810	83	109	60	38	93	88	117	86	40	71
1820	38	46	59	63	51	67	90	63	94	60
1830	51	62	94	94	63	83	76	66	79	82
1840	96	56	51	73	88	56	59	38	90	134
1850	80	70	89	100	60	67	52	35	47	61
1860	58	46	100	88	32	64	122	78	93	88
1870	44	34	84	76	76	92	50	53	66	57
1880	59	50	45	41	86	158	87	51	69	115
1890	130	81	64	56	36	60	40	72	104	29
1900	47	122	50	60	52	73	128	107	85	69
1910	89	101	67	60	88	76	77	76	65	59
1920	76	80	66	66	48	45	67	70	78	50
1930	54	74	78	68	54	74	57	53	75	64
1940	70	98	93	89	78	64	44	65	84	88
1950	54	43	86	60	72	71	37	73	96	42
1960	61	73	90	58	49	82	73	82	95	92
1970	52	59	68	76	57	75	83	28	64	120
1980	89	73	54	79	59	62	71	61	74	64
1990	36	54	106	91	64	106	38	56	104	



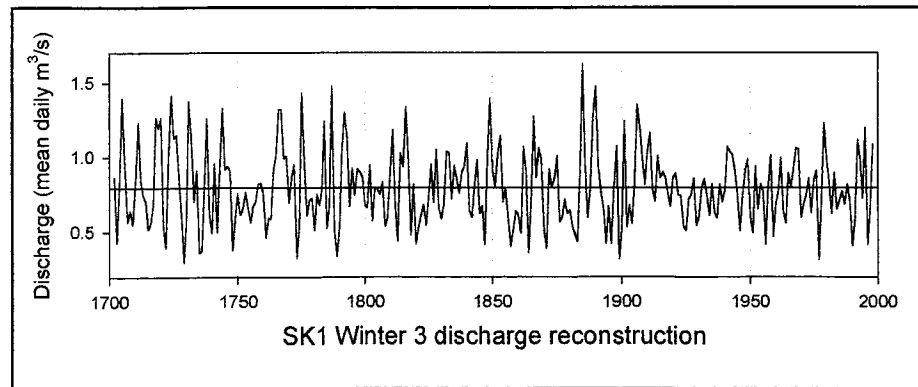
SITE SK1: Summer 2 reconstructed discharge.
 Units are mean daily cubic meters per second (m^3/s) $\times 100.$

Year	0	1	2	3	4	5	6	7	8	9
1698									71	71
1700	69	95	70	63	66	79	77	89	72	64
1710	70	71	75	87	86	83	63	64	55	82
1720	88	69	60	60	57	64	73	107	85	67
1730	66	74	65	104	97	84	66	87	86	72
1740	96	67	65	65	64	65	96	79	83	84
1750	83	78	83	87	83	83	75	75	75	94
1760	84	92	72	72	57	57	59	58	70	63
1770	66	102	83	64	69	77	74	77	89	76
1780	85	74	63	88	73	59	89	97	94	72
1790	65	61	74	63	75	63	69	65	76	75
1800	68	85	70	77	73	73	87	82	74	64
1810	79	90	67	73	55	66	81	69	101	85
1820	94	83	96	79	75	80	65	82	79	82
1830	66	68	73	65	70	70	67	66	60	76
1840	76	73	67	81	75	102	66	65	65	68
1850	61	60	71	67	82	94	93	89	91	98
1860	70	77	101	78	67	72	61	65	82	96
1870	71	81	69	68	83	80	80	84	83	92
1880	96	105	77	61	68	77	71	60	54	61
1890	64	73	92	79	106	75	74	111	89	71
1900	94	77	96	73	64	60	62	66	60	58
1910	67	69	63	68	64	68	70	76	68	70
1920	72	73	86	89	81	81	73	90	82	79
1930	74	77	82	73	85	83	76	81	75	66
1940	65	62	65	70	85	73	73	66	81	86
1950	70	85	70	78	96	74	73	93	77	81
1960	67	84	82	73	76	68	65	62	78	72
1970	77	70	83	69	72	107	75	70	66	70
1980	78	67	81	73	77	78	73	79	98	85
1990	70	70	74	59	98	72	71			



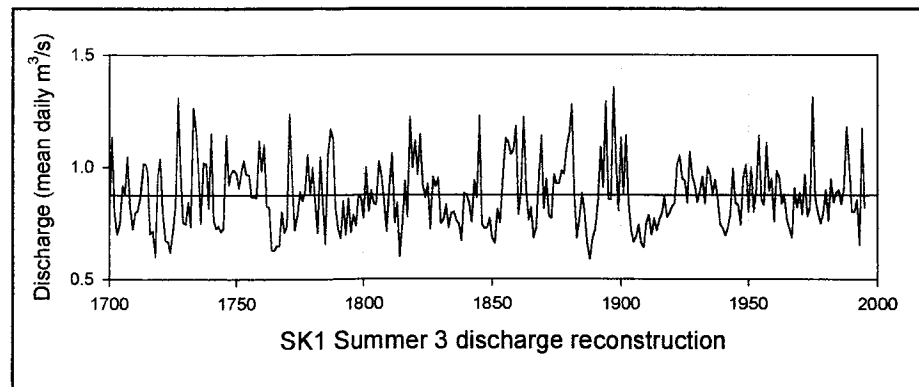
SITE SK1: Winter 3 reconstructed discharge.
 Units are mean daily cubic meters per second (m^3/s) $\times 100$.

Year	0	1	2	3	4	5	6	7	8	9
1702			86	43	80	140	94	57	64	55
1710	84	123	85	75	70	52	56	69	127	119
1720	127	53	40	99	141	113	115	87	62	30
1730	56	137	112	70	91	36	38	80	126	62
1740	49	96	50	92	132	92	94	92	38	58
1750	76	62	66	77	66	56	67	70	82	82
1760	76	46	59	59	91	101	132	132	99	101
1770	70	87	95	33	54	143	99	61	71	73
1780	51	75	68	78	124	52	67	148	51	34
1790	53	106	130	114	68	93	75	92	90	87
1800	68	66	95	58	79	79	75	83	53	60
1810	89	119	67	44	103	94	134	97	48	82
1820	42	53	62	68	54	73	95	70	105	66
1830	59	68	104	103	72	95	85	76	90	94
1840	109	64	60	81	98	62	68	42	100	140
1850	92	81	103	115	70	79	58	41	51	64
1860	61	49	107	92	36	70	127	86	106	99
1870	51	39	92	80	86	101	57	60	72	62
1880	64	54	49	43	90	163	96	59	79	127
1890	148	95	77	66	42	67	42	80	107	32
1900	52	124	53	68	55	81	135	120	99	81
1910	104	116	79	71	101	86	90	87	76	67
1920	87	89	75	74	54	51	72	75	86	54
1930	61	79	85	75	61	82	62	59	82	70
1940	78	107	104	102	91	74	50	74	91	99
1950	61	49	94	65	82	77	42	80	101	47
1960	68	77	100	64	56	89	80	92	106	106
1970	60	69	75	86	63	85	91	31	72	123
1980	99	83	62	90	65	71	77	69	82	70
1990	41	59	111	99	73	120	42	66	109	



SITE SK1: Summer 3 reconstructed discharge.
 Units are mean daily cubic meters per second (m^3/s) $\times 100$.

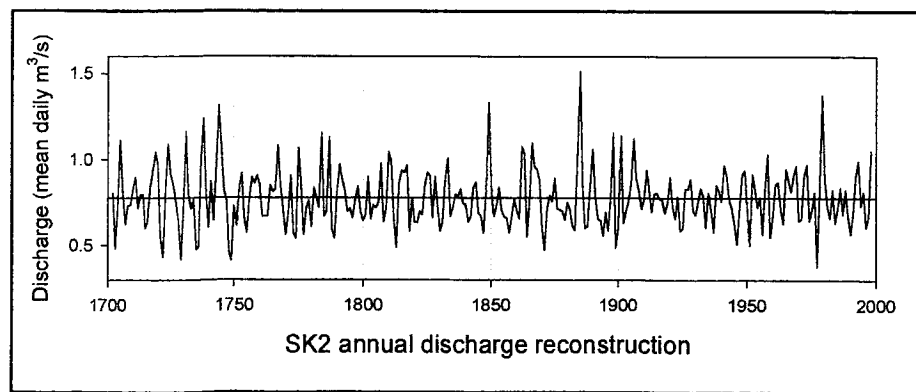
Year	0	1	2	3	4	5	6	7	8	9
1698									80	80
1700	78	113	80	70	74	92	88	104	82	72
1710	80	80	87	102	101	97	70	71	60	96
1720	104	78	67	67	62	72	83	131	100	75
1730	74	84	73	126	116	99	75	102	101	82
1740	115	76	72	73	71	73	114	92	97	99
1750	97	91	97	103	96	97	87	87	86	112
1760	98	110	82	82	63	63	65	65	80	71
1770	74	124	97	72	78	89	85	89	105	88
1780	100	85	70	104	84	66	105	117	113	82
1790	72	68	85	70	86	71	78	73	87	86
1800	77	100	80	89	84	83	102	96	85	71
1810	91	106	75	84	60	75	94	78	122	100
1820	112	97	115	92	86	92	72	95	91	95
1830	75	76	83	73	79	80	76	74	67	88
1840	88	84	75	94	86	123	74	72	73	77
1850	68	66	81	75	96	113	111	106	107	118
1860	79	89	122	91	76	82	68	73	96	114
1870	81	94	78	77	96	92	93	98	97	109
1880	115	128	89	68	77	88	80	66	59	68
1890	72	84	109	91	129	86	85	136	104	81
1900	113	88	114	84	71	67	69	74	66	64
1910	75	79	70	77	72	77	79	87	77	79
1920	83	84	101	105	95	94	84	107	96	92
1930	84	89	96	84	100	97	88	94	86	74
1940	73	69	73	79	99	84	83	74	95	101
1950	80	100	80	91	114	85	83	111	89	95
1960	76	98	95	84	88	76	72	69	91	82
1970	89	79	96	78	82	131	87	80	75	79
1980	90	76	94	84	89	90	83	91	118	100
1990	80	80	85	65	117	82	81			



SITE SK2: Annual reconstructed discharge.

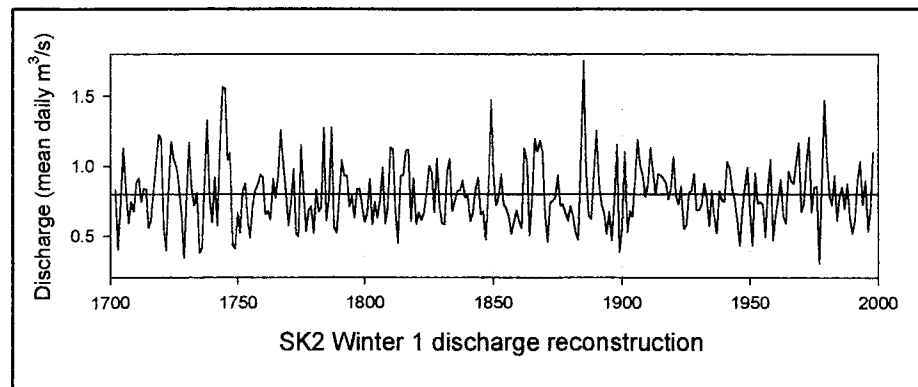
Units are mean daily cubic meters per second (m^3/s) $\times 100$.

Year	0	1	2	3	4	5	6	7	8	9
1702			80	48	72	111	80	63	73	74
1710	84	90	72	79	79	60	64	84	94	105
1720	97	56	44	83	109	92	85	75	63	42
1730	76	116	80	71	77	48	50	100	124	80
1740	61	87	65	97	131	108	82	77	47	41
1750	73	62	85	92	66	58	77	90	86	91
1760	86	67	67	67	85	81	83	108	86	72
1770	57	69	91	57	54	107	86	57	72	76
1780	61	84	78	72	116	67	70	113	60	54
1790	81	97	88	82	70	72	66	77	84	70
1800	65	68	90	65	74	72	75	98	64	71
1810	105	99	66	49	86	94	93	97	58	78
1820	64	64	70	68	86	93	90	66	90	74
1830	58	64	89	101	67	72	80	78	83	75
1840	74	64	67	84	87	69	67	57	82	133
1850	86	67	73	84	71	67	66	58	67	77
1860	70	66	108	104	55	75	110	96	94	88
1870	60	48	72	79	76	89	72	71	70	65
1880	75	71	62	59	106	151	86	60	62	85
1890	106	79	66	65	56	70	59	79	116	49
1900	61	114	63	70	76	86	112	89	82	71
1910	77	94	82	70	80	81	77	77	69	75
1920	90	73	66	78	59	60	83	83	89	71
1930	68	76	83	79	61	81	71	58	85	82
1940	76	97	91	77	72	63	51	73	92	94
1950	73	50	92	83	72	78	57	85	103	55
1960	67	86	87	71	63	95	88	81	91	96
1970	65	66	91	97	65	71	81	38	81	137
1980	88	73	66	83	63	72	84	69	82	67
1990	57	69	91	99	73	81	61	67	105	



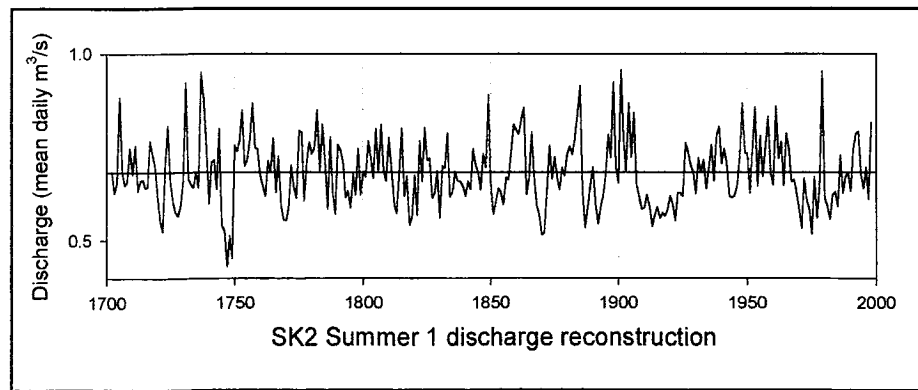
SITE SK2: Winter 1 reconstructed discharge.
 Units are mean daily cubic meters per second (m^3/s) $\times 100$.

Year	0	1	2	3	4	5	6	7	8	9
1702			83	40	73	113	82	59	74	68
1710	89	91	74	84	83	56	61	82	101	122
1720	120	56	40	85	117	104	99	85	66	34
1730	77	117	84	72	81	38	42	90	133	77
1740	60	91	57	116	156	156	104	109	45	41
1750	66	52	82	87	60	48	71	82	86	94
1760	92	65	68	61	91	77	93	125	102	82
1770	57	73	98	52	50	115	83	53	68	71
1780	52	83	67	70	127	61	76	128	56	52
1790	78	104	93	93	71	78	63	83	84	71
1800	60	66	91	58	74	63	75	99	59	71
1810	113	112	67	45	93	94	111	112	61	91
1820	59	67	62	66	81	100	96	67	105	72
1830	59	58	96	105	68	75	82	82	90	77
1840	79	60	66	83	91	66	67	47	84	147
1850	94	72	79	94	73	70	63	51	60	68
1860	61	55	113	103	50	76	119	110	118	110
1870	66	46	74	75	77	94	71	73	67	61
1880	71	65	53	47	108	175	97	65	62	94
1890	125	89	72	66	51	67	47	77	115	38
1900	56	110	52	68	64	89	119	100	93	78
1910	87	113	96	80	94	93	91	88	76	84
1920	106	79	72	85	55	58	80	82	94	68
1930	69	73	88	78	57	82	64	52	82	75
1940	74	103	98	84	76	61	43	68	85	99
1950	68	43	95	73	74	72	49	84	104	47
1960	65	77	90	64	59	96	89	87	103	116
1970	67	73	102	121	67	85	85	30	89	147
1980	104	79	72	93	61	78	85	70	88	63
1990	52	61	90	103	72	89	53	69	109	



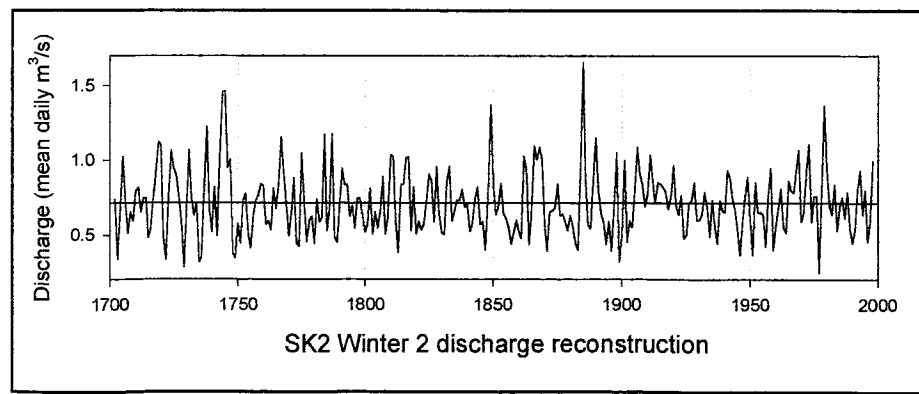
SITE SK2: Summer 1 reconstructed discharge.
 Units are mean daily cubic meters per second (m^3/s) $\times 100.$

Year	0	1	2	3	4	5	6	7	8	9
1702			68	63	66	88	68	65	66	75
1710	68	76	63	66	66	64	64	77	73	70
1720	62	55	52	71	81	66	61	58	57	59
1730	66	92	67	65	64	68	64	95	88	75
1740	60	71	71	64	80	54	53	43	51	45
1750	76	74	77	85	70	72	77	87	75	74
1760	67	65	62	71	69	77	63	72	60	55
1770	55	59	70	64	61	79	79	61	71	76
1780	73	75	85	69	81	71	58	78	63	57
1790	76	74	71	62	63	59	68	62	75	62
1800	68	67	77	72	67	80	68	81	69	66
1810	77	70	60	57	68	80	62	67	54	56
1820	67	57	77	66	80	71	72	61	63	69
1830	56	70	69	79	62	63	68	66	66	65
1840	62	66	64	75	70	69	64	73	70	89
1850	66	57	61	64	63	60	67	66	74	81
1860	80	79	82	86	62	66	79	67	59	57
1870	52	52	63	76	67	72	67	64	70	67
1880	73	75	73	78	84	92	64	53	59	65
1890	70	60	54	59	62	68	78	72	92	70
1900	65	96	77	68	87	72	84	65	62	58
1910	59	62	59	54	57	59	56	57	57	58
1920	62	60	55	63	63	62	76	74	70	68
1930	63	72	68	71	64	69	76	66	78	81
1940	71	75	70	62	62	62	65	72	87	74
1950	73	63	75	86	65	78	67	75	83	68
1960	65	86	72	76	65	79	75	66	66	63
1970	58	53	67	61	59	52	67	56	64	95
1980	61	59	56	62	63	59	73	63	67	68
1990	63	75	79	79	68	64	70	61	82	



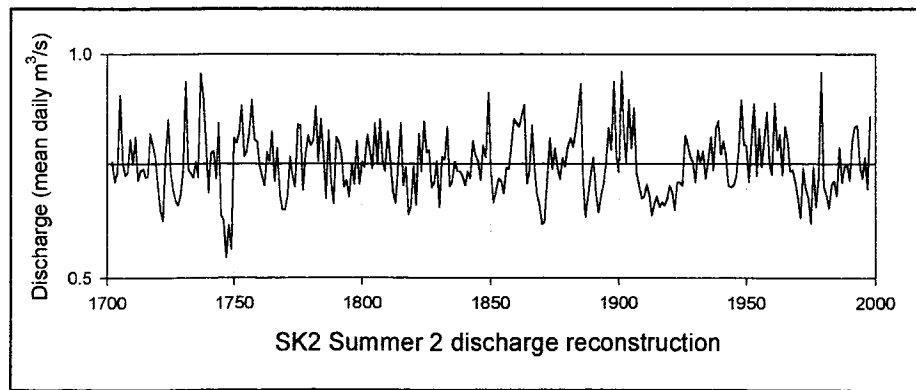
SITE SK2: Winter 2 reconstructed discharge.
 Units are mean daily cubic meters per second (m^3/s) $\times 100.$

Year	0	1	2	3	4	5	6	7	8	9
1702			74	34	64	102	73	51	65	59
1710	79	81	65	74	74	48	53	73	91	112
1720	110	48	34	76	107	95	90	76	58	29
1730	69	107	75	63	72	32	35	80	122	68
1740	52	82	50	106	146	146	95	100	38	34
1750	58	45	73	78	52	41	63	73	77	84
1760	83	57	59	53	81	68	84	115	92	73
1770	49	65	88	44	42	105	74	46	60	62
1780	44	74	59	62	117	53	67	117	48	45
1790	69	94	84	84	62	70	54	74	74	63
1800	52	58	81	50	65	54	66	89	51	62
1810	103	102	59	38	84	84	102	102	53	82
1820	51	59	53	58	72	90	86	59	96	64
1830	51	50	86	96	59	66	73	73	80	69
1840	70	52	58	74	82	57	59	40	75	137
1850	85	63	70	84	64	61	55	44	52	60
1860	52	48	103	93	43	67	109	100	108	100
1870	58	39	65	66	68	84	63	64	59	53
1880	63	56	45	40	98	166	87	57	54	85
1890	115	80	64	58	44	59	40	68	105	32
1900	49	100	45	59	55	80	108	91	84	69
1910	78	104	86	71	85	84	82	79	67	75
1920	97	70	64	76	48	50	71	73	85	60
1930	60	64	78	69	49	73	55	44	73	66
1940	65	93	89	74	67	53	36	60	76	89
1950	59	36	85	65	65	63	42	75	95	40
1960	56	68	81	55	51	86	80	78	93	107
1970	59	65	92	111	59	76	76	25	79	136
1980	94	70	64	84	53	69	75	61	78	55
1990	44	53	80	93	64	80	46	60	99	



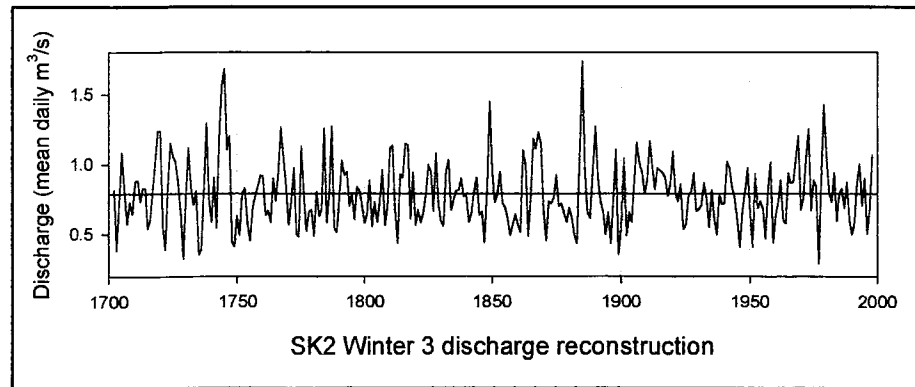
SITE SK2: Summer 2 reconstructed discharge.
 Units are mean daily cubic meters per second (m^3/s) $\times 100.$

Year	0	1	2	3	4	5	6	7	8	9
1702			76	71	74	91	76	73	74	81
1710	75	81	72	74	74	72	73	82	80	77
1720	71	65	63	78	85	74	70	67	66	69
1730	74	94	74	73	72	76	72	96	91	81
1740	69	78	78	72	85	64	63	55	62	57
1750	81	80	82	89	77	78	83	90	81	81
1760	75	73	71	78	76	83	72	79	69	65
1770	65	68	77	73	70	84	84	70	78	82
1780	80	81	88	76	86	78	68	83	71	67
1790	81	80	78	70	72	68	75	71	81	71
1800	76	75	82	79	74	85	76	86	76	74
1810	83	77	69	67	76	85	71	75	64	66
1820	75	66	82	74	85	78	79	70	71	76
1830	66	77	77	84	70	71	76	74	74	73
1840	71	74	72	81	77	76	72	80	77	91
1850	74	67	70	72	72	69	75	74	80	86
1860	85	84	87	89	71	74	84	75	69	66
1870	62	63	72	81	74	79	75	72	77	75
1880	79	81	79	83	88	93	73	64	68	73
1890	77	69	65	68	71	75	84	79	94	77
1900	74	96	82	76	90	79	88	73	70	68
1910	68	71	69	64	67	68	66	67	66	68
1920	71	69	65	71	71	71	82	80	77	76
1930	71	79	76	78	72	76	81	74	84	85
1940	78	81	77	71	70	71	73	79	90	80
1950	80	71	81	89	73	83	75	81	87	76
1960	73	89	79	82	73	84	81	74	74	71
1970	68	64	74	70	68	62	75	66	72	96
1980	70	69	66	71	72	68	79	71	75	76
1990	72	81	84	84	76	72	77	70	86	



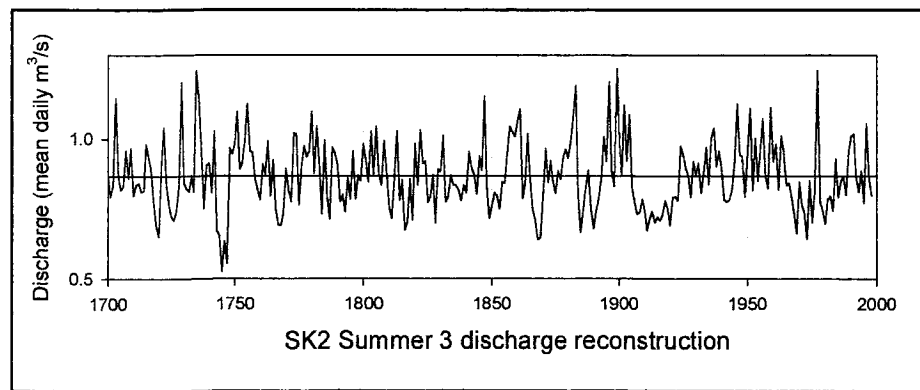
SITE SK2: Winter 3 reconstructed discharge.
 Units are mean daily cubic meters per second (m^3/s) $\times 100$.

Year	0	1	2	3	4	5	6	7	8	9
1702			82	39	72	108	81	57	73	65
1710	88	89	74	83	83	54	60	79	100	124
1720	124	56	39	84	115	106	102	87	67	33
1730	77	112	84	71	81	35	39	84	129	75
1740	59	90	55	119	157	168	110	120	45	41
1750	63	49	79	83	58	46	68	78	84	92
1760	92	64	67	59	90	74	94	126	105	84
1770	57	74	97	50	48	113	80	52	66	68
1780	49	80	63	68	126	58	77	127	55	52
1790	76	103	92	95	70	79	61	84	81	71
1800	58	64	88	55	73	59	74	96	57	69
1810	112	113	67	44	93	91	115	114	61	94
1820	57	67	58	65	78	99	95	67	108	71
1830	59	55	96	103	67	74	81	82	90	77
1840	79	59	65	81	91	64	66	44	83	145
1850	94	73	79	95	72	70	61	49	57	64
1860	57	52	110	100	49	75	118	111	123	115
1870	67	46	73	72	76	92	70	72	65	59
1880	69	62	50	44	105	173	98	65	62	95
1890	127	91	74	66	50	65	43	75	110	35
1900	55	104	49	66	59	87	116	101	94	79
1910	89	116	98	82	97	96	94	90	77	86
1920	109	80	73	86	54	57	78	80	94	67
1930	68	71	87	76	55	81	61	50	79	72
1940	72	102	98	84	76	60	41	66	80	97
1950	65	41	93	69	73	69	47	82	101	44
1960	63	72	89	60	58	93	87	87	104	120
1970	67	75	103	125	67	88	85	29	89	142
1980	106	80	73	94	60	79	83	69	87	61
1990	50	58	87	100	71	90	51	68	107	



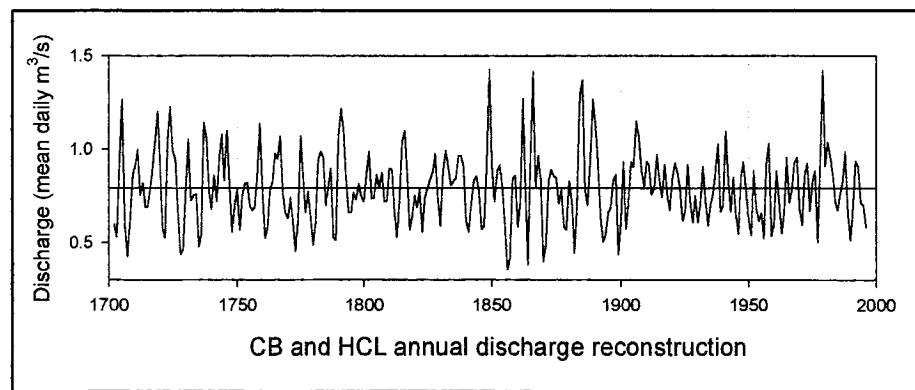
SITE SK2: Summer 3 reconstructed discharge.
 Units are mean daily cubic meters per second (m^3/s) $\times 100.$

Year	0	1	2	3	4	5	6	7	8	9
1700	87	79	83	115	87	82	83	96	86	97
1710	80	84	84	81	81	98	94	89	78	69
1720	65	90	104	83	76	72	71	74	84	120
1730	84	82	81	87	81	124	114	96	75	91
1740	91	81	103	67	65	53	64	55	97	95
1750	99	110	89	91	99	112	96	95	86	82
1760	78	91	87	99	80	92	75	69	69	74
1770	89	81	77	102	102	76	90	98	94	96
1780	110	88	104	91	73	100	79	71	97	95
1790	91	77	80	74	86	79	96	79	87	85
1800	98	92	85	103	87	104	87	84	99	88
1810	76	72	86	103	78	85	67	70	86	71
1820	98	83	103	91	92	77	79	87	70	89
1830	88	101	78	79	87	84	83	82	78	83
1840	81	96	90	87	80	94	89	115	83	72
1850	76	81	80	75	85	84	94	104	103	101
1860	106	111	79	84	102	85	75	71	64	65
1870	80	97	84	92	85	81	89	86	94	96
1880	93	100	109	119	81	67	74	82	89	76
1890	68	74	78	86	101	92	120	89	83	125
1900	99	87	112	92	109	83	78	73	74	79
1910	74	67	71	74	70	72	71	73	78	75
1920	69	79	79	78	98	94	90	87	79	92
1930	87	91	81	88	97	84	101	104	90	96
1940	90	78	77	78	82	92	112	94	94	79
1950	96	111	82	100	85	96	107	87	82	111
1960	92	98	82	101	96	83	84	79	73	66
1970	85	77	74	64	85	70	81	124	77	75
1980	70	79	80	74	93	79	85	87	80	96
1990	101	102	86	81	89	77	105	86	80	



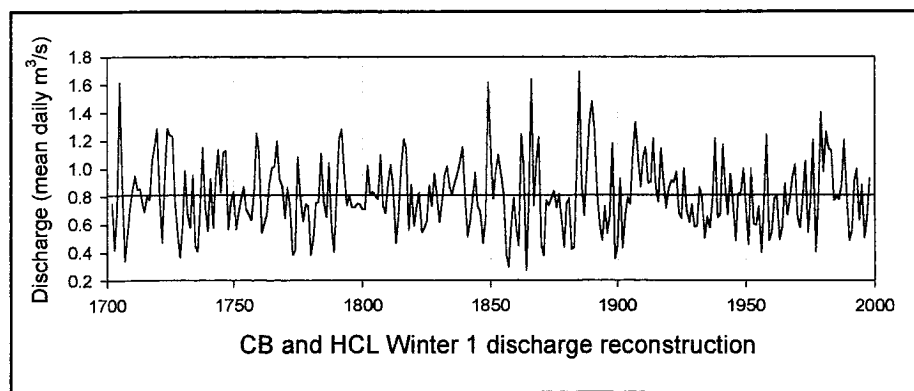
SITES CB and HCL: Annual reconstructed discharge.
 Units are mean daily cubic meters per second (m^3/s) $\times 100$.

Year	0	1	2	3	4	5	6	7	8	9
1702			60	53	91	126	59	42	61	87
1710	92	100	76	82	69	69	77	88	105	120
1720	92	58	53	105	123	99	95	64	44	46
1730	76	105	73	75	76	48	54	114	106	78
1740	68	86	72	96	108	83	110	80	56	70
1750	78	57	75	81	82	70	68	69	86	114
1760	80	52	58	78	83	98	95	107	77	66
1770	63	74	60	46	63	107	86	66	77	63
1780	49	61	95	99	95	70	81	90	53	51
1790	108	122	110	84	66	66	77	73	81	75
1800	72	87	99	74	74	86	79	87	72	72
1810	90	89	67	53	72	105	110	88	57	64
1820	75	69	78	56	74	79	84	88	98	75
1830	59	88	99	91	81	83	84	96	97	91
1840	61	56	70	83	86	78	57	59	91	143
1850	93	72	88	92	80	60	35	42	84	86
1860	59	71	127	80	38	95	141	79	96	84
1870	40	48	83	89	86	84	71	78	59	57
1880	83	72	44	70	129	137	78	70	92	127
1890	114	92	63	50	54	66	69	84	86	44
1900	62	93	57	70	93	90	115	107	90	79
1910	93	91	76	79	97	83	74	92	76	67
1920	84	92	88	79	62	67	92	73	61	75
1930	61	71	91	73	59	70	76	89	103	66
1940	70	110	84	67	85	65	55	85	93	80
1950	62	54	89	69	62	66	52	92	103	54
1960	60	88	72	55	66	95	72	78	93	95
1970	68	60	87	92	67	83	88	50	94	142
1980	91	104	96	87	72	67	76	84	98	66
1990	51	69	94	91	71	70	58			



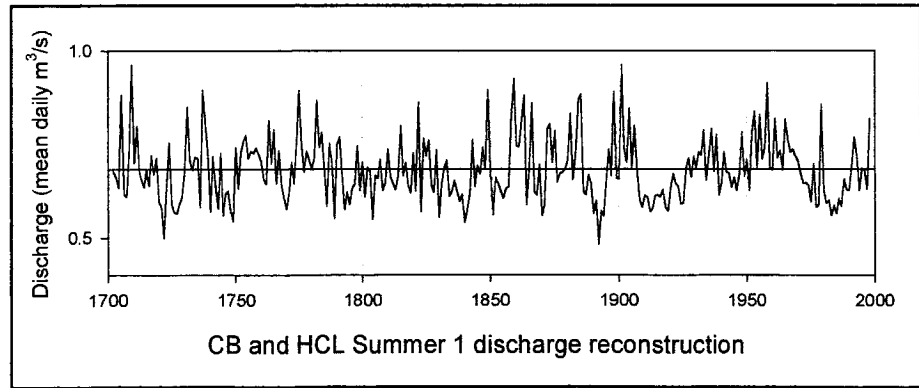
SITES CB and HCL: Winter 1 reconstructed discharge.
 Units are mean daily cubic meters per second (m^3/s) $\times 100$.

Year	0	1	2	3	4	5	6	7	8	9
1702			75	42	71	161	90	34	53	71
1710	85	95	85	86	75	69	79	78	106	116
1720	129	80	47	91	129	124	123	78	54	37
1730	58	98	68	58	95	45	41	72	115	74
1740	56	92	58	92	114	83	112	113	57	76
1750	83	57	68	79	87	71	68	63	82	125
1760	112	54	62	67	89	100	101	119	92	88
1770	64	87	74	39	42	108	81	62	75	73
1780	38	50	75	76	111	76	65	104	58	40
1790	81	122	128	98	74	81	72	72	75	75
1800	71	71	102	81	83	81	78	110	74	68
1810	90	102	85	47	66	101	121	114	56	88
1820	59	72	83	55	58	63	88	73	97	81
1830	62	76	96	101	87	81	90	96	104	116
1840	80	51	63	79	97	73	69	47	65	161
1850	118	78	99	110	96	82	39	30	60	79
1860	57	45	125	101	27	77	164	74	105	123
1870	46	38	77	74	79	84	72	82	64	44
1880	75	79	43	44	103	169	90	66	100	134
1890	148	127	83	61	49	73	54	66	118	36
1900	46	93	43	66	79	74	110	133	108	87
1910	109	116	90	91	122	88	77	114	91	72
1920	86	91	90	98	69	65	100	70	62	74
1930	59	59	87	79	50	66	58	79	122	65
1940	67	117	87	67	96	74	49	82	83	100
1950	73	46	100	61	60	73	40	76	124	49
1960	54	79	80	49	59	89	67	78	94	103
1970	65	58	80	105	55	77	121	41	78	140
1980	98	126	114	113	77	81	78	89	120	82
1990	49	55	91	100	63	88	51	65	93	



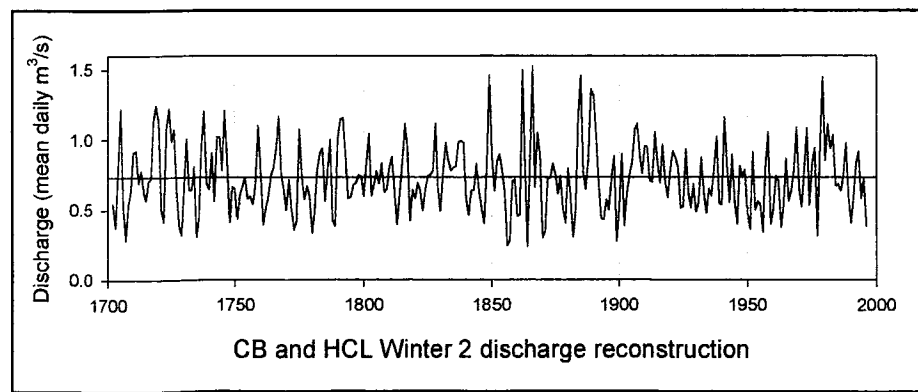
SITES CB and HCL: Summer 1 reconstructed discharge.
 Units are mean daily cubic meters per second (m^3/s) $\times 100$.

Year	0	1	2	3	4	5	6	7	8	9
1702			68	66	63	88	62	61	74	96
1710	70	80	68	65	63	68	64	72	67	71
1720	60	58	50	64	75	59	57	57	59	61
1730	68	85	71	68	71	71	58	90	81	72
1740	57	72	64	58	73	56	62	62	57	54
1750	74	63	73	76	77	71	73	73	74	72
1760	70	65	64	81	70	79	65	73	64	61
1770	58	62	70	65	74	89	75	68	73	71
1780	68	71	87	74	78	68	58	75	70	55
1790	75	77	67	57	62	59	63	64	74	63
1800	70	61	69	68	55	67	66	71	63	65
1810	74	66	65	63	66	80	67	70	64	62
1820	73	63	86	57	77	72	76	64	62	73
1830	55	64	69	71	61	62	65	63	60	62
1840	54	57	62	76	64	69	67	74	68	90
1850	68	56	66	65	62	61	63	64	83	93
1860	75	74	81	88	59	69	86	62	61	70
1870	56	59	79	80	70	79	65	67	67	68
1880	71	83	65	73	87	88	63	61	67	64
1890	57	60	48	57	56	65	74	67	89	66
1900	66	96	74	70	85	69	80	68	60	58
1910	61	61	57	58	61	61	61	63	58	57
1920	63	67	65	64	59	59	68	71	66	72
1930	69	73	72	79	65	72	79	68	77	61
1940	65	73	68	67	63	66	63	67	78	66
1950	71	63	78	84	68	83	71	74	91	69
1960	68	82	71	73	68	82	76	73	74	72
1970	70	67	64	65	64	60	70	58	59	86
1980	63	59	60	56	59	57	60	58	66	63
1990	63	69	77	72	63	69	68	63	82	



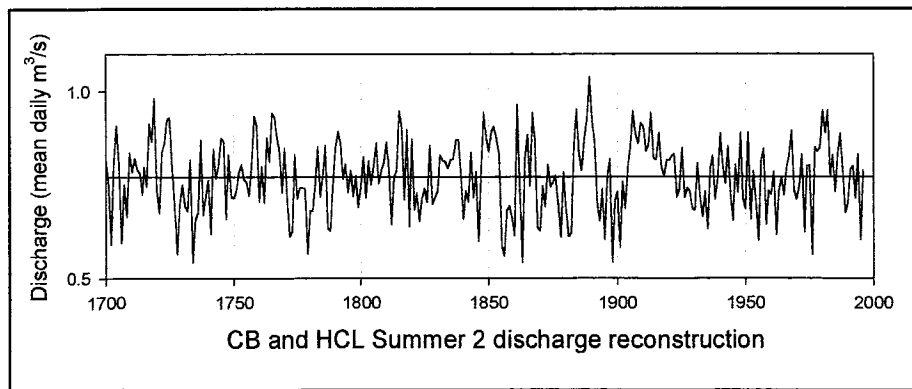
SITES CB and HCL: Winter 2 reconstructed discharge.
 Units are mean daily cubic meters per second (m^3/s) $\times 100$.

Year	0	1	2	3	4	5	6	7	8	9
1702			54	38	79	122	52	29	53	63
1710	91	92	69	78	62	57	70	72	113	124
1720	113	51	42	108	122	99	107	64	38	32
1730	64	101	64	64	81	30	44	96	120	69
1740	64	91	56	102	102	78	121	87	41	66
1750	65	43	61	67	73	58	59	54	68	110
1760	78	39	51	59	74	80	93	116	76	64
1770	50	71	50	36	43	107	73	58	67	59
1780	33	48	78	90	94	56	77	100	42	38
1790	100	115	116	89	58	59	68	69	74	73
1800	60	84	104	60	68	77	69	83	62	64
1810	80	88	63	39	61	84	112	94	42	64
1820	58	69	64	50	64	74	75	77	112	65
1830	49	77	98	85	78	80	81	98	99	98
1840	57	46	64	64	83	64	52	40	80	146
1850	90	64	85	90	77	62	25	28	70	71
1860	45	46	150	81	24	87	152	66	105	89
1870	30	35	72	73	83	75	61	74	51	41
1880	79	59	31	49	116	146	77	64	86	136
1890	131	103	69	44	43	57	50	73	88	28
1900	51	90	39	60	74	84	107	112	90	76
1910	95	95	71	70	105	84	69	97	70	59
1920	79	92	87	81	51	53	93	63	51	68
1930	48	55	87	63	48	65	60	79	103	55
1940	54	116	82	55	90	57	40	81	74	79
1950	48	36	91	50	56	54	34	80	105	40
1960	50	74	70	37	53	87	56	64	78	109
1970	65	52	79	108	53	83	94	31	95	145
1980	85	111	94	103	67	68	64	75	98	61
1990	41	58	83	91	58	73	39	59		



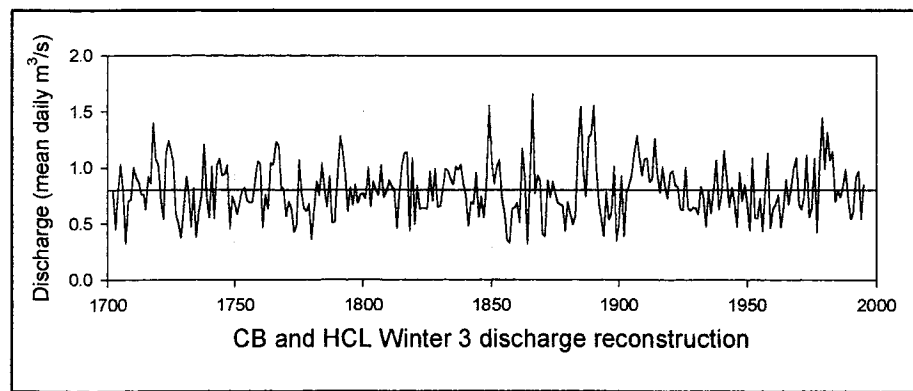
SITES CB and HCL: Summer 2 reconstructed discharge.
 Units are mean daily cubic meters per second (m^3/s) $\times 100$.

Year	0	1	2	3	4	5	6	7	8	9
1700	82	76	59	80	91	81	59	75	66	84
1710	78	82	79	78	72	80	74	91	87	98
1720	74	67	84	86	92	93	80	69	56	70
1730	75	69	68	82	54	66	68	87	67	72
1740	76	62	85	77	80	88	87	66	83	72
1750	71	73	78	80	76	76	72	80	93	91
1760	70	80	70	88	81	94	93	88	84	73
1770	85	72	61	63	83	71	74	74	74	57
1780	68	68	76	85	72	77	86	63	63	75
1790	85	89	86	77	81	73	79	72	77	69
1800	75	82	72	81	75	80	86	75	79	81
1810	86	80	64	77	79	95	90	71	90	64
1820	87	68	73	65	71	74	70	86	70	72
1830	73	83	81	81	79	82	82	87	87	78
1840	66	73	70	84	72	78	60	79	94	88
1850	84	89	91	87	83	59	56	68	69	66
1860	61	96	74	54	82	88	75	94	87	64
1870	63	75	69	80	74	76	77	70	61	78
1880	69	61	62	86	95	83	79	88	92	104
1890	92	86	70	65	74	60	77	82	54	71
1900	73	58	76	69	79	85	95	88	86	91
1910	91	84	86	94	82	82	89	80	77	81
1920	81	83	83	72	74	85	72	74	73	69
1930	68	81	72	66	73	63	79	83	71	76
1940	89	80	75	85	72	65	80	73	89	71
1950	68	89	66	79	70	60	81	85	64	73
1960	72	78	62	73	77	72	79	83	90	73
1970	71	75	83	62	80	80	56	85	84	85
1980	95	89	95	77	83	73	83	89	79	67
1990	70	79	80	71	83	60	79	76		



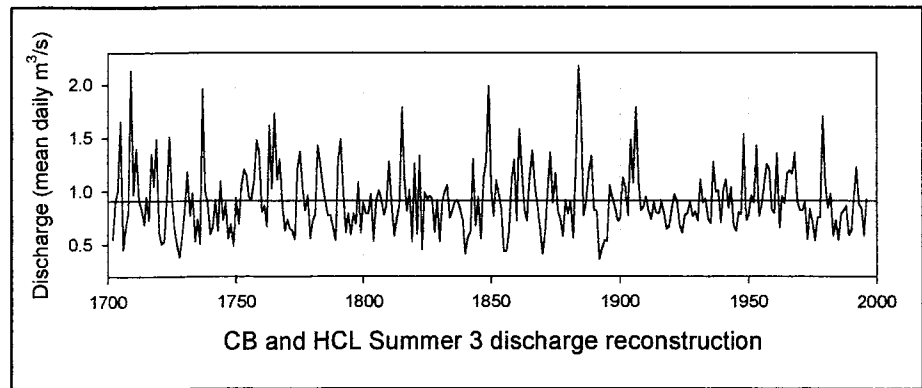
SITES CB and HCL: Winter 3 reconstructed discharge.
 Units are mean daily cubic meters per second (m^3/s) $\times 100$.

Year	0	1	2	3	4	5	6	7	8	9
1702			79	45	79	103	79	33	70	72
1710	100	91	86	76	76	63	92	86	140	107
1720	103	71	54	112	124	116	105	58	50	38
1730	65	92	76	47	82	38	60	75	121	72
1740	55	101	55	102	108	93	94	102	46	74
1750	68	58	68	80	81	70	69	69	89	105
1760	104	47	75	63	104	103	122	120	83	81
1770	56	69	64	43	49	106	77	63	61	67
1780	36	60	87	75	104	80	65	92	50	52
1790	92	128	115	94	61	82	67	85	68	76
1800	77	72	100	65	87	80	75	102	74	78
1810	88	83	81	46	78	103	113	114	44	108
1820	49	84	63	64	64	63	97	70	99	65
1830	66	81	99	97	90	85	101	98	103	86
1840	74	48	69	67	95	56	74	55	82	156
1850	107	86	101	107	74	60	35	33	63	65
1860	69	51	117	92	32	89	166	77	93	88
1870	41	39	88	73	87	78	69	67	66	43
1880	69	58	49	58	121	154	97	74	127	130
1890	156	100	70	54	38	78	53	60	101	35
1900	50	92	39	78	85	95	115	129	110	93
1910	108	108	87	90	126	93	78	100	82	72
1920	95	97	84	83	63	62	100	64	62	65
1930	64	58	82	74	48	79	59	80	107	63
1940	75	115	91	65	82	70	47	95	70	85
1950	67	44	109	55	55	72	43	79	112	46
1960	63	67	75	47	63	89	67	82	99	108
1970	68	63	73	111	56	64	108	42	102	145
1980	99	131	106	114	70	80	73	84	98	72
1990	54	61	91	96	54	84	45			



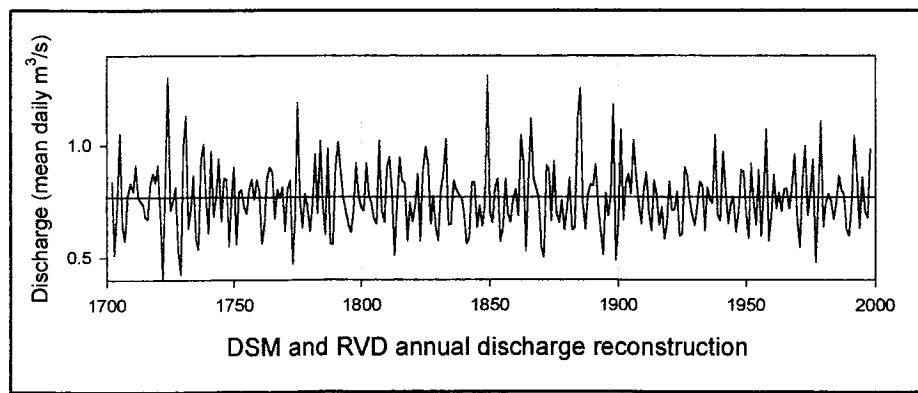
SITES CB and HCL: Summer 3 reconstructed discharge.
 Units are mean daily cubic meters per second (m^3/s) $\times 100$.

Year	0	1	2	3	4	5	6	7	8	9
1702			55	89	101	166	46	67	81	213
1710	97	140	92	83	69	95	73	135	105	149
1720	62	51	54	94	151	91	64	50	38	59
1730	85	118	77	98	53	74	51	196	100	89
1740	60	67	92	63	109	73	89	56	69	49
1750	93	70	106	120	115	95	92	110	148	136
1760	81	87	67	162	102	173	111	130	89	63
1770	74	65	63	55	121	137	103	82	96	56
1780	72	79	143	126	105	90	77	77	66	54
1790	129	149	103	61	79	59	79	70	108	61
1800	89	79	80	97	54	91	101	93	78	87
1810	128	89	58	75	88	179	112	81	101	52
1820	126	60	133	46	99	93	95	94	62	92
1830	53	90	100	105	75	82	90	92	83	73
1840	41	57	62	130	68	95	55	111	128	199
1850	102	77	110	98	84	43	43	62	112	129
1860	72	159	120	83	72	114	138	105	88	66
1870	41	62	101	136	90	117	81	74	58	91
1880	79	91	56	124	218	178	77	90	117	133
1890	82	82	36	46	54	53	106	94	85	72
1900	75	113	103	77	148	108	179	111	82	86
1910	94	81	73	89	80	79	90	80	65	67
1920	84	97	91	68	61	78	79	91	77	81
1930	73	111	90	93	74	70	128	100	101	70
1940	102	111	84	104	69	63	81	78	153	73
1950	78	96	89	143	77	87	107	125	121	83
1960	80	136	66	95	89	117	119	116	136	91
1970	83	82	90	55	83	72	54	76	76	171
1980	108	85	98	58	73	55	79	82	86	60
1990	63	96	123	88	85	59	92	73		



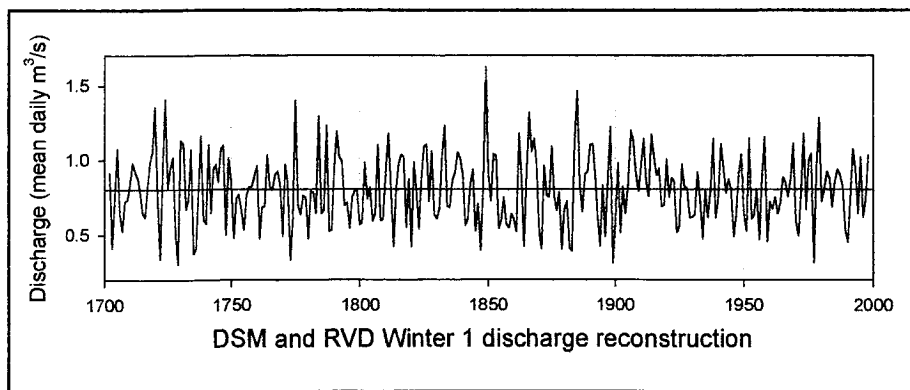
SITES DSM and RVD: Annual reconstructed discharge.
 Units are mean daily cubic meters per second (m^3/s) $\times 100$.

Year	0	1	2	3	4	5	6	7	8	9
1702			84	51	72	105	63	57	77	83
1710	79	91	77	75	73	68	67	83	88	83
1720	91	69	41	84	130	71	75	81	53	42
1730	100	113	63	72	87	58	54	94	100	75
1740	61	97	68	77	94	66	85	85	55	75
1750	90	56	79	80	73	70	81	85	76	85
1760	80	56	65	85	90	88	67	80	77	81
1770	62	81	84	47	68	119	76	63	78	73
1780	62	74	96	70	102	74	60	98	56	56
1790	90	101	88	77	71	65	61	70	92	77
1800	72	71	92	78	74	67	65	102	71	66
1810	91	95	78	51	73	95	84	83	57	74
1820	66	73	87	57	89	99	91	65	77	63
1830	57	80	87	103	65	65	84	80	78	77
1840	70	56	59	83	83	64	73	64	74	131
1850	71	65	82	85	57	63	85	69	66	76
1860	81	69	104	93	53	84	112	85	81	77
1870	55	50	91	89	66	93	70	65	75	62
1880	72	86	62	64	112	126	74	63	78	82
1890	82	91	73	61	51	79	69	77	118	49
1900	66	107	67	83	87	78	102	86	74	65
1910	81	88	70	62	84	78	64	72	58	65
1920	84	71	71	79	60	61	90	87	76	69
1930	64	73	84	82	62	81	76	74	104	69
1940	66	97	80	65	74	77	62	70	89	88
1950	70	59	92	75	64	89	60	79	107	57
1960	69	87	72	79	71	80	81	72	82	96
1970	67	54	83	100	69	79	94	48	76	111
1980	64	74	78	75	67	74	87	80	78	63
1990	60	74	104	89	63	86	70	68	98	



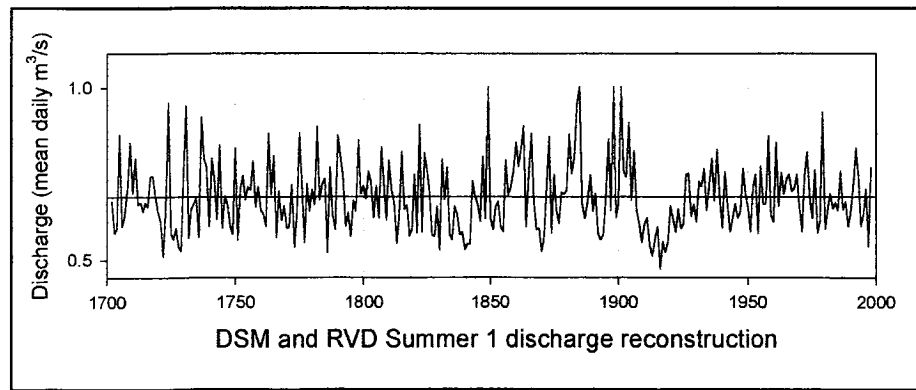
SITES DSM and RVD: Winter 1 reconstructed discharge.
 Units are mean daily cubic meters per second (m^3/s) $\times 100$.

Year	0	1	2	3	4	5	6	7	8	9
1702			91	42	76	108	65	53	73	73
1710	84	98	92	87	76	65	62	82	98	105
1720	136	77	34	95	141	81	94	102	52	31
1730	113	111	67	73	107	37	40	77	116	60
1740	57	110	64	94	97	85	107	110	50	101
1750	85	48	74	77	66	53	76	82	82	90
1760	96	47	68	69	103	83	80	91	92	82
1770	49	97	85	33	62	140	70	64	76	75
1780	47	79	78	65	129	64	67	123	52	53
1790	92	119	102	99	70	71	54	75	79	79
1800	57	59	98	74	81	59	64	110	59	61
1810	91	118	81	42	80	98	103	102	55	87
1820	42	98	79	54	88	109	110	72	106	64
1830	61	68	103	123	69	68	86	92	105	101
1840	91	56	61	84	94	52	70	40	82	162
1850	90	73	104	103	54	60	75	57	55	64
1860	60	52	117	89	42	90	132	106	114	97
1870	52	40	96	76	75	109	76	66	78	41
1880	67	72	42	39	112	146	85	65	91	92
1890	110	111	89	60	42	83	48	86	122	31
1900	59	98	51	82	64	84	120	113	91	79
1910	96	114	86	76	117	103	90	95	69	70
1920	100	75	88	86	51	56	97	82	81	62
1930	62	64	92	73	47	80	62	79	114	61
1940	73	111	96	78	87	80	49	63	90	104
1950	65	53	115	60	64	80	47	88	116	46
1960	72	67	75	64	71	88	85	76	87	111
1970	59	50	76	118	67	100	104	31	95	128
1980	72	81	92	88	69	85	94	90	82	53
1990	45	74	107	94	64	102	62	73	103	



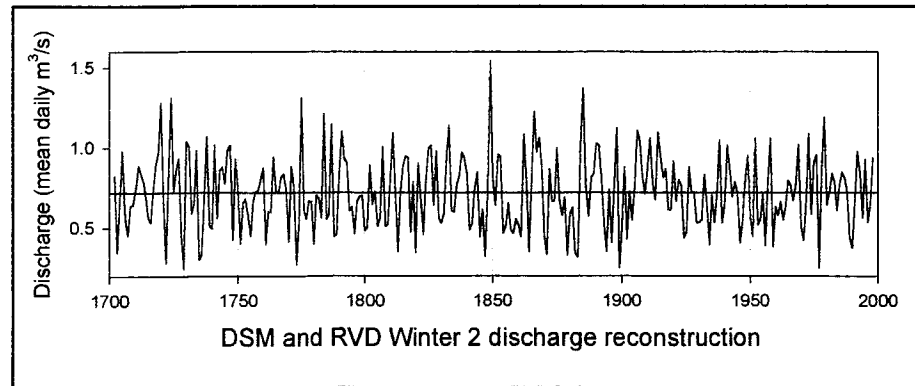
SITES DSM and RVD: Summer 1 reconstructed discharge.
 Units are mean daily cubic meters per second (m^3/s) $\times 100$.

Year	0	1	2	3	4	5	6	7	8	9
1702			67	58	59	86	60	63	71	84
1710	70	79	66	67	64	67	66	74	74	68
1720	64	61	51	66	96	58	56	59	54	53
1730	76	95	57	65	66	68	57	92	79	77
1740	60	79	73	62	83	59	69	66	60	58
1750	82	56	71	74	68	71	70	79	66	71
1760	65	63	60	87	69	80	57	70	62	66
1770	59	60	72	54	64	87	72	55	72	64
1780	70	66	89	67	72	74	52	77	63	59
1790	86	80	74	60	64	57	67	64	85	69
1800	71	68	76	73	62	71	62	83	72	62
1810	79	70	67	55	64	81	65	66	57	59
1820	75	58	89	58	81	76	70	57	57	65
1830	53	79	68	77	57	56	65	63	57	58
1840	53	55	55	73	68	66	61	80	62	100
1850	62	59	66	67	60	58	79	69	71	76
1860	84	77	82	89	60	75	87	68	59	59
1870	52	56	71	86	58	75	64	61	70	69
1880	70	87	75	80	95	100	66	62	67	75
1890	64	69	58	56	57	68	85	64	100	62
1900	66	100	76	74	90	67	82	65	61	55
1910	60	62	54	51	56	60	48	55	52	55
1920	66	62	58	65	59	61	75	75	63	66
1930	61	73	71	77	64	72	79	67	82	68
1940	59	76	67	58	62	66	62	64	77	69
1950	65	58	71	75	58	77	66	66	86	63
1960	61	84	66	75	69	74	75	70	71	75
1970	66	58	75	81	68	62	76	58	61	93
1980	59	65	69	65	67	64	76	65	67	60
1990	64	72	82	74	60	63	71	54	77	



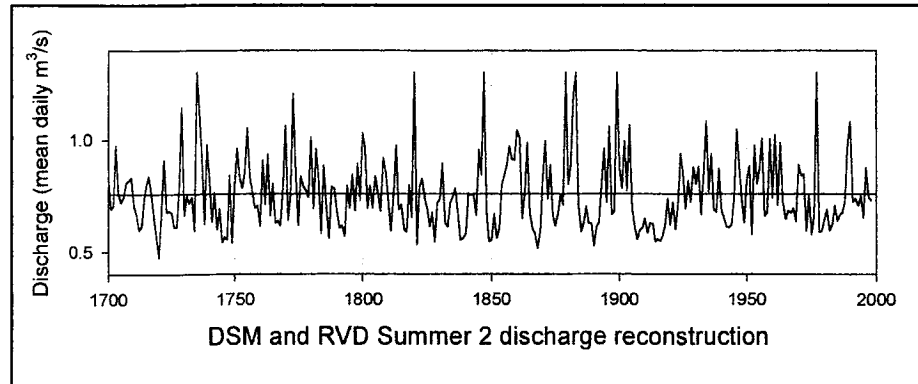
SITES DSM and RVD: Winter 2 reconstructed discharge.
 Units are mean daily cubic meters per second (m^3/s) $\times 100$.

Year	0	1	2	3	4	5	6	7	8	9
1702			82	35	67	98	56	45	64	64
1710	75	89	84	79	67	56	53	73	89	97
1720	128	68	28	86	131	73	86	93	45	25
1730	104	101	59	65	98	30	33	67	107	52
1740	49	101	56	86	88	77	99	101	42	93
1750	76	40	65	68	58	45	67	73	73	81
1760	88	40	60	60	94	73	72	82	84	73
1770	41	88	76	27	53	131	61	55	67	66
1780	40	70	68	56	121	55	59	115	45	46
1790	83	110	93	91	61	63	46	67	70	70
1800	48	51	89	65	73	51	56	101	51	52
1810	81	109	72	35	71	88	95	94	47	79
1820	35	90	70	46	79	100	101	64	98	56
1830	53	59	94	114	61	60	77	83	97	93
1840	83	49	53	75	85	44	62	32	73	154
1850	81	64	96	94	46	52	65	49	47	55
1860	51	44	108	79	35	81	123	97	106	89
1870	45	33	87	67	67	100	67	58	69	33
1880	59	63	34	32	102	137	76	57	82	84
1890	103	102	80	52	35	74	41	77	112	25
1900	50	88	43	73	55	75	111	105	82	71
1910	87	106	77	68	109	95	82	87	62	61
1920	91	67	80	77	44	48	88	73	72	53
1930	53	55	83	64	39	71	53	71	104	53
1940	64	102	87	70	79	71	41	55	81	95
1950	57	45	106	52	55	71	39	79	106	38
1960	63	58	66	55	63	80	76	67	78	102
1970	51	42	67	109	59	91	95	25	87	119
1980	64	72	84	79	61	77	85	81	73	45
1990	37	65	97	85	56	93	53	65	93	



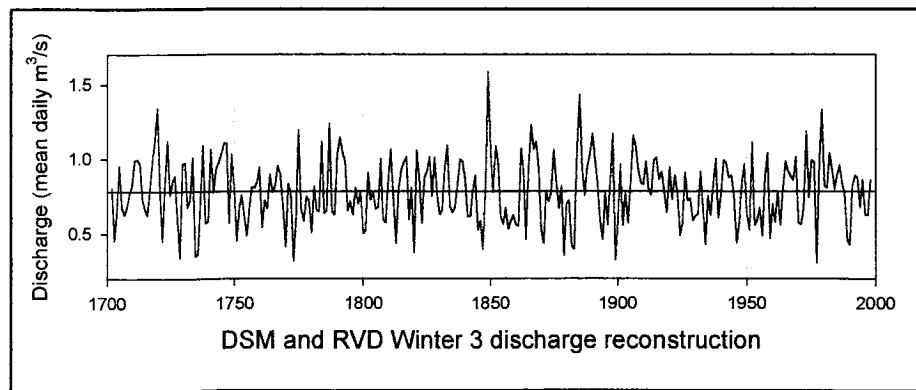
SITES DSM and RVD: Summer 2 reconstructed discharge.
 Units are mean daily cubic meters per second (m^3/s) $\times 100$.

Year	0	1	2	3	4	5	6	7	8	9
1700	83	69	71	98	76	72	75	81	82	83
1710	71	67	60	62	74	80	84	76	65	56
1720	48	67	91	68	68	68	61	61	79	115
1730	66	75	72	74	60	130	113	92	63	98
1740	83	64	77	60	70	54	57	56	84	54
1750	79	96	83	78	86	105	84	77	70	71
1760	62	91	71	94	66	80	63	64	62	79
1770	106	64	76	121	86	62	84	79	78	74
1780	101	69	96	83	58	89	70	56	79	79
1790	68	61	62	57	79	70	85	69	90	73
1800	103	97	70	79	70	84	76	68	92	86
1810	74	59	74	98	69	71	60	59	80	65
1820	130	53	79	83	74	69	61	67	54	72
1830	73	90	63	61	72	75	79	67	55	56
1840	58	76	76	75	67	96	84	130	68	55
1850	56	67	56	61	80	84	88	97	92	91
1860	104	101	65	76	99	67	60	58	52	59
1870	83	100	74	89	66	62	67	76	71	130
1880	80	89	120	130	72	59	63	70	63	63
1890	53	61	63	79	96	72	106	67	68	130
1900	88	79	100	77	107	69	61	56	60	61
1910	65	58	63	63	55	56	55	57	62	74
1920	62	72	60	71	94	85	69	81	72	88
1930	81	88	67	86	108	77	94	69	68	87
1940	68	65	61	61	63	74	105	88	74	63
1950	83	89	58	98	80	87	101	66	68	100
1960	74	102	71	99	72	65	68	67	70	64
1970	89	84	85	60	76	58	66	130	59	59
1980	64	69	60	63	71	64	67	67	73	98
1990	108	72	74	71	75	65	88	75	73	



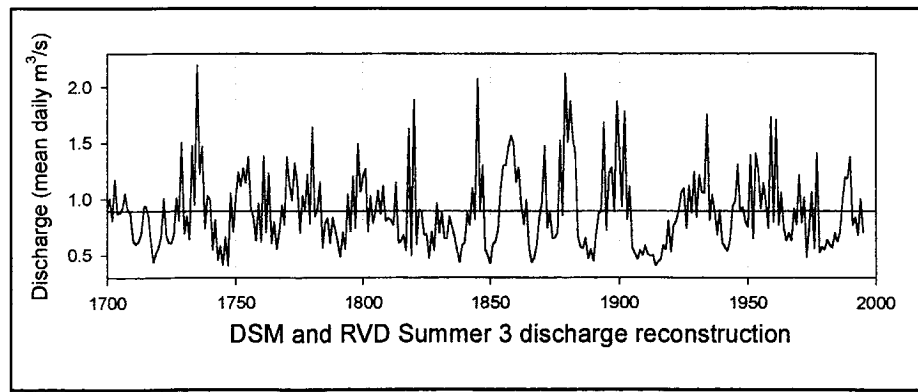
SITES DSM and RVD: Winter 3 reconstructed discharge.
 Units are mean daily cubic meters per second (m^3/s) $\times 100$.

Year	0	1	2	3	4	5	6	7	8	9
1702			80	46	65	95	68	63	68	77
1710	82	99	100	97	72	67	62	79	98	113
1720	134	79	45	83	112	76	85	88	58	34
1730	96	98	68	73	101	35	37	72	109	57
1740	58	106	77	94	98	104	111	111	57	103
1750	81	45	67	76	62	48	66	81	81	84
1760	94	54	72	67	90	78	82	95	90	68
1770	41	83	77	32	59	119	67	58	75	72
1780	50	81	66	65	111	63	66	124	65	63
1790	103	114	105	98	65	71	63	81	70	79
1800	50	52	91	73	77	67	68	100	59	57
1810	86	106	75	44	80	93	98	101	59	81
1820	38	106	87	57	88	92	101	75	101	77
1830	63	66	94	109	69	64	68	83	100	98
1840	87	61	62	79	89	52	58	40	79	159
1850	105	78	108	99	61	56	67	53	59	62
1860	56	55	107	92	46	94	123	106	111	94
1870	52	43	79	71	77	106	84	67	82	35
1880	70	72	42	39	104	143	94	76	95	103
1890	117	100	83	59	46	78	56	84	117	32
1900	59	96	55	77	57	83	116	109	93	84
1910	83	98	79	76	99	101	86	91	78	64
1920	94	73	89	77	49	57	90	72	73	59
1930	62	63	91	68	43	75	62	83	100	61
1940	76	99	98	88	89	75	44	57	84	97
1950	63	52	111	56	59	68	49	87	104	47
1960	70	58	78	56	79	98	92	89	86	101
1970	57	56	68	119	74	99	98	30	96	133
1980	82	81	104	93	80	89	96	83	77	46
1990	43	82	89	87	67	86	62	62	86	



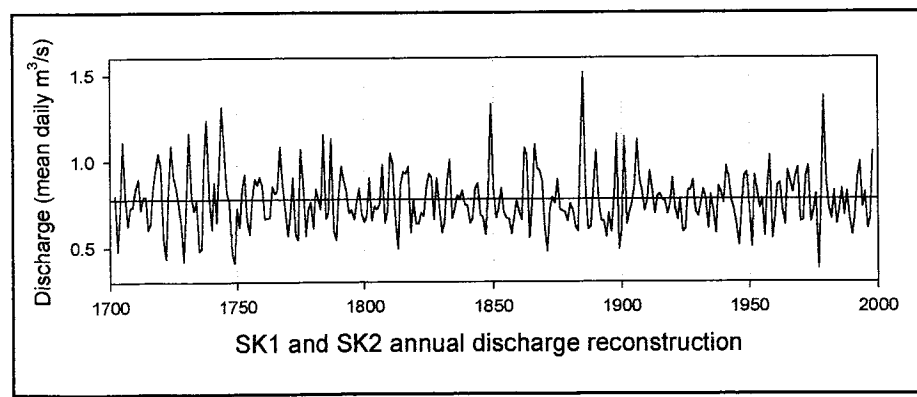
SITES DSM and RVD: Summer 3 reconstructed discharge.
 Units are mean daily cubic meters per second (m^3/s) $\times 100$.

Year	0	1	2	3	4	5	6	7	8	9
1700	91	101	81	117	87	88	93	105	91	88
1710	63	60	63	70	94	94	85	64	44	52
1720	57	67	101	67	61	61	68	101	81	151
1730	70	85	64	148	95	220	122	147	74	103
1740	100	55	81	46	58	41	66	41	105	71
1750	101	124	112	128	115	138	91	83	63	96
1760	62	139	70	123	61	80	56	72	94	78
1770	138	113	99	132	115	70	103	91	122	78
1780	164	85	92	115	57	79	83	61	84	73
1790	62	49	70	55	104	71	120	74	150	107
1800	121	127	71	103	78	90	108	86	111	81
1810	83	81	77	115	61	63	68	54	163	50
1820	189	60	91	90	68	69	47	71	54	96
1830	70	88	65	65	85	76	66	55	44	59
1840	61	88	77	110	82	208	91	130	55	50
1850	43	59	62	73	110	130	130	147	157	150
1860	115	128	93	77	99	57	44	47	58	82
1870	97	148	74	88	65	66	70	152	85	212
1880	151	188	153	140	67	58	56	65	47	55
1890	45	70	87	89	169	72	123	128	89	188
1900	141	94	179	82	111	57	52	46	55	50
1910	59	51	49	50	41	44	47	59	55	81
1920	53	77	80	90	106	110	74	112	88	124
1930	84	121	106	105	175	81	104	89	68	90
1940	61	57	54	64	94	98	131	89	93	80
1950	75	139	65	141	126	92	114	98	74	173
1960	80	171	77	106	74	63	70	63	92	77
1970	122	79	101	48	76	106	56	141	53	57
1980	55	63	59	57	70	62	71	98	119	118
1990	138	77	84	68	100	70	102			



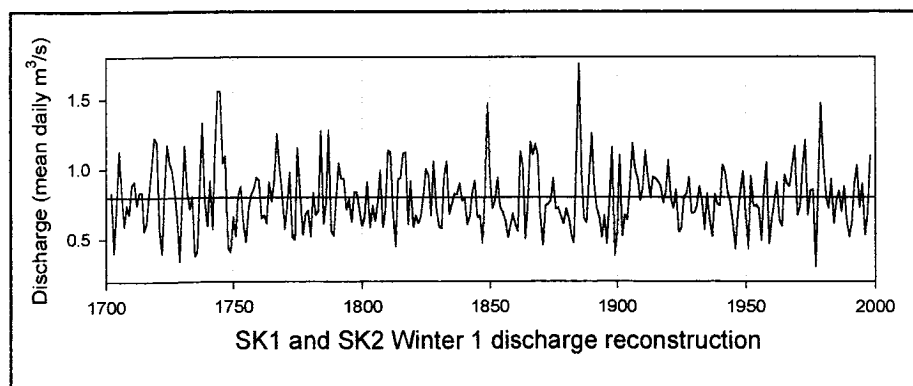
SITES SK1 and SK2: Annual reconstructed discharge.
 Units are mean daily cubic meters per second (m^3/s) $\times 100$.

Year	0	1	2	3	4	5	6	7	8	9
1702			80	48	72	111	80	63	73	74
1710	84	90	72	79	79	60	64	84	94	105
1720	97	56	44	83	109	92	85	75	63	42
1730	76	116	80	71	77	48	50	100	124	80
1740	61	87	65	97	131	108	82	77	47	41
1750	73	62	85	92	66	58	77	90	86	91
1760	86	67	67	67	85	81	83	108	86	72
1770	57	69	91	57	54	107	86	57	72	76
1780	61	84	78	72	116	67	70	113	60	54
1790	81	97	88	82	70	72	66	77	84	70
1800	65	68	90	65	74	72	75	98	64	71
1810	105	99	66	49	86	94	93	97	58	78
1820	64	64	70	68	86	93	90	66	90	74
1830	58	64	89	101	67	72	80	78	83	75
1840	74	64	67	84	87	69	67	57	82	133
1850	86	67	73	84	71	67	66	58	67	77
1860	70	66	108	104	55	75	110	96	94	88
1870	60	48	72	79	76	89	72	71	70	65
1880	75	71	62	59	106	151	86	60	62	85
1890	106	79	66	65	56	70	59	79	116	49
1900	61	114	63	70	76	86	112	89	82	71
1910	77	94	82	70	80	81	77	77	69	75
1920	90	73	66	78	59	60	83	83	89	71
1930	68	76	83	79	61	81	71	58	85	82
1940	76	97	91	77	72	63	51	73	92	94
1950	73	50	92	83	72	78	57	85	103	55
1960	67	86	87	71	63	95	88	81	91	96
1970	65	66	91	97	65	71	81	38	81	137
1980	88	73	66	83	63	72	84	69	82	67
1990	57	69	91	99	73	81	61	67	105	



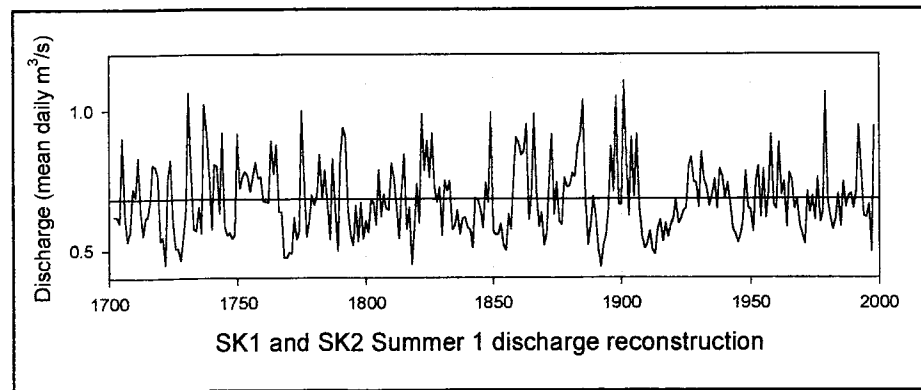
SITES SK1 and SK2: Winter 1 reconstructed discharge.
 Units are mean daily cubic meters per second (m^3/s) $\times 100$.

Year	0	1	2	3	4	5	6	7	8	9
1702			83	40	73	113	82	59	74	68
1710	89	91	74	84	83	56	61	82	101	122
1720	120	56	40	85	117	104	99	85	66	34
1730	77	117	84	72	81	38	42	90	133	77
1740	60	91	57	116	156	156	104	109	45	41
1750	66	52	82	87	60	48	71	82	86	94
1760	92	65	68	61	91	77	93	125	102	82
1770	57	73	98	52	50	115	83	53	68	71
1780	52	83	67	70	127	61	76	128	56	52
1790	78	104	93	93	71	78	63	83	84	71
1800	60	66	91	58	74	63	75	99	59	71
1810	113	112	67	45	93	94	111	112	61	91
1820	59	67	62	66	81	100	96	67	105	72
1830	59	58	96	105	68	75	82	82	90	77
1840	79	60	66	83	91	66	67	47	84	147
1850	94	72	79	94	73	70	63	51	60	68
1860	61	55	113	103	50	76	119	110	118	110
1870	66	46	74	75	77	94	71	73	67	61
1880	71	65	53	47	108	175	97	65	62	94
1890	125	89	72	66	51	67	47	77	115	38
1900	56	110	52	68	64	89	119	100	93	78
1910	87	113	96	80	94	93	91	88	76	84
1920	106	79	72	85	55	58	80	82	94	68
1930	69	73	88	78	57	82	64	52	82	75
1940	74	103	98	84	76	61	43	68	85	99
1950	68	43	95	73	74	72	49	84	104	47
1960	65	77	90	64	59	96	89	87	103	116
1970	67	73	102	121	67	85	85	30	89	147
1980	104	79	72	93	61	78	85	70	88	63
1990	52	61	90	103	72	89	53	69	109	



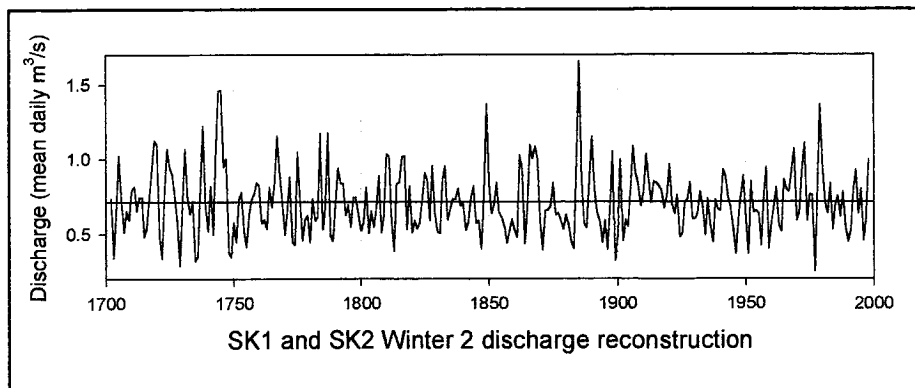
SITES SK1 and SK2: Summer 1 reconstructed discharge.
 Units are mean daily cubic meters per second (m^3/s) $\times 100$.

Year	0	1	2	3	4	5	6	7	8	9
1702			62	62	60	90	62	53	57	72
1710	69	83	64	55	62	62	67	81	80	77
1720	53	54	45	76	82	60	51	51	47	55
1730	64	106	79	58	57	65	56	102	93	78
1740	57	81	80	63	92	58	55	56	54	56
1750	92	72	77	78	77	71	77	81	76	76
1760	67	67	67	89	77	88	64	64	47	47
1770	49	49	62	54	57	100	76	55	60	70
1780	66	70	84	68	79	66	54	83	65	50
1790	83	94	90	64	55	52	66	53	67	54
1800	60	56	68	67	59	79	62	70	65	64
1810	81	76	66	54	71	84	58	65	45	57
1820	73	60	99	79	89	76	92	72	67	72
1830	55	75	71	75	57	59	64	56	61	62
1840	58	57	51	69	68	65	58	74	67	99
1850	57	55	56	59	52	50	63	58	76	90
1860	89	84	86	95	61	70	99	71	58	64
1870	52	56	75	91	63	74	60	59	76	73
1880	73	77	76	87	92	104	69	52	59	69
1890	62	50	44	52	55	65	87	71	105	67
1900	66	111	83	62	90	69	91	65	55	50
1910	52	57	50	49	58	61	53	59	55	59
1920	61	68	60	61	64	65	80	83	74	74
1930	65	85	75	72	66	70	75	65	79	76
1940	69	74	67	57	56	53	56	61	78	65
1950	64	57	75	80	62	79	62	71	91	66
1960	65	88	70	74	58	77	75	65	68	59
1970	55	52	71	63	69	61	76	60	64	106
1980	67	62	57	61	70	58	74	65	69	70
1990	65	71	95	79	62	62	66	49	94	



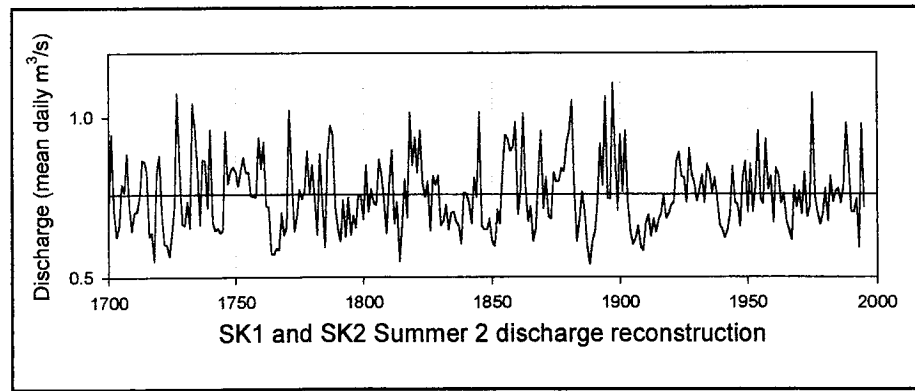
SITES SK1 and SK2: Winter 2 reconstructed discharge.
 Units are mean daily cubic meters per second (m^3/s) $\times 100$.

Year	0	1	2	3	4	5	6	7	8	9
1702			74	34	64	102	73	51	65	59
1710	79	81	65	74	74	48	53	73	91	112
1720	110	48	34	76	107	95	90	76	58	29
1730	69	107	75	63	72	32	35	80	122	68
1740	52	82	50	106	146	146	95	100	38	34
1750	58	45	73	78	52	41	63	73	77	84
1760	83	57	59	53	81	68	84	115	92	73
1770	49	65	88	44	42	105	74	46	60	62
1780	44	74	59	62	117	53	67	117	48	45
1790	69	94	84	84	62	70	54	74	74	63
1800	52	58	81	50	65	54	66	89	51	62
1810	103	102	59	38	84	84	102	102	53	82
1820	51	59	53	58	72	90	86	59	96	64
1830	51	50	86	96	59	66	73	73	80	69
1840	70	52	58	74	82	57	59	40	75	137
1850	85	63	70	84	64	61	55	44	52	60
1860	52	48	103	93	43	67	109	100	108	100
1870	58	39	65	66	68	84	63	64	59	53
1880	63	56	45	40	98	166	87	57	54	85
1890	115	80	64	58	44	59	40	68	105	32
1900	49	100	45	59	55	80	108	91	84	69
1910	78	104	86	71	85	84	82	79	67	75
1920	97	70	64	76	48	50	71	73	85	60
1930	60	64	78	69	49	73	55	44	73	66
1940	65	93	89	74	67	53	36	60	76	89
1950	59	36	85	65	65	63	42	75	95	40
1960	56	68	81	55	51	86	80	78	93	107
1970	59	65	92	111	59	76	76	25	79	136
1980	94	70	64	84	53	69	75	61	78	55
1990	44	53	80	93	64	80	46	60	99	



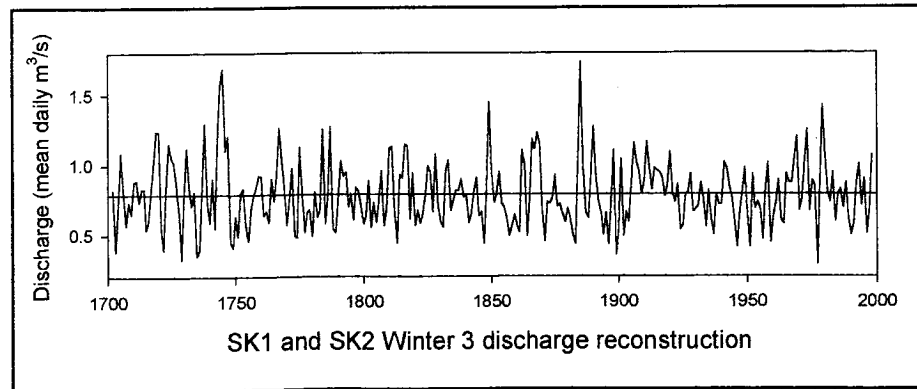
SITES SK1 and SK2: Summer 2 reconstructed discharge.
 Units are mean daily cubic meters per second (m^3/s) $\times 100$.

Year	0	1	2	3	4	5	6	7	8	9
1700	69	95	70	63	66	79	77	89	72	64
1710	70	71	75	87	86	83	63	64	55	82
1720	88	69	60	60	57	64	73	107	85	67
1730	66	74	65	104	97	84	66	87	86	72
1740	96	67	65	65	64	65	96	79	83	84
1750	83	78	83	87	83	83	75	75	75	94
1760	84	92	72	72	57	57	59	58	70	63
1770	66	102	83	64	69	77	74	77	89	76
1780	85	74	63	88	73	59	89	97	94	72
1790	65	61	74	63	75	63	69	65	76	75
1800	68	85	70	77	73	73	87	82	74	64
1810	79	90	67	73	55	66	81	69	101	85
1820	94	83	96	79	75	80	65	82	79	82
1830	66	68	73	65	70	70	67	66	60	76
1840	76	73	67	81	75	102	66	65	65	68
1850	61	60	71	67	82	94	93	89	91	98
1860	70	77	101	78	67	72	61	65	82	96
1870	71	81	69	68	83	80	80	84	83	92
1880	96	105	77	61	68	77	71	60	54	61
1890	64	73	92	79	106	75	74	111	89	71
1900	94	77	96	73	64	60	62	66	60	58
1910	67	69	63	68	64	68	70	76	68	70
1920	72	73	86	89	81	81	73	90	82	79
1930	74	77	82	73	85	83	76	81	75	66
1940	65	62	65	70	85	73	73	66	81	86
1950	70	85	70	78	96	74	73	93	77	81
1960	67	84	82	73	76	68	65	62	78	72
1970	77	70	83	69	72	107	75	70	66	70
1980	78	67	81	73	77	78	73	79	98	85
1990	70	70	74	59	98	72	71			



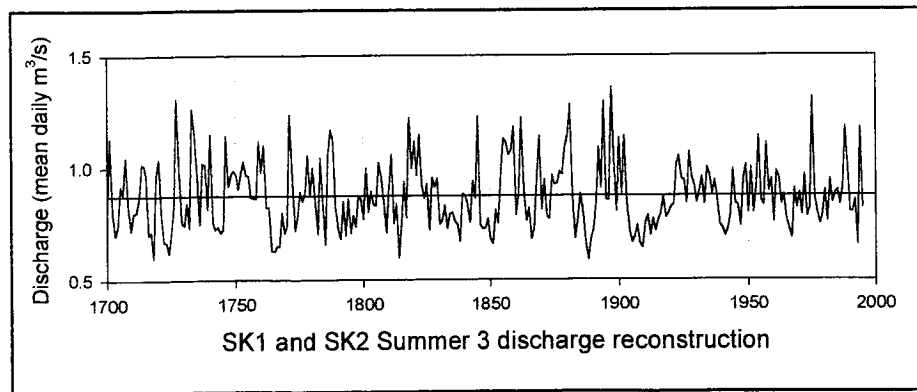
SITES SK1 and SK2: Winter 3 reconstructed discharge.
 Units are mean daily cubic meters per second (m^3/s) $\times 100$.

Year	0	1	2	3	4	5	6	7	8	9
1702			82	39	72	108	81	57	73	65
1710	88	89	74	83	83	54	60	79	100	124
1720	124	56	39	84	115	106	102	87	67	33
1730	77	112	84	71	81	35	39	84	129	75
1740	59	90	55	119	157	168	110	120	45	41
1750	63	49	79	83	58	46	68	78	84	92
1760	92	64	67	59	90	74	94	126	105	84
1770	57	74	97	50	48	113	80	52	66	68
1780	49	80	63	68	126	58	77	127	55	52
1790	76	103	92	95	70	79	61	84	81	71
1800	58	64	88	55	73	59	74	96	57	69
1810	112	113	67	44	93	91	115	114	61	94
1820	57	67	58	65	78	99	95	67	108	71
1830	59	55	96	103	67	74	81	82	90	77
1840	79	59	65	81	91	64	66	44	83	145
1850	94	73	79	95	72	70	61	49	57	64
1860	57	52	110	100	49	75	118	111	123	115
1870	67	46	73	72	76	92	70	72	65	59
1880	69	62	50	44	105	173	98	65	62	95
1890	127	91	74	66	50	65	43	75	110	35
1900	55	104	49	66	59	87	116	101	94	79
1910	89	116	98	82	97	96	94	90	77	86
1920	109	80	73	86	54	57	78	80	94	67
1930	68	71	87	76	55	81	61	50	79	72
1940	72	102	98	84	76	60	41	66	80	97
1950	65	41	93	69	73	69	47	82	101	44
1960	63	72	89	60	58	93	87	87	104	120
1970	67	75	103	125	67	88	85	29	89	142
1980	106	80	73	94	60	79	83	69	87	61
1990	50	58	87	100	71	90	51	68	107	



SITES SK1 and SK2: Summer 3 reconstructed discharge.
 Units are mean daily cubic meters per second (m^3/s) $\times 100$.

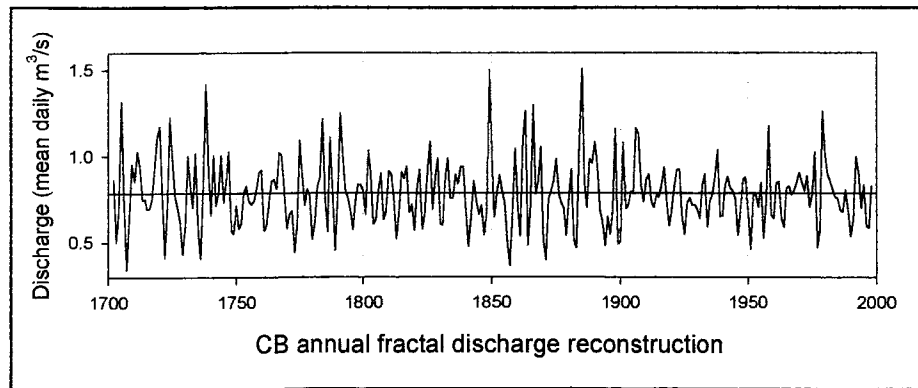
Year	0	1	2	3	4	5	6	7	8	9
1700	78	113	80	70	74	92	88	104	82	72
1710	80	80	87	102	101	97	70	71	60	96
1720	104	78	67	67	62	72	83	131	100	75
1730	74	84	73	126	116	99	75	102	101	82
1740	115	76	72	73	71	73	114	92	97	99
1750	97	91	97	103	96	97	87	87	86	112
1760	98	110	82	82	63	63	65	65	80	71
1770	74	124	97	72	78	89	85	89	105	88
1780	100	85	70	104	84	66	105	117	113	82
1790	72	68	85	70	86	71	78	73	87	86
1800	77	100	80	89	84	83	102	96	85	71
1810	91	106	75	84	60	75	94	78	122	100
1820	112	97	115	92	86	92	72	95	91	95
1830	75	76	83	73	79	80	76	74	67	88
1840	88	84	75	94	86	123	74	72	73	77
1850	68	66	81	75	96	113	111	106	107	118
1860	79	89	122	91	76	82	68	73	96	114
1870	81	94	78	77	96	92	93	98	97	109
1880	115	128	89	68	77	88	80	66	59	68
1890	72	84	109	91	129	86	85	136	104	81
1900	113	88	114	84	71	67	69	74	66	64
1910	75	79	70	77	72	77	79	87	77	79
1920	83	84	101	105	95	94	84	107	96	92
1930	84	89	96	84	100	97	88	94	86	74
1940	73	69	73	79	99	84	83	74	95	101
1950	80	100	80	91	114	85	83	111	89	95
1960	76	98	95	84	88	76	72	69	91	82
1970	89	79	96	78	82	131	87	80	75	79
1980	90	76	94	84	89	90	83	91	118	100
1990	80	80	85	65	117	82	81			



APPENDIX C. FRACTAL TRANSFORM RECONSTRUCTIONS

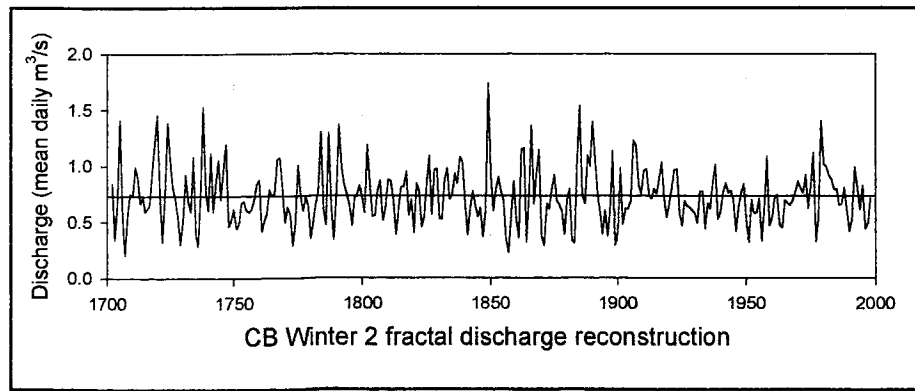
Site CB: Fractal Annual discharge reconstruction.
 Units are mean daily cubic meters per second (m^3/s) $\times 100$.

Year	0	1	2	3	4	5	6	7	8	9
1702			86	50	69	132	71	34	63	96
1710	86	103	94	75	75	70	70	75	92	111
1720	117	77	41	71	122	99	78	70	62	43
1730	60	100	83	70	102	58	41	84	142	92
1740	66	100	71	79	101	73	85	103	57	55
1750	71	58	62	79	83	74	72	74	81	90
1760	92	57	60	73	86	86	81	102	101	81
1770	58	67	68	44	61	109	89	72	81	77
1780	52	62	82	88	122	77	56	111	80	45
1790	76	125	101	80	76	69	58	74	84	84
1800	80	67	104	90	61	64	80	90	63	68
1810	91	90	77	52	67	91	87	94	68	72
1820	57	81	92	58	67	90	109	70	87	99
1830	61	60	87	99	76	76	89	84	94	94
1840	69	48	64	86	74	67	71	55	69	150
1850	102	65	79	89	80	73	50	37	69	104
1860	72	54	110	126	49	72	130	78	86	105
1870	51	40	75	80	86	99	79	73	70	54
1880	76	93	52	47	108	151	85	70	98	96
1890	108	95	69	61	48	65	55	69	116	49
1900	51	108	70	72	80	79	116	113	83	74
1910	87	90	74	70	78	77	84	94	74	60
1920	70	83	92	92	65	55	73	76	72	72
1930	69	64	83	90	59	74	78	89	104	65
1940	66	83	88	82	80	76	54	69	87	88
1950	67	46	77	78	71	85	53	73	117	66
1960	64	85	85	64	59	81	83	78	80	85
1970	90	85	80	89	71	78	103	47	58	126
1980	102	90	86	81	76	76	69	68	81	69
1990	54	63	100	91	70	84	60	58	83	



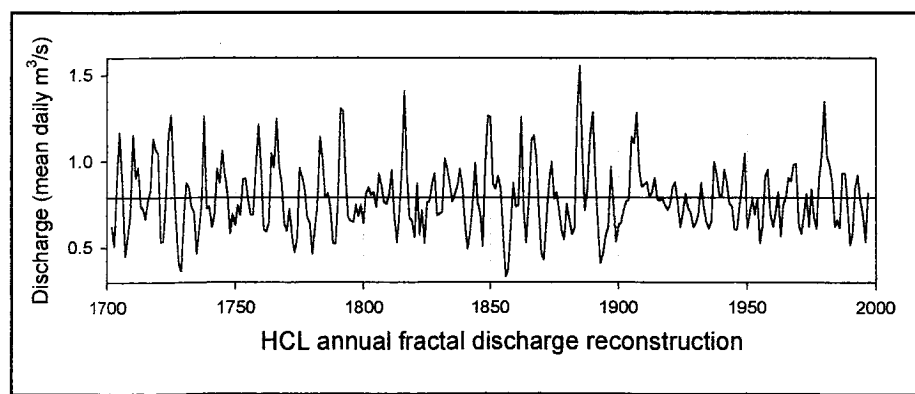
Site CB: Fractal Winter 2 discharge reconstruction.
 Units are mean daily cubic meters per second (m^3/s) $\times 100$.

Year	0	1	2	3	4	5	6	7	8	9
1702			84	34	66	141	56	21	54	74
1710	73	98	89	67	72	59	62	65	94	121
1720	145	75	32	76	138	106	82	71	55	30
1730	51	92	69	59	108	39	28	73	153	78
1740	61	111	59	85	105	70	94	119	46	52
1750	62	45	48	67	68	61	59	61	70	84
1760	87	42	51	57	79	73	75	106	107	80
1770	50	63	57	29	48	100	72	60	72	65
1780	35	49	65	76	130	61	47	129	65	34
1790	71	136	99	83	75	65	47	71	74	82
1800	72	58	119	84	55	56	78	87	51	62
1810	88	87	70	39	61	81	81	94	56	70
1820	40	85	77	45	54	84	109	56	96	98
1830	52	52	88	98	70	74	93	84	108	103
1840	67	38	62	77	66	55	63	37	60	173
1850	92	60	79	90	78	70	36	23	56	86
1860	51	36	115	116	32	71	136	66	94	114
1870	38	29	66	61	79	92	69	65	60	39
1880	70	79	34	31	107	154	74	66	109	100
1890	139	106	75	59	39	60	37	61	113	29
1900	40	98	48	62	61	69	122	119	83	74
1910	95	97	74	71	79	75	89	103	72	54
1920	66	80	96	97	58	46	68	65	63	60
1930	57	49	77	77	44	67	62	86	101	52
1940	59	76	85	76	77	70	41	63	76	84
1950	52	32	69	57	58	71	33	63	108	46
1960	53	71	74	47	45	69	67	65	69	77
1970	86	80	76	92	62	82	111	32	55	140
1980	102	99	91	88	79	79	65	66	80	61
1990	42	53	99	80	61	82	44	49	71	



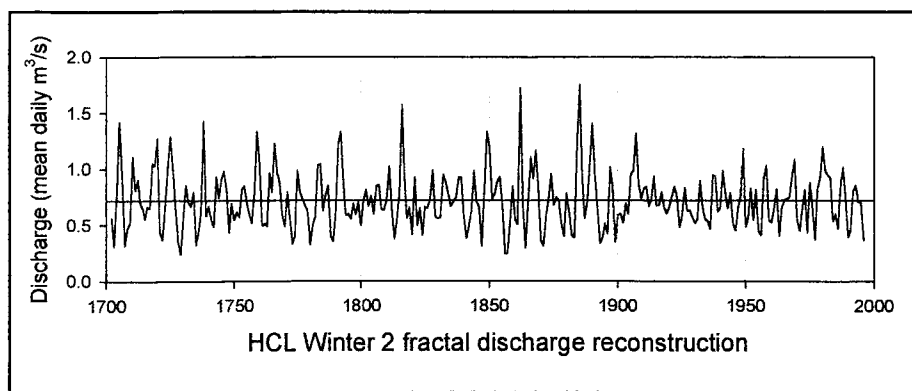
Site HCL: Fractal Annual discharge reconstruction.
 Units are mean daily cubic meters per second (m^3/s) $\times 100$.

Year	0	1	2	3	4	5	6	7	8	9
1702			62	51	88	117	88	45	56	69
1710	115	91	96	74	72	67	77	83	113	107
1720	104	53	54	77	115	127	92	63	41	36
1730	66	88	85	74	71	47	60	75	126	73
1740	74	62	69	96	88	106	93	82	58	70
1750	63	74	69	90	90	78	69	69	95	121
1760	98	61	59	65	104	96	124	98	87	64
1770	60	73	56	47	55	96	91	84	68	64
1780	46	62	74	114	102	79	81	74	52	52
1790	77	131	129	90	67	66	65	75	68	75
1800	64	82	85	81	82	73	93	87	76	75
1810	81	95	69	53	69	96	141	92	67	66
1820	56	87	58	71	53	76	77	87	93	68
1830	70	71	102	96	87	77	81	86	96	86
1840	63	49	59	75	99	76	70	51	98	126
1850	126	87	84	91	84	58	33	37	62	87
1860	74	74	126	73	53	76	112	115	101	72
1870	47	43	66	89	100	78	82	71	59	55
1880	75	66	58	62	130	156	104	72	84	115
1890	128	89	63	41	46	57	62	97	77	53
1900	63	64	72	77	78	114	110	129	96	85
1910	87	88	79	82	91	78	77	79	75	72
1920	75	85	88	76	62	70	81	73	70	62
1930	64	70	87	74	65	61	65	100	93	81
1940	79	95	88	76	74	61	60	74	89	105
1950	62	70	78	69	79	53	63	91	95	70
1960	62	70	82	57	75	80	90	89	98	99
1970	64	58	69	81	62	84	67	61	90	104
1980	135	103	98	89	62	66	61	93	93	75
1990	51	58	85	92	78	70	53	82		



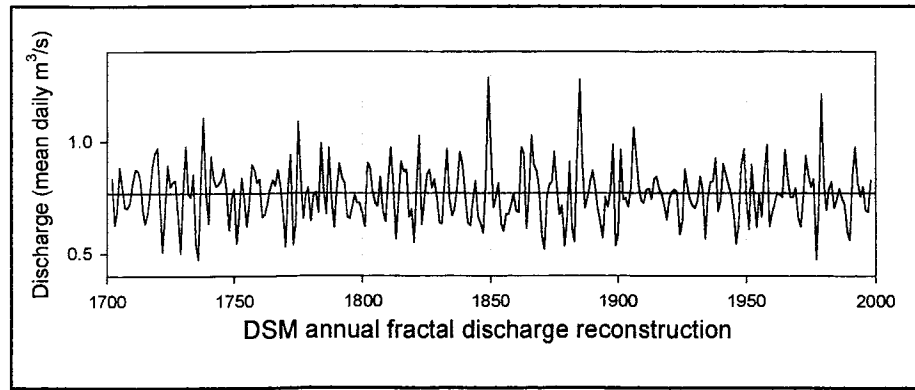
Site HCL: Fractal Winter 2 discharge reconstruction.
 Units are mean daily cubic meters per second (m^3/s) $\times 100$.

Year	0	1	2	3	4	5	6	7	8	9
1702			57	31	76	142	89	32	47	52
1710	111	81	91	69	64	55	66	65	105	103
1720	127	44	37	66	102	129	103	66	35	24
1730	56	85	70	67	79	32	44	62	143	58
1740	67	55	48	93	74	91	98	82	43	69
1750	54	62	57	81	85	71	60	52	78	133
1760	104	50	51	49	96	79	122	98	87	58
1770	49	79	54	33	40	99	79	74	67	63
1780	32	50	57	104	104	63	77	85	40	35
1790	61	122	133	88	59	60	55	69	59	70
1800	50	72	81	67	76	60	85	86	64	63
1810	72	102	66	38	55	79	157	92	56	66
1820	41	92	49	65	41	66	65	73	99	58
1830	56	57	95	89	78	67	71	74	92	92
1840	59	38	49	62	99	71	66	31	81	133
1850	119	74	77	89	93	67	25	25	54	84
1860	55	51	172	68	30	70	110	91	116	83
1870	35	31	58	73	96	68	75	72	50	40
1880	78	63	41	39	122	175	95	56	70	106
1890	141	95	66	33	38	51	42	101	85	35
1900	59	60	52	69	60	95	98	132	87	73
1910	83	85	67	73	93	67	67	79	66	60
1920	66	76	84	76	49	59	83	63	63	57
1930	52	55	90	67	55	53	46	95	94	62
1940	65	99	79	65	79	51	45	65	76	118
1950	48	56	83	54	81	44	41	92	103	54
1960	52	65	82	40	65	72	74	75	93	108
1970	55	45	63	82	43	88	65	37	83	92
1980	120	98	95	92	54	60	46	85	101	73
1990	39	45	80	85	71	70	36			



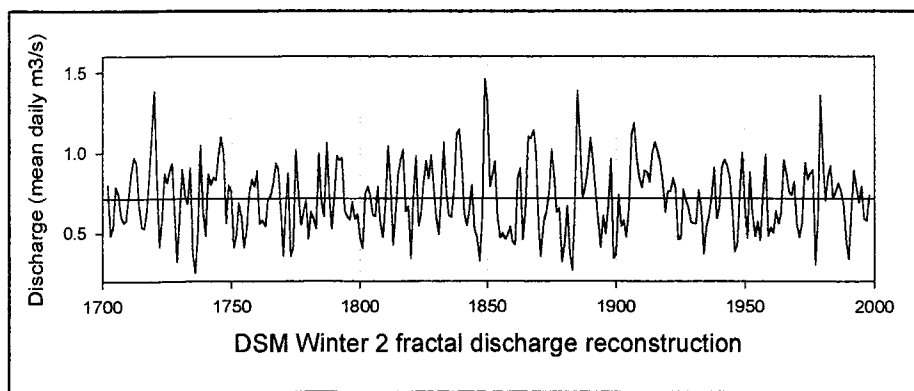
Site DSM: Fractal Annual discharge reconstruction.
 Units are mean daily cubic meters per second (m^3/s) $\times 100$.

Year	0	1	2	3	4	5	6	7	8	9
1702			84	63	69	89	80	71	70	73
1710	82	88	87	82	68	63	68	77	89	95
1720	97	72	51	69	89	80	82	83	67	50
1730	77	98	77	76	86	55	48	82	111	78
1740	64	93	84	80	81	83	88	79	61	75
1750	79	54	67	84	75	62	73	90	88	82
1760	83	66	67	72	79	83	80	88	80	68
1770	53	79	94	54	64	109	83	66	76	79
1780	64	76	77	68	99	77	68	97	76	62
1790	79	90	84	81	67	66	71	76	73	72
1800	68	62	91	89	78	73	71	84	69	64
1810	83	97	80	57	74	91	87	87	66	70
1820	55	81	103	63	74	85	88	79	83	75
1830	64	64	81	97	75	67	70	80	96	90
1840	77	64	63	73	82	66	63	59	81	129
1850	98	70	75	81	63	60	68	67	71	77
1860	69	68	98	95	61	76	103	90	87	79
1870	58	52	75	81	82	96	80	67	71	53
1880	65	91	61	55	95	128	92	70	75	82
1890	87	80	70	64	57	75	71	78	98	53
1900	59	96	74	74	71	79	106	94	80	74
1910	73	78	79	74	83	84	79	77	72	65
1920	74	77	79	77	59	64	88	80	74	71
1930	70	73	84	78	57	74	82	82	92	69
1940	73	90	85	81	77	68	54	63	89	97
1950	74	61	90	74	62	76	66	86	98	62
1960	68	72	77	76	75	96	83	75	75	79
1970	66	62	74	94	85	80	83	47	73	121
1980	81	70	79	82	70	74	79	75	72	60
1990	56	85	97	81	75	80	70	69	82	



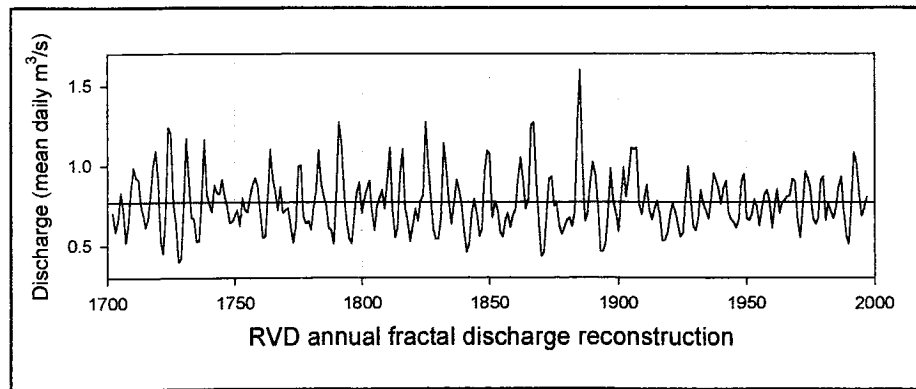
Site DSM: Fractal Winter 2 discharge reconstruction. Units are mean daily cubic meters per second (m^3/s) $\times 100$.

Year	0	1	2	3	4	5	6	7	8	9
1702			80	48	54	79	74	60	57	58
1710	73	87	97	94	68	54	53	64	88	113
1720	139	86	42	59	87	81	89	93	63	32
1730	61	90	74	68	91	36	25	50	105	63
1740	48	87	80	85	83	98	110	101	56	80
1750	76	41	49	69	61	41	51	74	83	79
1760	89	56	58	54	71	73	81	93	90	64
1770	36	66	88	35	41	102	77	55	63	70
1780	46	63	59	53	100	69	60	106	75	53
1790	72	98	95	97	64	60	58	69	58	62
1800	48	41	75	79	73	61	60	79	56	48
1810	68	104	81	43	61	86	95	102	64	67
1820	34	73	98	54	62	81	95	84	99	79
1830	60	49	75	106	77	61	60	76	112	115
1840	95	63	55	64	80	52	47	33	62	146
1850	131	79	86	94	60	47	50	46	49	54
1860	45	43	84	90	46	64	110	109	114	99
1870	54	36	58	64	76	102	86	63	65	32
1880	43	67	38	27	67	139	109	72	78	89
1890	109	96	78	58	41	61	49	67	96	35
1900	37	74	54	58	48	65	112	119	97	85
1910	78	89	88	82	100	107	101	95	82	63
1920	76	76	84	78	46	47	77	70	66	57
1930	56	56	77	66	37	54	60	73	91	59
1940	65	91	96	92	86	67	38	43	73	100
1950	67	47	88	61	48	57	46	73	99	48
1960	53	50	64	56	63	95	87	76	74	82
1970	56	47	56	94	83	88	89	31	60	136
1980	95	70	85	92	72	76	81	76	68	44
1990	34	64	89	79	69	79	59	58	73	



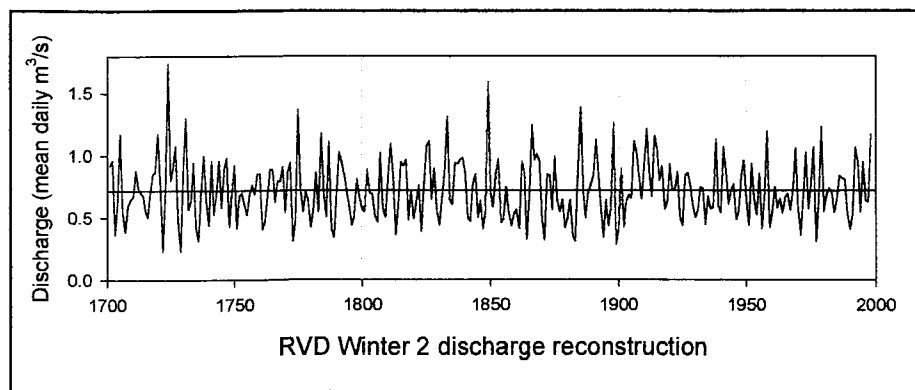
Site RVD: Fractal Annual discharge reconstruction.
 Units are mean daily cubic meters per second (m^3/s) $\times 100$.

Year	0	1	2	3	4	5	6	7	8	9
1702			70	58	66	83	72	52	64	85
1710	99	93	91	75	68	62	67	81	100	109
1720	92	53	45	71	124	120	77	63	40	42
1730	76	117	92	68	67	52	53	80	116	82
1740	77	71	88	83	82	92	81	74	64	65
1750	69	72	62	80	73	71	81	88	92	87
1760	71	55	56	81	110	92	84	72	87	71
1770	72	73	62	52	63	100	100	68	64	65
1780	60	74	83	110	89	82	76	61	60	51
1790	81	127	114	86	65	55	52	68	83	89
1800	70	79	85	91	70	59	75	80	85	73
1810	91	111	71	55	61	95	110	74	65	53
1820	63	73	65	78	81	127	102	82	60	54
1830	54	68	114	100	79	63	76	91	85	76
1840	59	46	51	70	79	70	56	61	96	109
1850	107	67	78	73	59	56	66	70	62	69
1860	73	92	105	91	73	79	125	127	92	65
1870	44	46	69	92	93	75	77	63	57	61
1880	66	67	62	71	128	160	104	65	70	89
1890	102	94	76	47	46	51	71	98	79	71
1900	58	79	99	81	93	111	110	111	76	70
1910	79	88	72	66	73	78	69	53	53	58
1920	69	76	72	64	56	58	79	99	81	62
1930	59	68	85	76	72	67	78	95	91	85
1940	76	86	90	70	66	65	61	66	90	95
1950	67	66	70	79	75	62	74	82	85	77
1960	61	74	85	70	77	78	81	81	91	90
1970	66	55	74	96	92	85	67	63	67	91
1980	93	66	77	71	67	74	87	93	72	56
1990	51	75	108	102	84	69	73	80		



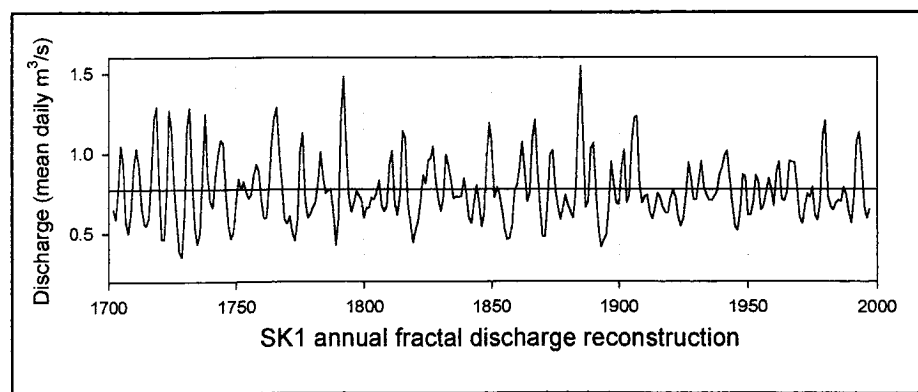
Site RVD: Fractal Winter 2 discharge reconstruction.
 Units are mean daily cubic meters per second (m^3/s) $\times 100$.

Year	0	1	2	3	4	5	6	7	8	9
1701		92	96	37	62	117	55	39	59	65
1710	66	88	73	70	68	56	51	71	85	87
1720	117	75	24	71	174	80	90	108	47	23
1730	91	130	57	64	94	42	32	71	99	63
1740	44	95	53	68	95	59	89	98	43	70
1750	92	42	68	70	61	52	69	76	69	85
1760	85	41	47	67	89	89	63	79	79	91
1770	54	87	94	31	48	137	73	55	70	64
1780	42	55	86	55	117	69	51	111	41	34
1790	70	103	94	84	71	59	44	52	81	67
1800	58	55	89	70	69	51	46	102	58	50
1810	84	109	85	36	60	94	92	96	48	72
1820	49	62	76	39	75	108	111	65	89	55
1830	44	65	87	131	65	61	94	93	97	98
1840	86	50	47	77	85	50	64	41	55	159
1850	70	58	84	97	46	49	74	53	44	53
1860	56	42	95	87	33	66	124	97	101	96
1870	49	32	85	84	57	99	64	55	64	42
1880	50	64	35	31	87	139	71	49	70	76
1890	85	113	86	58	34	65	44	58	126	28
1900	41	89	42	64	68	65	112	103	84	65
1910	94	121	87	67	115	106	80	91	58	63
1920	94	72	73	87	50	44	84	86	76	60
1930	50	56	74	73	44	67	57	58	113	60
1940	54	107	87	61	72	77	49	56	84	96
1950	64	44	94	66	52	86	42	65	119	42
1960	54	74	58	65	54	67	69	56	72	106
1970	58	36	67	102	57	76	107	31	63	123
1980	55	68	73	71	54	64	83	82	80	53
1990	41	53	106	95	55	95	64	63	117	



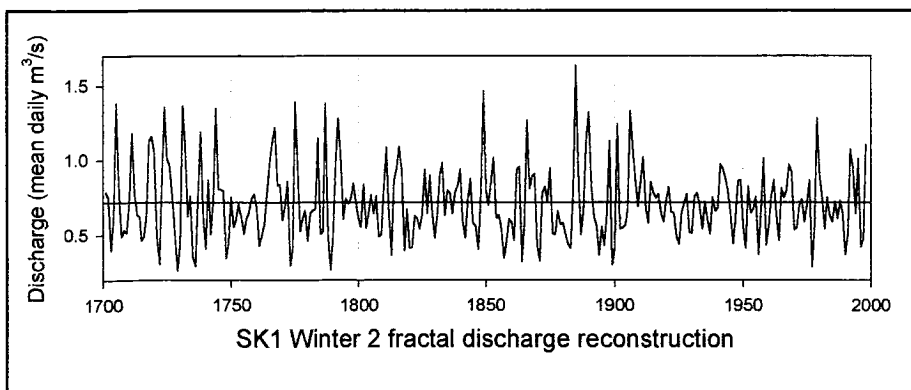
Site SK1: Fractal Annual discharge reconstruction.
 Units are mean daily cubic meters per second (m^3/s) $\times 100$.

Year	0	1	2	3	4	5	6	7	8	9
1702			65	59	78	105	93	58	50	64
1710	92	103	93	67	56	55	60	89	122	129
1720	84	47	47	75	127	115	80	59	39	36
1730	62	117	129	85	54	43	50	87	125	86
1740	70	66	86	98	108	106	75	55	47	51
1750	69	84	77	82	76	72	74	87	93	89
1760	71	59	60	79	107	122	129	101	81	59
1770	56	61	51	46	59	102	113	71	60	62
1780	67	70	82	101	86	75	77	78	63	43
1790	61	124	148	105	73	63	69	76	74	71
1800	60	66	66	72	71	76	83	68	64	67
1810	93	101	69	61	74	114	109	69	57	44
1820	52	58	71	87	81	96	97	104	83	72
1830	64	72	99	93	83	72	73	73	73	85
1840	75	60	56	69	80	70	54	63	98	119
1850	106	72	79	75	65	53	46	47	55	77
1860	81	91	107	90	70	75	110	121	91	69
1870	49	48	70	100	102	77	67	59	66	74
1880	68	64	60	75	125	155	111	66	70	103
1890	106	76	53	42	46	49	67	95	81	69
1900	68	92	102	70	73	107	122	123	81	69
1910	73	74	63	59	66	75	72	66	63	63
1920	72	77	73	60	55	59	74	94	84	71
1930	71	83	95	79	74	71	71	73	76	87
1940	91	99	101	85	69	55	52	64	87	86
1950	61	62	69	87	82	65	67	75	85	78
1960	67	89	95	72	70	75	95	95	94	78
1970	60	57	67	75	73	79	61	58	70	111
1980	121	73	67	65	69	71	70	79	74	64
1990	57	72	107	113	95	67	59	65		



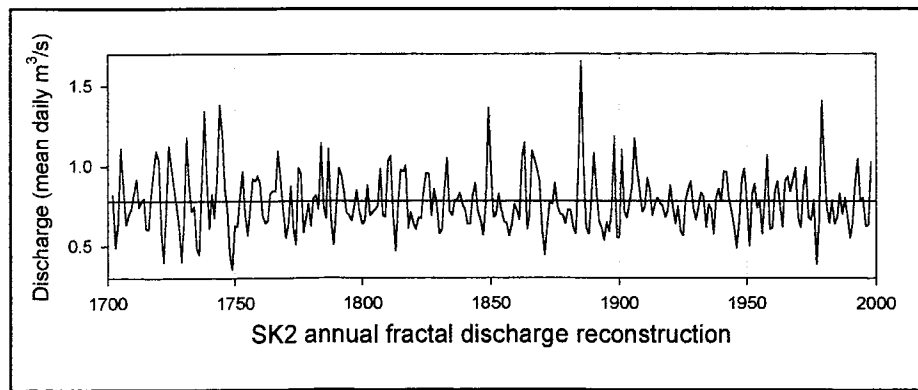
Site SK1: Fractal Winter 2 discharge reconstruction.
 Units are mean daily cubic meters per second (m^3/s) $\times 100$.

Year	0	1	2	3	4	5	6	7	8	9
1701		78	76	40	63	138	85	49	53	51
1710	71	118	77	63	62	46	49	64	114	116
1720	106	49	30	87	136	101	96	76	51	26
1730	44	136	109	62	76	35	29	77	119	62
1740	41	87	50	73	135	81	80	80	34	45
1750	75	55	61	70	62	51	61	66	74	77
1760	68	43	50	58	80	100	113	122	83	84
1770	60	69	86	30	41	139	97	53	61	66
1780	46	65	67	67	115	51	52	138	50	27
1790	49	98	128	102	61	74	71	74	85	72
1800	62	55	84	54	64	77	64	76	49	51
1810	82	109	64	37	87	94	109	94	39	67
1820	42	42	63	61	54	64	94	65	90	65
1830	48	63	91	98	63	80	78	64	79	83
1840	94	59	48	73	88	58	56	40	79	147
1850	80	70	86	102	62	64	54	34	46	61
1860	58	46	94	96	32	58	127	81	89	91
1870	44	33	78	82	73	95	51	50	66	57
1880	58	50	44	41	81	164	92	50	66	114
1890	132	83	62	57	36	56	43	65	113	30
1900	42	124	54	55	57	68	133	109	86	69
1910	87	102	68	58	86	78	75	77	65	59
1920	74	82	65	65	49	44	65	71	77	52
1930	51	76	78	70	54	72	60	51	75	66
1940	68	98	95	88	79	63	44	61	86	87
1950	57	41	83	65	68	76	37	67	101	43
1960	57	76	87	63	46	81	75	80	97	92
1970	54	55	70	74	59	70	87	29	56	128
1980	90	75	54	75	63	59	73	61	73	65
1990	37	50	107	95	65	101	42	48	110	



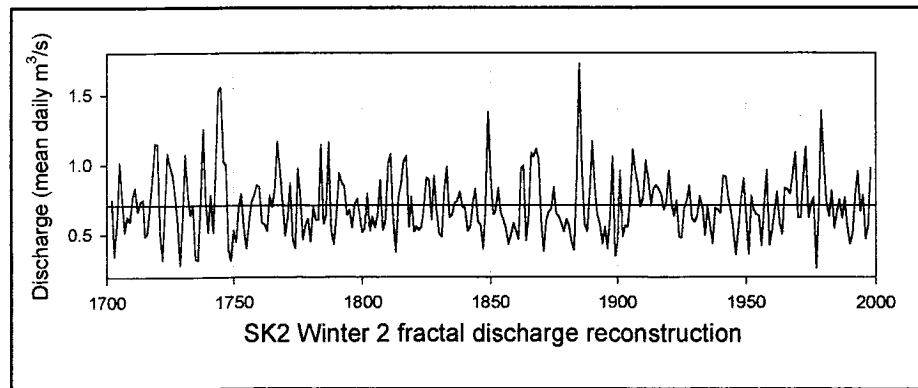
Site SK2: Fractal Annual discharge reconstruction.
 Units are mean daily cubic meters per second (m^3/s) $\times 100$.

Year	0	1	2	3	4	5	6	7	8	9
1702			82	49	65	111	88	63	70	74
1710	83	92	74	78	80	61	60	81	97	110
1720	103	59	40	72	112	100	88	76	62	40
1730	65	118	89	72	75	49	45	92	134	91
1740	61	82	68	92	138	119	87	74	46	36
1750	63	62	81	97	70	57	73	92	91	94
1760	89	69	64	66	83	84	84	110	92	73
1770	55	63	88	60	51	99	95	58	67	76
1780	62	80	82	73	114	75	67	111	66	51
1790	75	99	94	84	71	69	66	74	85	71
1800	64	66	88	69	71	73	75	98	69	68
1810	103	106	70	47	77	98	96	100	61	71
1820	64	60	68	67	84	96	95	69	86	77
1830	57	61	85	105	71	69	79	79	83	76
1840	73	64	64	82	89	72	66	57	77	136
1850	98	68	70	82	72	65	64	56	64	76
1860	72	66	105	115	60	69	109	104	98	91
1870	61	44	63	79	76	89	75	70	70	64
1880	73	72	62	57	101	166	102	61	58	80
1890	108	85	65	62	54	65	59	74	118	55
1900	55	110	72	67	76	87	117	98	84	71
1910	74	92	85	69	76	80	77	75	68	72
1920	88	75	64	75	59	57	79	86	90	74
1930	67	74	83	81	61	76	73	58	81	86
1940	78	97	96	80	72	62	49	66	92	98
1950	77	50	83	89	74	78	58	79	107	60
1960	62	84	90	75	62	91	93	84	92	99
1970	68	62	86	99	68	66	79	39	68	141
1980	101	74	64	79	64	68	83	70	80	68
1990	55	65	89	104	79	80	62	63	102	



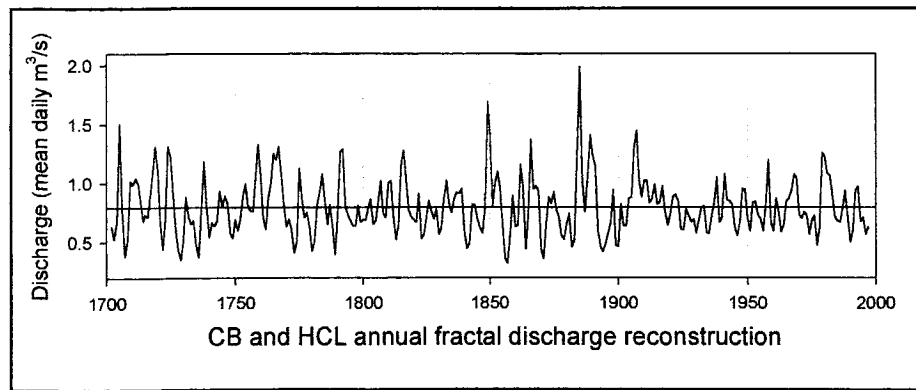
Site SK2: Fractal Winter 2 discharge reconstruction.
 Units are mean daily cubic meters per second (m^3/s) $\times 100$.

Year	0	1	2	3	4	5	6	7	8	9
1702			75	35	58	102	78	52	63	60
1710	77	83	67	74	75	49	51	71	92	115
1720	115	52	32	69	108	100	92	78	58	29
1730	61	107	80	64	71	33	32	75	125	75
1740	52	79	52	100	153	156	103	100	40	32
1750	53	45	69	79	54	41	59	73	78	86
1760	85	59	58	53	78	70	83	117	98	75
1770	50	61	87	47	40	97	79	47	57	62
1780	45	70	61	61	115	58	64	116	53	43
1790	66	94	87	85	64	68	55	71	76	64
1800	52	56	79	53	63	55	64	89	53	60
1810	101	107	62	38	76	87	103	106	56	77
1820	52	56	53	56	71	91	89	61	92	67
1830	51	49	82	98	62	64	73	74	81	70
1840	69	53	56	72	83	59	58	40	70	138
1850	93	65	68	84	66	60	54	43	50	58
1860	53	47	98	100	46	63	108	106	111	104
1870	60	38	60	66	68	84	65	63	58	52
1880	61	57	45	39	91	173	98	58	52	81
1890	117	85	64	57	43	56	40	64	106	35
1900	44	96	49	56	55	77	111	96	86	70
1910	77	103	90	72	83	85	83	79	68	74
1920	96	73	63	74	49	48	69	74	85	62
1930	59	63	77	70	50	70	57	44	69	68
1940	65	92	92	77	68	53	36	55	75	90
1950	62	36	78	68	65	64	42	70	96	43
1960	53	67	81	58	50	83	83	79	94	109
1970	62	63	90	113	63	72	77	26	68	139
1980	102	73	63	81	55	66	75	62	77	56
1990	44	51	78	95	67	78	47	57	98	



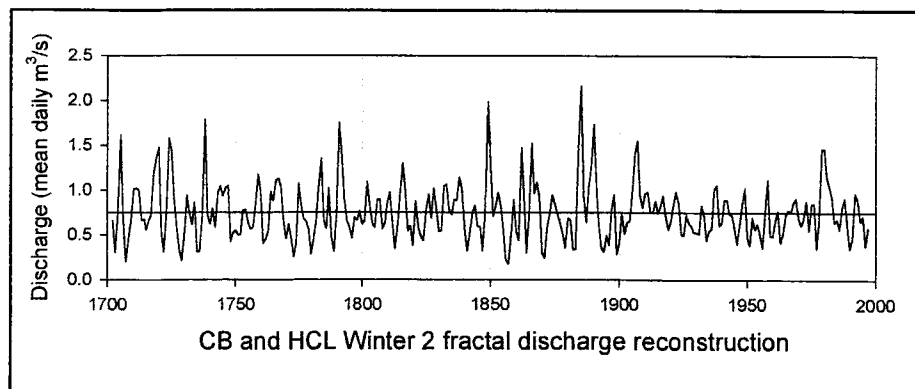
Sites CB-HCL: Fractal Annual discharge reconstruction.
 Units are mean daily cubic meters per second (m^3/s) $\times 100$.

Year	0	1	2	3	4	5	6	7	8	9
1702			63	53	69	151	78	39	52	102
1710	99	105	100	82	68	73	71	88	109	131
1720	111	65	44	70	131	124	94	61	43	35
1730	51	88	71	65	68	48	37	77	118	81
1740	55	66	64	68	93	80	89	83	58	54
1750	69	60	70	89	100	81	77	76	105	133
1760	106	70	61	87	101	125	120	131	108	82
1770	63	69	61	41	51	112	89	71	75	63
1780	43	51	81	92	108	86	65	81	63	40
1790	73	127	129	81	73	68	64	64	81	67
1800	69	69	79	87	65	68	83	102	74	71
1810	100	102	71	52	65	116	128	102	77	71
1820	69	67	91	53	56	70	85	77	70	78
1830	57	63	87	102	84	75	87	92	91	95
1840	58	45	50	82	82	70	62	58	80	169
1850	139	81	101	110	96	64	36	32	56	89
1860	63	65	116	97	44	73	137	96	97	93
1870	44	36	67	88	83	92	79	71	56	52
1880	66	74	46	52	124	199	103	76	106	141
1890	124	115	61	46	42	49	58	67	94	48
1900	47	82	64	64	87	88	131	145	102	88
1910	102	103	84	87	99	82	84	98	76	64
1920	75	89	91	85	61	60	78	73	67	69
1930	58	69	80	81	58	58	72	84	105	67
1940	72	108	86	85	82	62	55	68	95	95
1950	70	59	84	85	73	70	59	82	120	67
1960	60	87	76	59	65	85	87	94	108	104
1970	74	70	76	72	57	69	72	47	62	126
1980	123	108	107	90	71	68	67	79	94	71
1990	50	60	94	97	68	71	57	63		



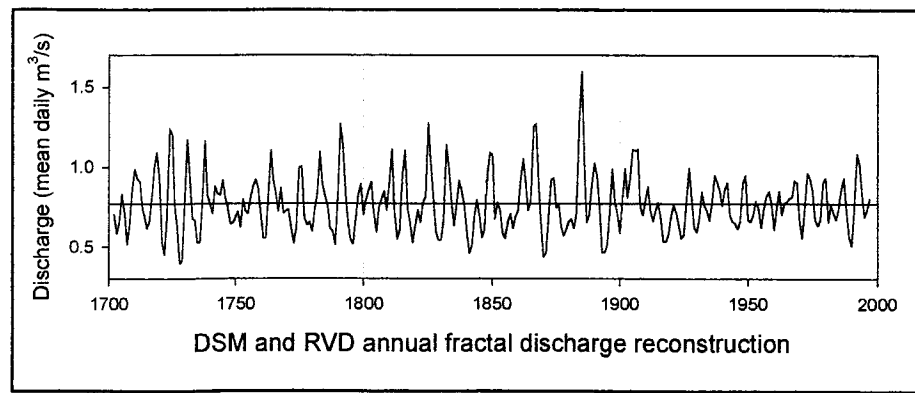
Sites CB-HCL: Fractal Winter 2 discharge reconstruction.
 Units are mean daily cubic meters per second (m^3/s) $\times 100$.

Year	0	1	2	3	4	5	6	7	8	9
1702			65	30	76	161	66	20	44	67
1710	101	102	100	66	67	56	65	72	119	136
1720	148	54	31	74	158	144	91	59	34	21
1730	50	94	75	61	86	31	31	72	179	72
1740	62	79	58	97	104	93	102	105	42	53
1750	54	50	50	77	78	64	56	58	84	117
1760	98	40	45	53	98	88	111	113	103	65
1770	45	62	46	25	41	107	83	67	64	56
1780	29	46	65	104	135	65	57	101	48	31
1790	72	175	138	90	66	58	46	69	66	76
1800	62	66	109	83	63	58	89	89	56	63
1810	86	97	63	34	58	95	130	99	54	60
1820	37	87	58	49	43	79	95	68	102	80
1830	53	54	104	106	77	73	89	88	114	100
1840	57	32	52	74	83	59	59	32	78	198
1850	128	70	82	97	81	54	21	18	50	89
1860	54	44	147	92	30	70	152	96	108	91
1870	30	24	59	73	94	85	73	62	50	35
1880	68	67	33	34	147	216	94	64	103	127
1890	173	105	61	36	31	49	39	78	95	28
1900	41	74	51	64	65	97	140	155	95	80
1910	96	98	75	76	88	74	83	93	70	56
1920	66	84	98	86	51	49	72	64	60	52
1930	52	51	83	72	44	55	57	101	105	60
1940	64	89	89	73	72	57	40	63	85	102
1950	47	38	69	56	62	50	36	76	111	49
1960	48	66	76	41	51	71	78	75	86	91
1970	68	60	68	88	55	84	85	35	68	146
1980	146	114	104	92	64	67	56	80	91	62
1990	35	46	96	89	65	70	38	57		



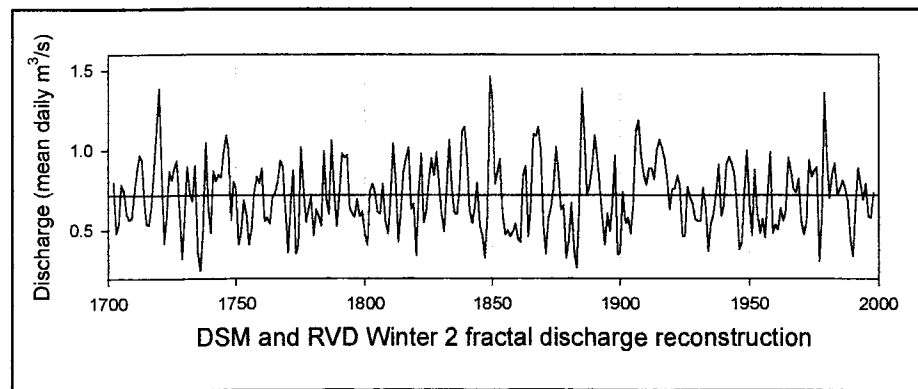
Sites DSM-RVD: Fractal Annual discharge reconstruction.
 Units are mean daily cubic meters per second (m^3/s) $\times 100.$

Year	0	1	2	3	4	5	6	7	8	9
1702			70	58	66	83	72	52	64	85
1710	99	93	91	75	68	62	67	81	100	109
1720	92	53	45	71	124	120	77	63	40	42
1730	76	117	92	68	67	52	53	80	116	82
1740	77	71	88	83	82	92	81	74	64	65
1750	69	72	62	80	73	71	81	88	92	87
1760	71	55	56	81	110	92	84	72	87	71
1770	72	73	62	52	63	100	100	68	64	65
1780	60	74	83	110	89	82	76	61	60	51
1790	81	127	114	86	65	55	52	68	83	89
1800	70	79	85	91	70	59	75	80	85	73
1810	91	111	71	55	61	95	110	74	65	53
1820	63	73	65	78	81	127	102	82	60	54
1830	54	68	114	100	79	63	76	91	85	76
1840	59	46	51	70	79	70	56	61	96	109
1850	107	67	78	73	59	56	66	70	62	69
1860	73	92	105	91	73	79	125	127	92	65
1870	44	46	69	92	93	75	77	63	57	61
1880	66	67	62	71	128	160	104	65	70	89
1890	102	94	76	47	46	51	71	98	79	71
1900	58	79	99	81	93	111	110	111	76	70
1910	79	88	72	66	73	78	69	53	53	58
1920	69	76	72	64	56	58	79	99	81	62
1930	59	68	85	76	72	67	78	95	91	85
1940	76	86	90	70	66	65	61	66	90	95
1950	67	66	70	79	75	62	74	82	85	77
1960	61	74	85	70	77	78	81	81	91	90
1970	66	55	74	96	92	85	67	63	67	91
1980	93	66	77	71	67	74	87	93	72	56
1990	51	75	108	102	84	69	73	80		



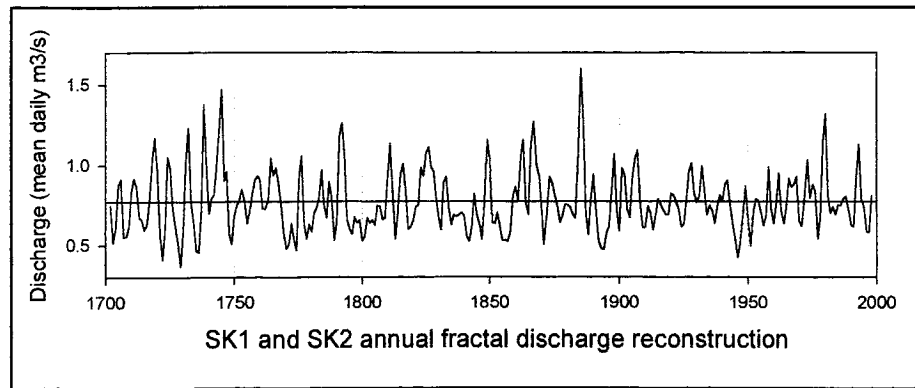
Sites DSM-RVD: Fractal Winter 2 discharge reconstruction.
 Units are mean daily cubic meters per second (m^3/s) $\times 100$.

Year	0	1	2	3	4	5	6	7	8	9
1702			80	48	54	79	74	60	57	58
1710	73	87	97	94	68	54	53	64	88	113
1720	139	86	42	59	87	82	89	93	63	32
1730	61	90	74	68	91	36	25	50	105	63
1740	48	87	81	85	83	98	110	101	56	80
1750	76	41	49	69	61	41	51	74	84	79
1760	89	56	58	54	71	73	81	93	90	64
1770	36	66	88	35	41	102	77	55	63	71
1780	47	63	59	53	100	69	60	106	75	53
1790	72	98	95	97	64	61	58	69	59	62
1800	48	41	75	79	74	61	60	79	56	48
1810	69	104	81	43	61	86	95	102	64	67
1820	34	73	98	55	62	81	95	84	99	79
1830	60	49	75	107	77	61	60	76	112	115
1840	95	63	55	64	80	53	47	33	62	146
1850	131	79	86	95	60	47	50	46	49	54
1860	45	43	84	90	46	65	110	109	115	99
1870	54	36	58	64	76	102	86	63	66	33
1880	43	67	38	27	67	139	109	72	78	89
1890	110	96	78	58	41	61	50	67	97	35
1900	37	74	55	58	48	66	112	119	97	85
1910	78	89	89	82	100	107	101	95	82	63
1920	76	76	84	78	46	47	77	71	66	57
1930	56	56	77	66	37	54	61	73	91	59
1940	65	91	96	92	86	67	38	43	73	100
1950	67	47	88	61	48	57	46	73	99	48
1960	54	50	64	56	63	95	87	76	74	82
1970	56	48	56	94	83	88	89	31	60	136
1980	95	70	85	92	72	76	81	76	68	44
1990	34	64	89	79	69	79	59	58	74	



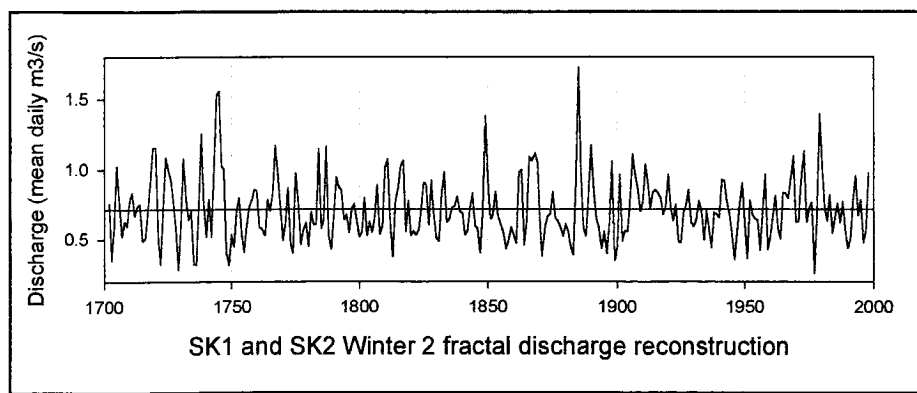
Sites SK1-SK2: Fractal Annual discharge reconstruction.
 Units are mean daily cubic meters per second (m^3/s) $\times 100$.

Year	0	1	2	3	4	5	6	7	8	9
1702			75	51	61	88	91	55	56	62
1710	83	91	87	68	66	60	63	80	104	117
1720	98	57	41	60	105	98	73	62	51	37
1730	59	102	123	76	64	47	46	73	138	102
1740	70	79	82	99	121	147	90	96	57	51
1750	68	74	78	85	78	64	71	82	91	93
1760	91	73	73	78	104	93	98	89	75	57
1770	48	51	63	53	47	92	105	63	54	63
1780	58	70	73	80	97	75	67	89	79	53
1790	65	118	126	105	66	60	57	68	64	65
1800	53	56	67	64	65	63	74	74	66	67
1810	92	113	84	54	70	93	101	85	60	62
1820	65	74	75	98	93	108	111	98	96	80
1830	67	59	89	93	73	63	69	68	69	70
1840	69	56	52	61	82	69	63	54	77	116
1850	104	64	63	70	61	53	53	52	58	81
1860	86	78	105	116	77	69	113	127	99	93
1870	70	50	70	93	89	81	74	64	68	75
1880	75	74	69	67	107	160	127	70	56	78
1890	94	71	52	48	47	57	61	83	107	72
1900	59	98	94	72	67	92	104	109	77	61
1910	61	74	70	60	68	79	76	72	69	69
1920	82	81	77	73	62	63	77	96	101	82
1930	77	80	100	84	69	75	71	64	74	81
1940	78	88	90	75	64	53	42	53	70	87
1950	65	50	70	79	78	70	62	69	99	73
1960	64	75	95	71	64	74	91	86	88	93
1970	65	62	77	103	80	87	84	54	67	114
1980	132	82	70	74	69	75	74	79	80	72
1990	63	62	93	112	79	74	59	58	81	



Sites SK1-SK2: Fractal Winter 2 discharge reconstruction.
 Units are mean daily cubic meters per second (m^3/s) $\times 100$.

Year	0	1	2	3	4	5	6	7	8	9
1702			75	35	58	102	78	52	63	60
1710	78	83	67	74	75	49	51	71	92	115
1720	115	52	32	69	108	100	93	78	58	29
1730	61	107	80	64	71	33	32	75	125	75
1740	52	79	52	100	153	156	103	100	40	32
1750	53	45	69	80	54	41	59	73	78	86
1760	85	59	58	53	78	70	83	117	98	75
1770	50	61	87	47	40	97	79	47	57	62
1780	45	70	61	61	115	58	64	116	53	43
1790	66	94	87	85	64	68	55	71	76	64
1800	52	56	80	53	63	55	65	89	54	60
1810	101	107	62	38	76	87	103	106	56	77
1820	53	56	53	56	71	91	89	61	92	67
1830	51	49	82	99	62	65	73	74	81	70
1840	69	53	56	73	83	59	58	40	70	138
1850	93	65	68	84	66	60	54	43	50	59
1860	53	47	98	100	46	63	109	106	112	104
1870	60	38	60	67	68	84	65	63	59	52
1880	61	57	45	39	91	173	98	58	53	81
1890	117	85	64	57	43	56	40	64	106	35
1900	44	96	49	56	56	77	111	96	86	70
1910	77	103	90	72	84	85	83	80	68	74
1920	96	73	63	75	49	48	69	74	85	62
1930	59	64	77	70	50	70	57	44	69	68
1940	65	92	92	77	68	53	36	55	75	90
1950	62	36	78	68	65	64	42	70	96	43
1960	53	67	81	58	50	83	83	79	94	109
1970	62	63	90	113	63	73	77	26	68	139
1980	102	73	63	82	55	66	75	62	77	56
1990	44	51	78	95	67	79	48	57	98	



REFERENCES

- Barefoot, A.C., Woodhouse, L.B., Hafley, W.L., and Wilson, E.H., 1974. Developing a Dendrochronology for Winchester, England. *Journal of the Institute of Wood Science*, Vol. 6, No. 5 (Issue 35), p. 34-40.
- Birkeland, P.W., 1984. *Soils and geomorphology*. Oxford University Press, New York, 372 p.
- Bland, J.M., and Altman, D.G., 1986. Statistical methods for assessing agreement between two methods of clinical measurement. *The Lancet*, February 8, p. 307-310.
- Box, G.E.P., and Jenkins, G.M., 1976. *Time Series Analysis, Forecasting and Control*. Holden-Day, Oakland, 575 p.
- Bradford, C., Taylor, L.G., Hinman, M.K., Marcovecchio, B., Peterson, W., Riley, J.P., Ross, L.S., and Shirley, H., 2000. Utah State Water Plan: West Colorado River Basin. State of Utah Division of Water Resources.
- Briffa, K., and Jones, P.D., 1990. Basic chronology statistics and assessment, in Cook, E.R., and Kairiukstis, L.A., eds., *Methods of Dendrochronology, Applications in the Environmental Sciences*, 394 p.
- Brooks, K.N., Ffolliott, P.F., Gregerson, H.M., and Debano, L.F., 1997. *Hydrology and the Management of Watersheds*, 2nd ed. Iowa State University Press, Ames, 502 p.
- Cleaveland, M.K., 2000. A 963-year reconstruction of summer (JJA) streamflow in the White River, Arkansas, USA, from tree-rings. *The Holocene*, Vol. 10, No. 1, p. 33-41.
- Cleaveland, M.K., and Stahle, D.W., 1989. Tree ring analysis of surplus and deficit runoff in the White River, Arkansas. *Water Resources Research*, Vol. 35, No. 6, p. 1391-1401.
- Cook, E.R., Briffa, K.R., Shiyatov, S., and Mazepa, V., 1990. Tree-Ring Standardization and Growth-Trend Estimation, in Cook, E.R., and Kairiukstis, L.A., eds., *Methods of Dendrochronology*. Kluwer Academic Press, Boston, 394 p.

- Cook, E.R., and Jacoby, G.C., 1983. Potomac River streamflow since 1730 as reconstructed by tree rings. *Journal of Climate and Applied Meteorology*, Vol. 22, No. 10, p. 1659-1672.
- Davis, J.C., 1986. *Statistics and Data Analysis in Geology*, 2nd ed. John Wiley and Sons, New York, 646 p.
- Fetter, C.W. Jr., 1980. *Applied Hydrogeology*. Charles E Merrill Publishing Company, London, 488 p.
- Fillmore, R., 2000. *The Geology of the Parks, Monuments and Wildlands of Southern Utah*. University of Utah Press, Salt Lake City, 268 p.
- Fritts, H.C., 1969. Bristlecone pine in the White Mountains of California: growth and ring-width characteristics. *Papers of the Laboratory of Tree Ring Research*, 4. University of Arizona Press.
- Fritts, H.C., 1976. *Tree Rings and Climate*. Academic Press, New York, 567 p.
- Fritts, H.C., Guiot, J, Gordon, G.A., and Schweingruber, F., 1990. Methods of calibration, verification, and reconstruction, in Cook, E.R., and Kairiukstis, L.A.,eds., *Methods of Dendrochronology*. Kluwer Academic Press, Boston, 394 p.
- Fritts, H.C., and Shatz, D.J., 1975. Selecting and characterizing Tree-Ring Chronologies for Dendroclimatic Analysis. *Tree-Ring Bulletin*, Vol. 35, p. 31-40.
- Fritts, H.C., and Holowaychuck, N., 1959. Some Soil Factors Affecting the Distribution of Beech in a Central Ohio Forest. *The Ohio Journal of Science* 59 (3): 167-186.
- García-Ruiz, J.M., and Otálora, F., 1992. Fractal trees and Horton's laws. *Mathematical Geology*, Vol. 24, No. 1, p. 61-71.
- Gleick, J., 1987. *Chaos, Making a New Science*. Viking Press, 352 p.

- Graf, J.B., Webb, R.H., and Hereford, R., 1991. Relation of sediment load and flood-plain formation to climatic variability, Paria River drainage basin, Utah and Arizona. *Geological Society of America Bulletin*, Vol. 103, p. 1405-1415.
- Graybill, D.A., 1989. The Reconstruction of Prehistoric Salt River Streamflow, in Graybill, D.A., Gregory, D.A., Nials, F.L., Fish, S.K., Gasser, R.E., Miksicek, C.H., and Szuter, C.R., eds., *The 1982-1984 Excavations at Las Colinas, Environment and Subsistence*. Cultural Resource Management Division, Arizona State Museum, University of Arizona, Archaeological Series 162, Vol. 5.
- Hack, J.T., 1957. Studies of longitudinal profiles in Virginia and Maryland. *U.S.G.S. Prof. Paper* 294-B.
- Hardman, G., and Reil, O.E., 1936. The relationship between tree-growth and stream runoff in the Truckee River basin, California-Nevada. *The University of Nevada Agricultural Research Station, Bulletin No.* 141, p. 1-38.
- Hawley, F.M., 1937. Relationship of Southern Cedar growth to precipitation and runoff. *Ecology*, Vol. 18, No. 3, p. 398-405.
- Hereford, R., 1986. Modern alluvial history of the Paria River drainage basin, southern Utah. *Quaternary Research*, 25, p. 293-311.
- Hereford, R., Jacoby, G.C., and McCord, V.A.S., 1996. Late Holocene alluvial geomorphology of the Virgin River in the Zion National Park area, southwest Utah. *Geological Society of America Special Paper* 310, 41 p.
- Holmes, R.L., Adams, R.K., and Fritts, H.C., 1986. Tree-ring chronologies of western North America: California, eastern Oregon and northern Great Basin, with procedures used in the chronology development work, including users manuals for computer programs COFECHA and ARSTAN. *Laboratory of Tree-Ring Research, University of Arizona, Chronology Series VI*, 182 p.
- Hurst, H.E., 1957. A suggested statistical model of some time series which occur in nature. *Nature*, Vol. 180, p. 494.

- Hurst, H.E., Black, R.P., and Simaika, Y.M., 1965. *Long-Term Storage, an Experimental Study*. Constable and Company, London, 145 p.
- Hurst, H.E., Black, R.P., and Simaika, Y.M., 1946. The Nile basin, the future Conservation of the Nile. S.O.P Press, Cairo , Physical Department Paper No. 51, 178 p.
- Jenny, H., 1941. Factors of Soil Formation, A System of Quantitative Pedology, 5thed. McGraw-Hill, New York, 281 p.
- Jones, P.D., Briffa, K.R., and Pilcher, J.R., 1984. Riverflow reconstruction from tree rings in southern Britain. *Journal of Climatology*, Vol. 4, p. 461-472.
- Kelsey, M.R., 1998. *Hiking and Exploring the Paria River*, 3rd ed. Kelsey Publishing, Provo, Utah, 224 p.
- Kendall, M., and Ord, J.K., 1990. *Time Series*, 3rd ed. Oxford University Press, New York, 296 p.
- Kulatilake, P.H.S.W., and Um, J., 1999. Requirements for accurate quantification of self-affine roughness using the roughness-length method. *International Journal of Rock Mechanics and Mining Science*, Vol. 36, p. 5-18.
- Kulatilake, P.H.S.W., Um, J., and Pan, G., 1998. Requirements for accurate quantification of self-affine roughness using the variogram method. *International Journal of Solids Structures*, Vol. 35, Nos. 31-32, p. 4167-4189.
- Kusumayudha, S.B., Zen, M.T., Notosiswoyo, S., and Gautama, R.S., 2000. Fractal analysis of the Oyo River, cave systems, and topography of the Gunungsewa karst area, central Java, Indonesia. *Hydrogeology Journal*, 8:271-278.
- Loaiciga, H.A., Haston, L., and Michaelson, J., 1993. Dendrohydrology and long-term hydrologic phenomena. *Reviews of Geophysics*, Vol. 31, No. 2, p.151-171.
- Malamud, B.D., and Turcotte, D.L., 1999. Self-affine time series: I. Generation and analyses, in Dmowska, R., and Saltzman, B., eds., *Advances in Geophysics*, *Long-Range Persistence in Geophysical Time Series*, Vol. 40. Academic Press, New York, p. 1-90.

- Malinverno, A., 1990. A simple method to estimate the fractal dimension of a self-affine series. *Geophysical Research Letters*, Vol. 17, No. 11, p. 1953-1956.
- Mandelbrot, B.B., 1967. How long is the coast of Britain? Statistical self-similarity and fractional dimension. *Science*, Vol. 156, No. 3775, p. 636-638.
- Mandelbrot, B.B., 1977. *Fractals: Form, Chance, and Dimension*. W.H. Freeman, San Francisco, 365 p.
- Mandelbrot, B.B., 1983. *The Fractal Geomtry of Nature*. W.H. Freeman, San Francisco, 468 p.
- Meko, D.M., 2001. Reconstructed Sacramento River system runoff from tree rings. Report prepared for the California Department of Water Resources under Agreement No. B81923-SAP # 4600000193, 63 p.
- Meko, D.M., Therrill, M.D., Baisan, C.H., and Hughes, M.K., 2001. Sacramento River flow reconstructed to A.D. 869 from tree rings. *Journal of the American Water Resources Association*, in Press.
- Meko, D.M., and Graybill, D.A., 1995. Tree-ring reconstruction of upper Gila River discharge. *Water Resources Bulletin*, Vol. 31, No. 4, p. 605-616.
- Meko, D.M., and Stockton, C.W., 1984. Secular variations in streamflow in the western United States. *Journal of Climate and Applied Meteorology*, Vol. 23, p. 889-897.
- Pelletier, J.D., and Turcotte, D.L., 1999. Self-affine time series: II. Applications and models, in Dmowska, R., and Saltzman, B., eds., *Advances in Geophysics, Long-Range Persistence in Geophysical Time Series*, Vol. 40. Academic Press, New York, p. 91-175.
- Phipps, R.L., 1972. Tree rings, stream runoff, and precipitation in central New York-a reevaluation. *U.S.G.S. Professional Paper* 800-B, p. B259-B264.
- Phipps, R.L., 1983. Streamflow of the Occoquan River in Virginia as reconstructed from tree-ring series. *Water Resources Bulletin*, Vol. 19, No. 5, p. 735-743.

- Ritter, D.F., Kochel, R.C., and Miller, J.R. 2002. *Process Geomorphology*, 4th. ed. Wm. C. Brown Publishers, Boston, 560 p.
- Rodríguez-Iturbe, I., and Rinaldo, A., 1997. *Fractal River Basins, Chance and Self-Organization*. Cambridge University Press, 547 p.
- Rosso, R., Bacchi, B., and Barbera, P.L., 1991. Fractal relation of mainstream length to catchment area in river networks. *Water Resources Research*, Vol. 27, No. 3, p. 381-387.
- Schulman, E., 1945. Runoff histories in tree rings of the Pacific slope. *The Geographical Review*, Vol. 35, No. 1, p. 59-73.
- Schulman, E., 1950. Dendroclimatic histories in the Bryce Canyon area, Utah. *Tree-Ring Bulletin*, Vol. 17, No. 1/2, p. 2-16.
- Schulman, E., 1951. Tree-ring indices of rainfall, temperature, and river flow, in Malone, T.F., ed., *Compendium of Meteorology*, American Meteorological Society, p. 1024-1029.
- Schulman, E., 1956. *Dendroclimatic Changes in Semiarid America*. University of Arizona Press, 142 p.
- Shroder, J.F. Jr., 1978. Dendrogeomorphological analysis of mass movement on Table Cliffs Plateau, Utah. *Quaternary Research* 9, p. 168-185.
- Skau, C.M., 1964. Interception, Throughfall, and Stemflow in Utah and Alligator Juniper Cover Types of Northern Arizona. *Forest Science*, vol. 10, No. 3, p. 283-287.
- Smith, L.P., and Stockton, C.W., 1981. Reconstructed stream flow for the Salt and Verde Rivers from tree-ring data. *Water Resources Bulletin*, Vol. 17, No. 6, p. 939-947.
- Sokal, R.R., and Rohlf, F.J., 1973. *Introduction to Biostatistics*. W.H. Freeman and Company, San Francisco, 368 p.

- Stockton, C.W., 1976. Long-term streamflow reconstruction in the upper Colorado River basin using tree rings, in Clyde, C.G., Falkenborg, D.H., and Riley, J.P., eds., *Colorado River Basin Modeling Studies*, seminar proceedings, Utah State University, Logan, p. 401-441.
- Stokes, M.A. and Smiley, T.L., 1996. *An Introduction to Tree-Ring Dating*. The University of Arizona Press, Tucson, 73 p.
- Strackee, J., and Jansma, E., 1992. The statistical properties of mean sensitivity - a reappraisal. *Dendrochronologia*, Vol. 10. p. 121-135.
- Swenson, H.K. and Bayer, J., 1990. Soil survey of Panguitch area, Utah, parts Garfield, Iron, Kane, and Piute Counties. U.S.D.A., SCS, 354 p. plus maps.
- Takayasu, H., 1993. Power-law distribution of river basin sizes, in Vicsek, T., Schlesinger, M., and Matsushita, M., eds. *Fractals in Natural Sciences*, World Scientific, London, p. 521-528.
- Tarboton, D.G., Bras, R.L., and Rodriguez-Iturbe, I., 1988. The fractal nature of river networks. *Water Resources Research*, Vol. 24, No. 8, p. 1317-1322.
- Turcotte, D.L., 1992. *Fractals and Chaos in Geology and Geophysics*. Cambridge University Press, New York.
- Turcotte, D.L., 1994. Fractal theory and the estimation of extreme floods. *Journal of Research of the National Institute of Standards and Technology*, Vol. 99, p.377-389.
- Weisberg, S., 1985. *Applied Linear Regression*, 2nd ed. John Wiley and Sons, New York.
- Wigley, T.M.L., Briffa, K.R., and Jones, P.D., 1984. On the average value of correlated time series, with applications in dendroclimatology and hydrometeorology. *Journal of Climate and Applied Meteorology*, Vol. 23, p. 201-213.
- Wright, R.D., and Mooney, H.A., 1965. Substrate-oriented distribution of bristlecone pine in the White Mountains of California. *American Midland Naturalist*, Vol. 72, No. 2, p. 257-284.